University of São Paulo
"Luiz de Queiroz" College of Agriculture

Investigating the use of defect-containing timber from young *Eucalyptus* plantations for manufacturing engineered products

Bruno Monteiro Balboni

Thesis presented to obtain the degree of Doctor in Science, Area: Forest Resources. Option in: Forest Products Technology

Piracicaba
2022

Bruno Monteiro Balboni
Forest Engineer and Biologist

Investigating the use of defect-containing timber from young *Eucalyptus* plantations for manufacturing engineered products

versão revisada de acordo com a Resolução CoPGr 6018 de 2011

Advisor:
Prof. Dr. **JOSÉ NIVALDO GARCIA**

Thesis presented to obtain the degree of Doctor in Science, Area: Forest Resources. Option in: Forest Products Technology

Piracicaba
2022

Dados Internacionais de Catalogação na Publicação
DIVISÃO DE BIBLIOTECA – DIBD/ESALQ/USP

Balboni, Bruno Monteiro

Investigating the use of defect-containing timber from young Eucalyptus plantations for manufacturing engineered products / Bruno Monteiro Balboni. - - versão revisada de acordo com a Resolução CoPGr 6018 de 2011. - - Piracicaba, 2022.

92 p.

Tese (Doutorado) - - USP / Escola Superior de Agricultura “Luiz de Queiroz”.

1. Silvicultura de ciclos curtos 2. Madeira juvenil 3. Nós 4. Empenamentos I. Título

Àqueles que sempre me deram apoio incondicional,
que me estimularam a buscar o meu melhor, sempre.
Aos meus pais e mentores, ***Adilson*** *e* ***Amarilis****,*

DEDICO

AGRADECIMENTOS

Esta foi uma longa jornada. Inúmeros desafios, dos mais diferentes tipos, surgiram, mas sempre acompanhados de alguém disposto a ajudar. Fiquei bastante satisfeito com o resultado alcançado neste projeto, mas seguramente, eu não teria atingido este nível de qualidade sozinho. Uma importante fase desta trajetória ocorreu em território onde a língua portuguesa não é familiar, assim, teremos, adicionalmente, uma versão em inglês dos agradecimentos. Portanto, todos aqueles que ajudaram de alguma forma poderão acompanhar esta seção.

Primeiramente, quero agradecer aos meus pais, Adilson e Amarilis pela criação fantástica que tive e pelo grande exemplo que são na minha vida. Obrigado por terem buscado respostas científicas, e não religiosas, para as perguntas existenciais de uma criança com sede de conhecimento. Este foi, sem dúvida, o início do meu caminho rumo à ciência. Obrigado ao Be, por ter se juntado a este time e pelas diversas ajudas com "economiquês". E obrigado aos outros três membros da família, Cléo, Katara e Mindiga, por sempre tornarem minha vida mais leve.

Um agradecimento especial ao meu orientador e amigo, Prof. José Nivaldo Garcia, que ora Garcia, com sua matemática apurada, ora José, nas cervejas e vinhos científicos, e ora Nivaldo, com seus conselhos paternais, me guiou até o término desta tese. Sou muito grato pela confiança e liberdade que tive para a escolha do tema, do caminho a ser seguido e das perguntas a serem feitas. Estas são as raízes dos meus maiores crescimentos ao longo deste doutorado.

Agradeço aos professores Marcelo Ribeiro e Brand Wessels, que, apesar da impossibilidade de oficializarmos, atuaram como meus coorientadores no doutorado e se tornaram parceiros científicos fundamentais.

Sou muito grato à minha grande parceira Alessandra Batista, cuja ajuda foi essencial em cada etapa desse doutorado, seja nos intermináveis ensaios mecânicos e medições, nas suas opiniões e sugestões sempre muito válidas, ou no suporte nos momentos de frustração.

Ao amigo e super técnico Facco, sempre bem disposto a ajudar e cuja experiência foi fundamental para realizar tudo o que foi feito no projeto. Aos técnicos dos outros laboratórios que sempre deram todo o suporte sempre que necessário, Sid, Biro, Cido, Amarildo.

À Giovana, nosso anjo da guarda dentro do PPG em Recursos Florestais, que além dos conselhos e orientações esteve sempre conosco para escutar nossas dores. A todo o pessoal da Seção de Apoio à Pós-Graduação, em especial ao meu amigo Alexandre, que forneceu uma enorme ajuda para a obtenção da bolsa de doutorado sanduíche. À equipe da Biblioteca, com todo o auxílio prestado na edição e formatação desta tese.

À Luty pelos diversos conselhos nos momentos de dúvida, ao Jotatê e ao Ari pelos papos estatísticos, à Bruna e ao Rafa pelas várias assistências.

Aos amigos Marina, Caio, Denise, Alê, José Eduardo, Thiago, Gabriel, pelos momentos de descontração, conversas científicas, cervejas, cafés e rucas, certamente um dos pontos fortes da minha pós-graduação. Ao Fado pela amizade e por me apresentar seu irmão, o que mudou os rumos deste projeto para melhor.

A todas as pessoas queridas da África do Sul que tornaram este país minha segunda casa. Em especial, à Bernie, por ter me acolhido em sua família maluca e incrível, ao Roland e à Suzanne por terem me adotado, e todos outros membros da família: CarolAnne, Monique, Dominique, Neil, Sky, Rosie, e Ashley. Ao meu grande broder da viagem, Jesse, pela amizade, parceria e pela grande ajuda que ele e o MJ me deram com tudo o que precisei. À Pamela pela ajuda com a fuga pra Namíbia. Ao Phillip, Justin, Michiel, Nick, Vanessa, Zahra, Tobi, Wilmore, Sadiq, Bright, Prof. Ben, Prof. Dave, Prof. Deon, Anton, Nickki, Jeanne, Zimele & Sino, Brian, Saskia, and Ryan.

À Zitral, por meio de sua equipe, em especial Valdir e Denis, que abriram as portas da serraria e doaram a madeira utilizada neste projeto, e ao Roberto Rubin que prontamente ofereceu seu caminhão para buscarmos a madeira.

À CAPES, pela bolsa de doutorado pleno e de doutorado sanduíche que recebi para o desenvolvimento deste projeto e que me permitiu viver uma grande experiência na África do Sul e crescer ainda mais neste processo. Ao grande Kikuchi (CAPES), que cuidou de todo encaminhamento da minha bolsa de doutorado sanduíche, pela sua energia positiva, pelo cuidado e simpatia.

E a todos aqueles que, em meio a tantas pessoas importantes, possam ter faltado à minha memória, mas que também foram fundamentais para a conclusão desta minha etapa.

Meus mais profundos agradecimentos!

AKNOWLEDGMENTS

It was a long journey, where numerous challenges of the most distinct types showed up, but always accompanied by someone willing to help. I am quite happy with the results achieved in this project, but it would not be possible to reach this quality level if I were working by myself. A very important stage of this path happened in a land where Portuguese is not spoken, so, we will have, additionally, an English version of the acknowledgments. This way, all of those who helped in some way will be able to follow this section.

First of all, I want to thank my parents, Adilson and Amarilis, for their fantastic raising and the great example they are in my life. Thank you for always looking for scientific, and not religious, answers to the existential questions of a kid thirsty for knowledge. It was, no doubt, the beginning of my path toward science. Thanks, Be, for joining the team and for the help with "economic dialect." Thanks to the other three elements of the family, Cléo, Katara and Mindiga, for always making my life lighter.

A special acknowledgment to my advisor and friend, Prof. José Nivaldo Garcia, who sometimes Garcia, with his complex math, sometimes José, during our scientific beer and wine, and sometimes Nivaldo, with his fatherly advice, guided me to the end of this thesis. I am very grateful for the trust and freedom I had to choose the subject, the path to be followed, and the questions to be made. These are the roots of my greatest growth through this Ph.D.

Thanks to Professors Marcelo Ribeiro and Brand Wessels, who, although impossible of turning it official, acted as my co-supervisors and became fundamental scientific partners.

I am very grateful to my great partner, Alessandra Batista, whose help was essential in each step of this Ph.D., with those infinite mechanical tests and measurements, the always-valuable opinions and suggestions, and the support in moments of frustration.

To the friend and super technician, Facco, who is always willing to help, whose experience was fundamental to the completion of the project. To the technicians from other labs, who always helped every time I needed them, Sid, Biro, Cido e Amarildo.

To Giovana, our guardian angel inside our Post-Grad program, who, besides the advice and guidance, was always there to listen to our pain. To everyone from the Graduate Studies Office, especially my friend Alexandre, who gave me great help in obtaining the grant to study abroad. To the library team with all support in editing the thesis.

To Luty for the many pieces of advice in moments of doubt, to Jotatê and Ari for the statistical talks, to Bruna and Rafa for their assistance.

To my friends Marina, Caio, Denise, Alê, Joseph Edwards, Thiago, and Gabriel, for the moments of distraction, scientific talks, beers, coffee, and rucas, certainly a strong point of my Ph.D. To Fado, for his friendship and for introducing me to his brother, what changed the direction of this project for the better.

To all dear people from South Africa who made that country my second home. Especially, to Bernie, for having welcomed me into her crazy and amazing family, to Roland and Suzanne for adopting me, and all other family members: CarolAnne, Monique, Dominique, Neil, Sky, Rosie, and Ashley. To my best mate in South Africa, Jesse, for his friendship and the great help he and MJ gave me with everything I needed. To Pamela, for helping me escape to Namibia. To Phillip, Justin, Michiel, Nick, Vanessa, Zahra, Tobi, Wilmore, Sadiq, Charles, Bright, Prof. Ben, Prof. Dave, Prof. Deon, Anton, Nikki, Jeanne, Zimele & Sino, Brian, Saskia, and Ryan.

To Zitral, through their team, especially Valdir and Denis, who opened the doors of the sawmill and donated all timber used in this project, and to Roberto Rubin, who promptly offered his truck to get the timber.

To CAPES, for both full Ph.D. and doctoral internship grants to develop this project, which allowed me to live a great experience in South Africa and to become even better. To the great Kikuchi (CAPES) who took care of my grant process, for his positive energy, care, and sympathy.

And to all those who, among so many important people, may have got lost in my memory, but which were also fundamental for the conclusion of this step.

My deepest thanks!

BIOGRAFIA

O menino dos dinossauros cresceu. Experimentou. Viveu. Voou.

“Descobri como é bom chegar quando se tem paciência. E para se chegar, onde quer que seja, aprendi que não é preciso dominar a força, mas a razão. É preciso, antes de mais nada, querer”.

Amyr Klink

SUMÁRIO

RESUMO

Investigação do uso de madeira com defeitos de florestas jovens de *Eucalyptus* para fabricação de produtos engenheirados

A crescente demanda por madeira no mundo tem levado a buscas por fontes sustentáveis desta matéria prima. Florestas jovens de *Eucalyptus* são uma potencial fonte de madeira, devido a seu rápido crescimento e alta adaptabilidade a diversas condições climáticas. Árvores jovens normalmente apresentam características indesejáveis, como nós, empenamentos e altas porcentagens de madeira juvenil, além de gerar madeira serrada de seção transversal de dimensões limitadas, o que pode ser superado pela fabricação de produtos engenheirados. Nosso objetivo foi avaliar alguns pontos chaves, do ponto de vista da qualidade e propriedades mecânicas, para adoção de madeira de plantações de ciclo curto de *Eucalyptus* na fabricação de produtos engenheirados de madeira. Dentre os clones de *Eucalyptus* altamente produtivos já utilizados na indústria de bioenergia brasileira, foram identificados alguns com propriedades da madeira desejáveis mesmo em idades precoces (sete anos). Um índice de arqueamento e encurvamento foi desenvolvido com madeira adulta e jovem de *E. grandis*, que nos permite identificar e segregar porções de madeira cuja distorção localizada é muito severa, auxiliando o uso das seções pouco empenadas na composição de lamelas emendadas para produtos engenheirados de madeira. Ao avaliar a resistência de adesão em madeira com nós de *E. grandis* jovens em relação à madeira sem defeitos, foi encontrado que a presença de nós afeta a resistência da adesão da madeira em densidades acima de 0.65 g cm^{-3}, reforçando os benefícios da estratificação de lamelas em vigas laminadas. Lamelas de alta densidade são posicionadas em zonas que demandam maiores tensões de compressão e tração, mas onde a tensão de cisalhamento é menor. Este fato, junto à baixa proporção de nós na superfície das lamelas, torna a influência dos nós na adesão da madeira de *Eucalyptus* jovens, pouco significante. Foram construídas e ensaiadas vigas laminadas coladas de madeira de *E. grandis* jovens com diferentes níveis de encurvamento, adicionando pré-tensão às vigas. A pré-tensão não influenciou a capacidade de carga das vigas como hipotetizado. Porém, as vigas retornaram propriedades mecânicas adequadas para uso estrutural, ainda que 80% das lamelas não atendessem os requisitos mínimos estabelecidos em norma. Enquanto nós na zona de compressão não influenciaram o comportamento das vigas, os nós presentes na porção tracionada foram pontos onde a ruptura teve início. No entanto, apenas em uma das vigas o comportamento e a resistência na flexão foram afetados pelo nó, ainda que não suficiente para alterar a média e variação dos dados. Por sua vez, os nós não influenciaram o módulo de elasticidade na flexão, independente da posição. Os resultados demonstram que a madeira de eucaliptos jovens apresenta potencial para a fabricação de produtos engenheirados, especialmente em países onde o *Eucalyptus* já é uma cultura florestal bem estabelecida, como Brasil, África do Sul e Chile. Existem diversos benefícios em utilizar esta fonte de madeira serrada, desde produção e processamento rápidos, menores riscos, entrada financeira antecipada, até a possibilidade de se estabelecer plantios próximos ao mercado consumidor. Há, no entanto, a necessidade de se avaliar o rendimento de cada etapa de processamento e a viabilidade econômica da fabricação de produtos engenheirados de madeira provinda de plantações jovens de *Eucalyptus*.

Palavras-chave: Silvicultura de ciclos curtos, Madeira juvenil, Nós, Empenamentos

ABSTRACT

Investigating the use of defect-containing timber from young *Eucalyptus* plantations for manufacturing engineered products

The increasing demand for timber globally has led to a search for sustainable wood sources. Young *Eucalyptus* plantations are a potential source of timber, taking advantage of their fast growth and high adaptability to a wide range of climatic conditions. Young trees usually contain undesirable features, such as knots, warping, and high contents of juvenile wood, apart from providing timber of limited cross-sectional dimensions, what can be overcome by the manufacture of engineered products. We aimed to address some key points, from the wood quality and mechanical properties point of view, for the adoption of short-rotation *Eucalyptus* plantations to manufacture engineered wood products. Among the high-productive clones already in use in the Brazilian bioenergy industry, we have identified some with desirable wood mechanical properties even at early ages (seven years-old). We developed and tested a bow and spring index in young and mature *E. grandis* timber boards which allows us to identify and segregate timber portions whose localized distortion is too high, helping to use the low warping sections to compose finger-jointed lamellas for engineered wood products. When testing the adhesion strength on knot-containing timber from young *E. grandis* in relation to clear wood, we found that knots reduce wood adhesion strength only when density is above 0.65 g cm^{-3}, reinforcing the benefits of stratifying lamellas on glued laminated beams. High-density lamellas are positioned on zones with higher compression and tensile stress demand, but where shear stress is low. This fact, together with the low proportion of knots on lamellas' surfaces, makes the influence of knots on the adhesion of wood of young *Eucalyptus* less significant. We build an tested glued laminated beams using timber from young *E. grandis* with different levels of bow, adding presstress to the beams. Prestress did not influence the beams' load capacity as hypothesized. However, laminated beams returned mechanical properties adequate for structural applications, even though 80% of lamellas did not meet the minimum requirements of national timber standards. While knots in the compression zone did not influence the beams' behavior, knots on the tension side were the points where rupture started. However, only one beam had the bending behavior and strength affected by the knot, although not enough to affect the average and the variation of the data. In turn, knots did not influence beams' bending stiffness independently of their position. The results showed young *Eucalyptus* timber has a high potential for manufacturing engineered products, especially in countries where *Eucalyptus* is already well established as a forest culture, such as Brazil, South Africa, and Chile. There are several benefits of using this timber source, from the fast-growing raw material production and processing, lower risks, and earlier payout, to the possibility of establishing plantations close to the consumer market. There is, however, the need for assessing the yield of each processing step and the economic viability of manufacturing engineered wood products from young *Eucalyptus* forests.

Keywords: Short rotation forestry, Juvenile wood, Knots, Warping

1. INTRODUCTION

The construction industry was responsible alone for more than 40% of the global carbon emission related to energy production and consumption in 2015 (Abergel et al., 2017). This fact led to a significant increase in the energy efficiency of buildings, which, together with many buildings having no occupation (bridges, roads, tunnels, etc), the focus of investigations turned to embodied emissions instead of operational emissions (Huang et al., 2018). Embodied emissions can be defined as the carbon emitted during the manufacture of the materials used in the building and the construction process itself, including renewals (Cabeza et al., 2014). The replacement of steel and concrete for timber is one of the most efficient strategies to reduce CO_2 emissions (Oliver et al., 2014). However, some studies point out that stocking carbon in a standing forest is even more efficient for decreasing carbon emissions (Harmon et al., 1990; Nunery & Keeton, 2010). An alternative for stocking carbon in the forests and, at the same time, adopting timber on buildings is to use plantations forests as a wood source instead of native forests.

Although planted forests usually need long rotations for timber production, some species can provide the raw material for the timber industry at earlier ages, such as *Populus* sp. (Casado et al., 2012; Castro & Paganini, 2003), *Schizolobium parahyba* (Rosa et al., 2019), *Tectona grandis* e *Gmelina arborea* (Montero & Moya, 2015). Nevertheless, species from the genus *Eucalyptus* stand out at that point. Besides being the most planted hardwood in the world (Myburg et al., 2014) and one of the fastest-growing trees (Japarudin et al., 2020), eucalypts adapt to a wide variety of environments (Gonçalves et al., 2013).

However, *Eucalyptus* wood is mainly destined for low-value products, such as paper, reconstituted panels, or bioenergy, and the reason is the generation of several quality problems after processing or drying (Wessels et al., 2020). Brazil has almost 7.5 million hectares covered with *Eucalyptus* plantations (IBGE, 2020), and it could provide timber in replacement of those coming from natural forests or long rotation pine plantations. Derikvand et al. (2017) argue that the best destination for low-grade eucalyptus timber in Australia is through the manufacture of mass timber products, such as glued laminated timber and cross-laminated timber. The motivation for the mentioned authors to look for another timber source in Australia is the same as in other countries: wood demand is increasing, but forest plantation area does not follow the same trend and natural forests are not able to rationally supply the market with timber.

The basic concept behind engineered wood products is that timber pieces are connected to form a single element. Timber can be joined with glue, nails, screws, or dowels, and their main advantage is to produce a large element from timber with small dimensions (Abbott & Whale, 1987). Besides generating only timber with small sizes, young trees are mostly unpruned and constituted by juvenile wood only. Knots resulting from the unpruned branches usually harm wood mechanical properties, reaching decrease values of 50% or more (Abbott & Whale, 1987). Juvenile wood, in turn, has lower density and mechanical properties and is usually avoided for the manufacture of solid wood products, especially for structural purposes (Missanjo & Matsumura, 2016).

However, studies with wood from young *Eucalyptus* plantations have brought encouraging results. Fideles (2017) reported branch diameters from 7 to 9.9 mm in *Eucalyptus urophylla* at 18 months, the age when natural pruning starts to occur and branches stop growing. These values are considerably lower than those reported for *Pinus sylvestris*, with diameters ranging from 10 to 45 mm (Moberg, 2000). Knots with small diameters were also reported by Crafford and Wessels (2016), and it is the probable reason why knots in young *Eucalyptus* trees did not have major impacts on the mechanical properties of timber of structural sizes (Nocetti et al., 2017; Pagel et al., 2020).

Juvenile wood, in turn, is a minor problem in hardwoods compared to softwoods, the usual raw material for engineered wood products (Zobel & Sprague, 1998). Balboni et al. (2020) confirmed juvenile wood has lower strength than mature wood, but they share the same strength-to-density relationship. Products manufactured with juvenile wood from *Eucalyptus* plantations had returned adequate properties (Liao et al., 2017; Pagel et al., 2020), with a special reference to the roof trusses made with young *E. grandis* wood, which is already well established in the South African market (Wessels et al., 2020).

The high growth rates of *Eucalyptus* allow the establishment of short-rotation forests to provide raw material to the timber industry. These plantations harvested at young stages have some advantages over the classic forests managed for timber, whether planted or natural. Besides prompt availability of wood in some regions and countries, these forests can be planted close to the main consumer markets, avoiding extra costs with transport or importation. Shorter rotations have lower risks of fire, pests, wind damage (Griess et al., 2016), and do not require thinning or pruning. An earlier cash inflow also turns plantation forests into a more attractive investment opportunity. Young trees generate logs of small diameters, allowing the adoption of linear sawmills, which increases speed and reduces the costs of primary processing (Washusen, 2013).

There are still some challenges before adopting young *Eucalyptus* as a timber source, and we have identified some of them considering previous studies as well as the Brazilian scenario. The paper and the bioenergy industries in Brazil have several *Eucalyptus* clones and varieties with high growth rates and adapted to the environment. Although they were developed for reconstituted products or for providing energy, some of these clones or varieties may provide wood with adequate quality for solid products. Identifying them can reduce costs and time for developing a variety specifically for timber production. Knots have not shown impacts on wood mechanical properties, but they are zones that may reduce wood adhesion strength due to different grain angles and higher extractive contents (Davis, 1997). Their effect on adhesion is an important subject to be assessed since a weak adhesion may cause a structural failure. Timber warping is another point of relevance, because, as stated by Derikvand et al. (2017), timber standards are too severe and do not take into consideration low grade timber can be used to compose engineered products. We have also found some standards have an imprecise calculation of timber bow and crook that should be fixed to improve the use of warped timber.

In the present series of studies, we aim to address some key points, from the wood quality and mechanical properties point of view, to turn feasible the use of timber from young *Eucalyptus* plantations to manufacture engineered wood products.

References

Abbott, A. R., & Whale, L. R. J. (1987). An overview of the use of glued laminated timber (glulam) in the UK. Construction & Building Materials, 1(2), 104–110.

Abergel, T., Dean, B., & Dulac, J. (2017). Towards a zero-emission, efficient, and resilient buildings and construction sector. www.globalabc.org

Balboni, B. M., Batista, A. S., Rodrigues, R. de A., & Garcia, J. N. (2020). Relationship between strength and density in juvenile and mature Eucalyptus sp. wood. Brazilian Journal of Animal and Environmental Research, 3(3), 983–991. https://doi.org/10.34188/bjaerv3n3-019

Cabeza, L. F., Rincón, L., Vilariño, V., Pérez, G., & Castell, A. (2014). Life cycle assessment (LCA) and life cycle energy analysis (LCEA) of buildings and the building sector: A review. Renewable and Sustainable Energy Reviews, 29, 394–416. https://doi.org/https://doi.org/10.1016/j.rser.2013.08.037

Casado, M., Acuña, L., Basterra, L.-A., Ramón-Cueto, G., & Vecilla, D. (2012). Grading of structural timber of Populus × euramericana clone I-214. Holzforschung, 66(5), 633–638. https://doi.org/doi:10.1515/hf-2011-0153

Castro, G., & Paganini, F. (2003). Mixed glued laminated timber of poplar and Eucalyptus grandis clones. Holz Als Roh- Und Werkstoff, 61(4), 291–298. https://doi.org/10.1007/s00107-003-0393-6

Crafford, P. L., & Wessels, C. B. (2016). The potential of young, green finger-jointed Eucalyptus grandis lumber for roof truss manufacturing. Southern Forests, 78(1), 61–71. https://doi.org/10.2989/20702620.2015.1108618

Davis, G. (1997). The performance of adhesive systems for structural timbers. International Journal of Adhesion and Ahesives, 17(3), 247–255.

Derikvand, M., Nolan, G., Jiao, H., & Kotlarewski, N. (2017). What to Do with Structurally Low-Grade Wood from Australia ' s Plantation Eucalyptus ; Building Application ? BioResources, 12(1), 4–7.

Fideles, J. C. A. (2017). Oclusão da casca indica o início da formação de clear em árvores desramadas.

Gonçalves, J. L. D. M., Gonçalves, D. M., Alcarde, C., Rioyei, A., Duque, L., Couto, A., Stahl, J., Frosini, S., Ferraz, D. B., Paula, W. de, Henrique, P., Brancalion, S., Hubner, A., Bouillet, J. D., Laclau, J., Nouvellon, Y., & Epron, D. (2013). Integrating genetic and silvicultural strategies to minimize abiotic and biotic constraints in Brazilian eucalypt plantations. Forest Ecology and Management, 301, 6–27. https://doi.org/10.1016/j.foreco.2012.12.030

Griess, V. C., Uhde, B., Ham, C., & Seifert, T. (2016). Product diversification in South Africa ' s commercial timber plantations : a way to mitigate investment risk. Southern Forests, 78(2), 145–150. https://doi.org/10.2989/20702620.2015.1136508

Harmon, M. E., Ferrell, W. K., & Franklin, J. F. (1990). Effects on Carbon Storage of Conversion of Old-Growth Forests to Young Forests. Science, 247(4943), 699–702. https://doi.org/10.1126/science.247.4943.699

Huang, L., Krigsvoll, G., Johansen, F., Liu, Y., & Zhang, X. (2018). Carbon emission of global construction sector. Renewable and Sustainable Energy Reviews, 81, 1906–1916. https://doi.org/https://doi.org/10.1016/j.rser.2017.06.001

IBGE. (2020). Produção da Extração Vegetal e da Silvicultura—PEVS. In https://www.ibge.gov.br/estatisticas-novoportal/economicas/agricultura-e-pecuaria/9105-producao-da-extracao-vegetal-e-da-silvicultura.html . https://www.ibge.gov.br/estatisticas-novoportal/economicas/agricultura-e-pecuaria/9105-producao-da-extracao-vegetal-e-da-silvicultura.html

Japarudin, Y., Lapammu, M., Alwi, A., Warburton, P., Macdonell, P., Boden, D., Brawner, J., Brown, M., & Meder, R. (2020). Growth performance of selected taxa as candidate species for productive tree plantations in Borneo. Australian Forestry, 83(1), 29–38. https://doi.org/10.1080/00049158.2020.1727181

Liao, Y., Tu, D., Zhou, J., Zhou, H., Yun, H., Gu, J., & Hu, C. (2017). Feasibility of manufacturing cross-laminated timber using fast-grown small diameter eucalyptus lumbers. Construction and Building Materials, 132, 508–515. https://doi.org/10.1016/j.conbuildmat.2016.12.027

Missanjo, E., & Matsumura, J. (2016). Wood Density and Mechanical Properties of Pinus kesiya Royle ex Gordon in Malawi. Forests, 7(7). https://doi.org/10.3390/f7070135

Moberg, L. (2000). Models of Internal Knot Diameter for Pinus sylvestris. Scandinavian Journal of Forest Research, 15(2), 177–187. https://doi.org/10.1080/028275800750014984

Montero, R. S., & Moya, R. (2015). Reducing Warp and Checking in 4 by 4 Beams from Small-Diameter Tropical Species (Tectona grandis, Gmelina arborea, and Cordia alliodora) Obtained by Turning the Pith Inside Out. Forest Products Journal, 65(5–6), 285–291. https://doi.org/10.13073/FPJ-D-14-00089

Myburg, A. A., Grattapaglia, D., Tuskan, G. A., Hellsten, U., Hayes, R. D., Grimwood, J., Jenkins, J., Lindquist, E., Tice, H., Bauer, D., Goodstein, D. M., Dubchak, I., Poliakov, A., Mizrachi, E., Kullan, A. R. K., Hussey, S. G., Pinard, D., van der Merwe, K., Singh, P., … Schmutz, J. (2014). The genome of Eucalyptus grandis. Nature, 510(7505), 356–362. https://doi.org/10.1038/nature13308

Nocetti, M., Pröller, M., Brunetti, M., Dowse, G. P., & Wessels, C. B. (2017). Investigating the potential of strength grading green Eucalyptus grandis lumber using multi-sensor technology. BioResources, 12(4), 9273–9286. https://doi.org/10.15376/biores.12.4.9273-9286

Nunery, J. S., & Keeton, W. S. (2010). Forest carbon storage in the northeastern United States: Net effects of harvesting frequency, post-harvest retention, and wood products. Forest Ecology and Management, 259(8), 1363–1375. https://doi.org/https://doi.org/10.1016/j.foreco.2009.12.029

Oliver, C. D., Nassar, N. T., Lippke, B. R., & McCarter, J. B. (2014). Carbon, Fossil Fuel, and Biodiversity Mitigation With Wood and Forests. Journal of Sustainable Forestry, 33(3), 248–275. https://doi.org/10.1080/10549811.2013.839386

Pagel, C. L., Lenner, R., & Wessels, C. B. (2020). Investigation into material resistance factors and properties of young, engineered Eucalyptus grandis timber. Construction and Building Materials, 230, 117059. https://doi.org/10.1016/j.conbuildmat.2019.117059

Rosa, T. O., Terezo, R. F., Rios, P. D., Sampietro, J. A., & Rosa, G. O. (2019). Schizolobium Parahyba var. Amazonicum Glulam Classified by Non-destructive Tests. In Floresta e Ambiente: Vol. v. vol.26 num.2. Instituto de Florestas da Universidade Federal Rural do Rio de Janeiro.

Washusen, R. (2013). Processing methods for production of solid wood products from plantation- grown Eucalyptus species of importance to Australia (Issue April).

Wessels, C. B., Nocetti, M., Brunetti, M., Crafford, P. L., Pröller, M., Dugmore, M. K., Pagel, C., Lenner, R., & Naghizadeh, Z. (2020). Green-glued engineered products from fast growing Eucalyptus trees: a review. European Journal of Wood and Wood Products, 78(5), 933–940. https://doi.org/10.1007/s00107-020-01553-6

Zobel, B. J., & Sprague, J. R. (1998). Juvenile Wood in Forest Trees. Springer.

2. EVALUATING THE POTENTIAL FOR TIMBER PRODUCTION OF YOUNG FORESTS OF *Eucalyptus* spp. CLONES USED FOR BIOENERGY: WOOD DENSITY AND MECHANICAL PROPERTIES

B. M. Balboni[1], A. S. Batista[1] & J. N. Garcia[1]

[1]Department of Forest Sciences, University of São Paulo, Piracicaba, Brazil

https://doi.org/10.1080/00049158.2021.1945238

Abstract The Brazilian bioenergy industry is well developed and has numerous highly productive *Eucalyptus* spp. clones, the wood of which may suit the timber industry. We screened the mechanical wood properties of six bioenergy *Eucalyptus* spp. clones from young forests to find ones suitable for the timber industry. We evaluated shear strength, parallel compressive strength, strength and stiffness on static bending, and wood density. *Eucalyptus camaldulensis* clones had low strength and stiffness for their wood density and are less suitable for timber products. However, clones from *E. urophylla* and *E. urophylla* × *E. grandis* had specific strength and stiffness close to the values reported for mature *Eucalyptus* wood. Their average density ranged from 0.54 g cm^{-3} to 0.68 g cm^{-3} and, while the lightest wood had properties close to those of mature *Pinus elliottii* trees, the clone with the densest wood produced material similar to mature *E. urophylla*. We conclude that these clones have distinct wood properties, each with different potential applications. With better understanding of this timber source, young clonal *Eucalyptus* forests could be an asset to the timber industry in Brazil, substituting pine wood and providing raw material close to the main consumer markets.

Keywords short-rotation forestry; juvenile wood; wood density; specific strength; specific stiffness

2.1. Introduction

Eucalyptus trees are among the most productive in the world (Japarudin et al., 2020), with reported growth rates above 80 m^3 ha^{-3} y^{-1} (Gava and Gonçalves, 2008). Clonal *Eucalyptus* spp. silviculture has played an important role in establishing Brazil as a leading centre for forest plantations (Gonçalves et al., 2013). In general, the clones with the highest growth rates have been selected for use by the pulp, bioenergy and panel industries (Gonçalves et al., 2013). Many companies are also planting *Eucalyptus* spp. for timber production because of their high productivity but, because they were not developed for this purpose, there is little information about which clones are most suitable for timber production.

The bioenergy industry, on the other hand, is well developed in Brazil, and *Eucalyptus* spp. plantations are one of its biggest assets (Andrade et al. 2013). One of the properties most sought after from clonal eucalypts for charcoal production is denser wood because high-density wood generates products with higher mechanical properties (Moutinho et al., 2016; Pereiraet al., 2016) and greater energy content per volume (Dufournyet al., 2019). Because mechanical wood properties also have a strong correlation with wood density (Zhang, 1997; Balboniet al., 2020), clones developed for bioenergy might be suitable for timber production. Available *Eucalyptus* spp. clones have already been genetically improved to adapt to the local climate, maximise productivity and resistance to disease, and increase wood density. Hence, the timber industry may be able to take advantage of the availability of such clones,

avoiding the need for a program of genetic selection, which is a demanding activity in terms of time and cost (Resende et al., 2012).

Superior clones can be transitioned to classic long-rotation forests because many juvenile characteristics are maintained at older ages (Queiroz et al., 2019). Clonal forests can also be used for new engineered wood products (Derikvand et al., 2017), which adds value to young forests, enables production areas to be closer to consumer markets, and reduces pressure on native forests. The wood from these young forests is usually considered to have low net worth and has been underused, although according to McGavin and Leggate (2019) it has high potential for many high-added-value products. Young *Eucalyptus grandis* W.Hill, for example, is a promising material for structural engineered products (Pagel et al., 2020). There are still many challenges for the commercial production of structural products from young eucalypt trees (Derikvand et al,. 2017), but encouraging results with wood from short-rotation forests have recently been reported (Crafford and Wessels, 2016; Liao et al., 2017; Derikvand et al., 2018, 2020; Balboni et al., 2020; Wessels et al., 2020).

Finding bioenergy *Eucalyptus* spp. clones suitable for solid wood products can reduce costs and shorten the time for developing appropriate genetic material, increasing the relevance of Brazil's main forest plantation genus to the timber industry. Hence, in this study, our goal was to assess the mechanical properties of wood from six high-productivity bioenergy *Eucalyptus* spp. clones and determine their suitability for timber production.

2.2. Materials and methods

The clonal material came from a commercial plantation (Figure 1) with a spacing of 3.5 m × 2 m located at 620 m above sea level in the state of Goiás, Brazil (Figure 2). The plantation has a sandy soil and Aw climate (according to the Köeppen classification), with a dry season followed by a rainy spring-summer, and average annual rainfall of 1600 mm. According to commercial inventories performed in the plantation, the average increment rates of all clones are similar, at around 34 m^3 ha^{-1} y^{-1}. This site was selected because of the wide variety of eucalypt clones available, all of which were developed for bioenergy. For this study, we used all clones growing under the same conditions (i.e. soil type, terrain slope, spacing and age).

Figure 1. Clonal *Eucalyptus urophylla* (clone GG100) plantation (spacing 3.5 m × 2 m) at 7 years old. Photo taken during tree height measurement.

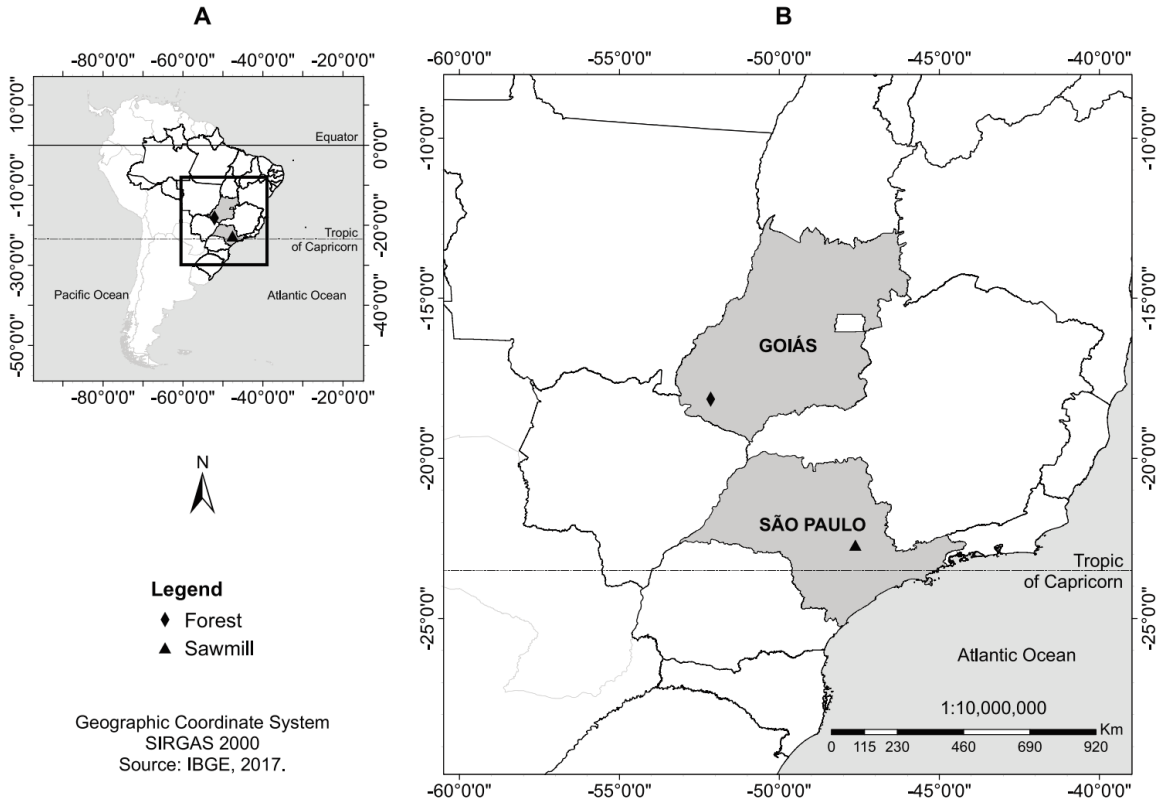

Figure 2. Map of South America with Brazil's borders in black (A) and a detailed area in Brazil (B) showing the location of the forest plantation studied (S 18°08′49.7", W 52°09′04.7") in the state of Goiás, as well as the sawmill where the logs were milled (S 22°42′23.0", W 47°37′40.9") in the state of São Paulo. Geographic Coordinate System SIRGAS 2000. Data source: IBGE (2021).

Ninety-six seven-year-old trees (16 per clone) were selected from six different bioenergy clones (Table 1) and harvested using a chainsaw; the first log of each (2 m long) was sent for sawmilling. We visually selected individual trees with high diameter and straightness as these are desirable characteristics for timber processing. The selected trees' diameters at breast height (DBH; 1.3 m from the ground) ranged from 18 to 21 cm, an interval that represents 10.28% of the 866 inventoried trees (Figure 3). The inventory and the harvesting were conducted in the same week, with tree DBH measured using a diameter tape. The DBH average and distribution of the six clones were very similar, so a single distribution is presented.

Table 1. Selected clones and their respective species (RNC, 2018)

Clone	Species	Species code
C219	*Eucalyptus urophylla* x *Eucalyptus grandis*	(u x g)
GG100	*Eucalyptus urophylla*	(u)
I144	*Eucalyptus urophylla*	(u)
I224	*Eucalyptus urophylla*	(u)
VM01	*Eucalyptus urophylla* x *Eucalyptus camaldulensis*	(u x c)
VM58	*Eucalyptus camaldulensis*	(c)

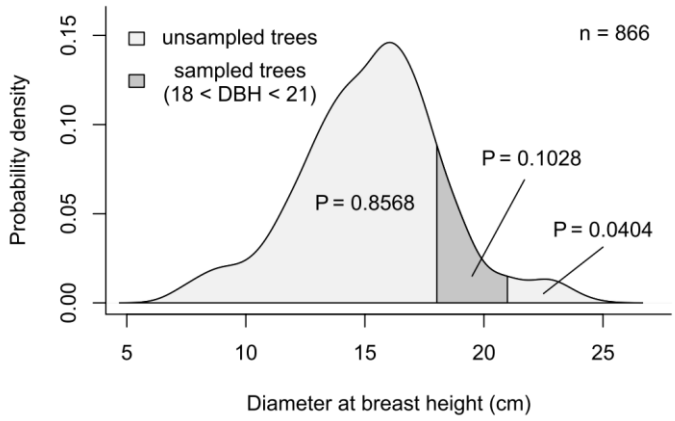

Figure 3. Probability density distribution of the tree's diameter at breast height (DBH) from the forest plantation studied, highlighting the range of DBH values of the sampled trees. P = probability of DBH to fall within the ranges pointed on the plot.

After harvesting, which occurred at the end of October (the middle of spring in the Southern Hemisphere), the logs were identified with their respective clone name and tree number and had both ends covered with plastic bags to avoid excessive water loss and end-splitting. The material was transported by truck to a sawmill at the University of São Paulo, Piracicaba Campus (Figure 2). Four days after arrival, the logs were processed using a vertical band saw with log carriage (Schiffer) to produce flat-sawn (tangential) boards with a nominal thickness of 30 mm. The milling pattern, shown in Figure 4, was adopted to minimise end-splits and crook and to obtain 30 mm × 30 mm slats of the outermost heartwood. We kept the slats stacked in a climate-controlled room at 25°C and 65% relative humidity until they reached constant mass and the moisture content (MC) required for mechanical testing (12%). When the slats achieved their equilibrium MC, they were processed using a single circular-saw blade, first to reduce the crosssection to 25 mm × 25 mm and then to cut to length to obtain the samples for mechanical testing. The samples were kept in the climate-controlled room for approximately two weeks until the tests were carried out.

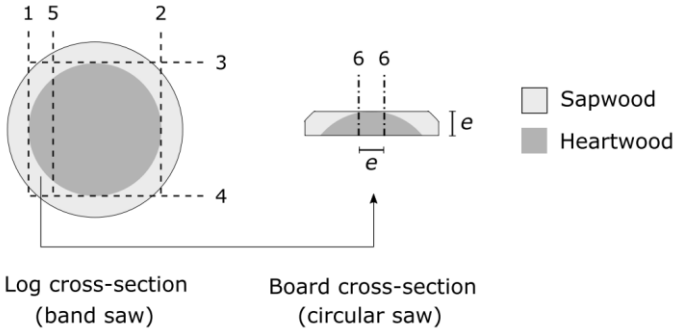

Figure 4. Milling pattern adopted. Numbers indicate the sawing sequence and e = 30 mm.

One sample from each tree was used for each of the various mechanical tests, which were carried out using a Universal Testing Machine (Pavitest 300 kN of load capacity). We followed the secondary method of the ASTM Standard D143 (ASTM 2014) for testing small clear-wood specimens in which no visual defects such as knots, sapwood or grain deviations were observed before or after the tests. The properties assessed were compression strength parallel to grain (f_{c0}), shear strength parallel to grain (f_{v0}), static bending strength (f_M), and stiffness in static bending (E_{M0}). Because the boards were 30 mm thick, we modified the shear samples: the shear

area was 25 mm × 25 mm instead of 50 mm × 50 mm. As the shear area adopted was one-quarter of the original area stated by the standard, the crosshead speed (0.6 mm min^{-1}) was reduced by the same rate. All samples' dimensions and test speeds are displayed in Table 2. We used compression-test samples to calculate the density at 12% MC ($\rho_{12\%}$), measuring dimensions with a digital caliper (precision of 0.01 mm) and mass with a semi-analytical scale (precision of 0.01 g).

Table 2. Sample size and crosshead speed for each mechanical test realized

Test	Sample dimensions (mm)	Crosshead speed
compression([1])	25 x 25 x 100([2])	0.3 mm/min
static bending	25 x 25 x 410	1.3 mm/min
shear	25 x 25([3])	0.15 mm/min

([1]) and density
([2]) span = 360 mm
([3]) shear area

For each variable, we analysed the normal distribution and homoscedasticity graphically by quantile-quantile plots and boxplots, respectively, with the R software (R Development Core Team, 2019). Because the data conformed to the theoretical assumptions of analyses of variance, this technique, followed by the Tukey test, was used to analyse data. The only exception was shear strength, for which homoscedasticity was not observed even after mathematical transformations (logarithmic, square root and angular) (Ribeiro-Oliveira et al., 2018). We adopted the Kruskal-Wallis non-parametric test to analyse this variable. The significance value for all tests was 5%.

The comparison of results for different clones was done graphically on transformed data. For each variable, the values of all treatments altogether had the mean subtracted and the result was divided by the standard deviation (Kissell and Poserina, 2017); that is, they were transformed to the standard normal distribution (mean = 0, standard deviation = 1). The standardised values were then plotted by treatment and presented together, allowing overall comparisons.

For the ratio between compressive strength and density at 12% MC, we calculated the specific strength and compared values with those of parent species grown in mature forests. We built linear regression models for the purpose of checking whether the wood's compressive strength could be predicted based on its density because the latter is simpler to obtain and the two parameters are strongly correlated (Armstrong et al., 1984). To compare the mechanical properties of wood from young eucalypts, we compared these models with models from the literature and data for mature eucalypts.

We applied a Pearson correlation test (a = 0.05) to assess the relationship between density and compressive strength at the clone level. All data analyses and graphs were carried out using the R software (R Development Core Team 2019).

In our experience in working with young *Eucalyptus* spp. wood, static bending strength has a weaker relationship with wood density than compression strength. A possible reason for this is that static bending is compound stress – in which compression, shear and tensile stresses occur (Gere and Goodno, 2008) – and other influences, rather than wood density, might be stronger in static bending than in compression. There was also a considerably larger amount of data available for various *Eucalyptus* spp. planted in Brazil related to compressive strength compared to that available for static bending. For the aforementioned reasons, we used

compression-test samples to conduct specific strength analysis at the sample level, while specific strength and stiffness on static bending were calculated with the averages for each clone.

2.3. Results and Discussion

2.3.1. Wood density and strength

The properties of the six bioenergy clones were significantly different, forming between three and four statistical groups for each property analysed (Figure 5). The highest values were from 31% to 50% greater than the lowest, indicating considerable differences between the clones.

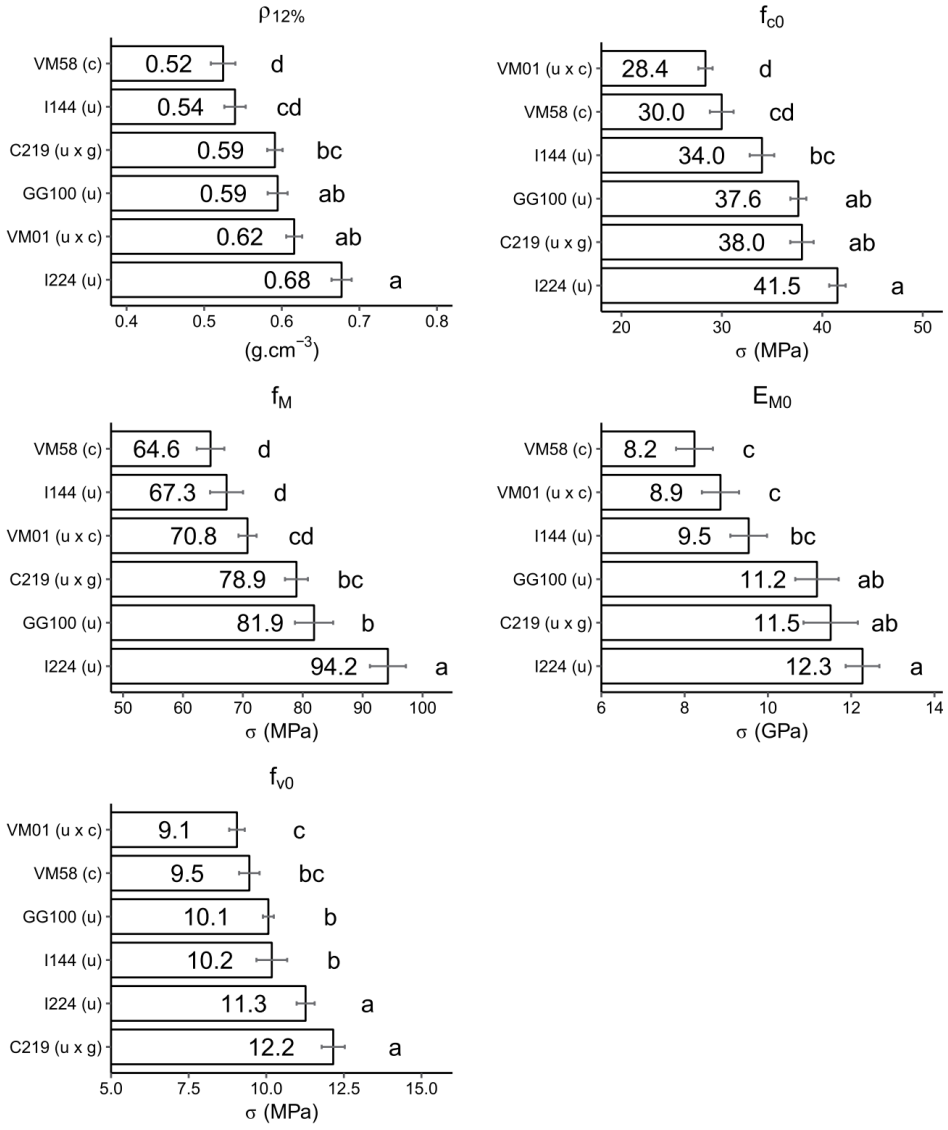

Figure 5. Wood properties with standard error bars. Different letters represent distinct statistical groups on the Tukey test (a = 0.05), except for f_{v0}, which was applied using a Kruskal-Wallis test.
$\varrho_{12\%}$ = density at 12% moisture content; f_{c0} = strength on compression parallel to grain; f_{v0} = strength on shear parallel to grain; f_M = strength on static bending; E_{M0} = stiffness on static bending.

I224 (u) had the densest wood and I144 (u) and VM58 (c) had the lowest densities. I224 also had, in general, the highest mechanical properties. Mechanical properties, however, were not necessarily proportional to wood density (Figure 6). For example, I144 was less dense than VM58 but had superior strength; VM01 (u × c) had the second-densest wood but always had mechanical properties among the lowest.

Young trees are constituted basically of juvenile wood, a tissue formed by the immature cambial meristem (Zobel and Sprague, 1998), with distinct characteristics from mature wood, such as lower density (Vaněrek et al., 2017). This is probably why the six clones had lower wood density than that reported for mature trees of the clones' parent species – *Eucalyptus urophylla* S.T.Blake, 0.739 g cm^{-3} (ABNT, 1997; Lahr et al., 2017); *E. grandis* 0.640 g cm^{-3} (ABNT, 1997); and *Eucalyptus camaldulensis* Dehnh., 0.899 g cm^{-3} (ABNT, 1997).

It is widely known that density has a strong positive influence on the mechanical properties of wood (Armstrong et al., 1984; Zhang, 1997; Kretschmann, 2010; Nickolas et al., 2020), but species, varieties and clones may not share the same relationship. I224 (u) had the highest density and mechanical properties, but VM01 (u × c) had the second-highest density but mechanical properties that were among the lowest (Figures 5 and 6). Other clones, such as C219 (u × g), GG100 (u) and I144 (u), had lower densities but their mechanical properties were proportionally low. VM58 (c), however, had low density and even lower mechanical properties.

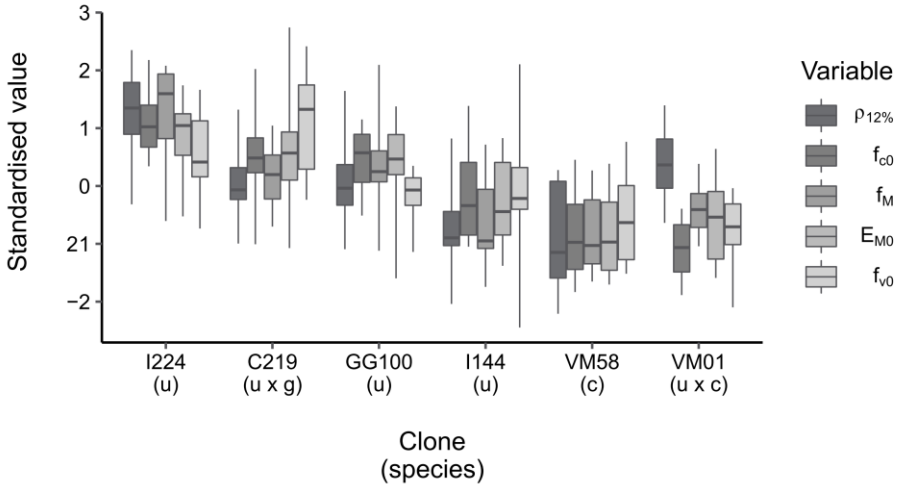

Figure 6. Standardised values for all variables.
$\rho_{12\%}$ = density at 12% moisture content; f_{c0} = strength on compression parallel to grain; f_{v0} = strength on shear parallel to grain; f_M = strength on static bending; E_{M0} = stiffness on static bending

2.3.2. Specific strength properties

The relationship of density to compressive strength showed a similar trend in all clones, apart from VM01 (u × c), the removal of which resulted in a much better coefficient of determination (Figure 7). At the clone level, only GG100 (u) and VM01 did not have a significant correlation between those variables, although P-values were close to the significance level adopted (Table 3). When analysing specific compression strength (the ratio between strength and density), three statistical groups were formed: C219 (u × g), GG100 (u), I144 (u), and I224 (u) with the highest averages; VM58 (c) in the intermediate group; and VM01 (u × c) with the lowest average. The four clones in the first group had the same specific strength as wood from mature trees (Figure 8) for their parent species. Even though we calculated specific strength on compression samples, approximately the same density–strength pattern was found for static bending (Figure 6). I144 was an exception; its specific bending strength (Table 4) was closer to

VM58 (c) than to the other clones in the same statistical group for specific compression strength. C219 (u × g), GG100 (u) and I224 (u) had not only the highest specific compression strength but also the highest specific bending strength and stiffness, and VM01 (u × c) had the lowest values for all three specific properties.

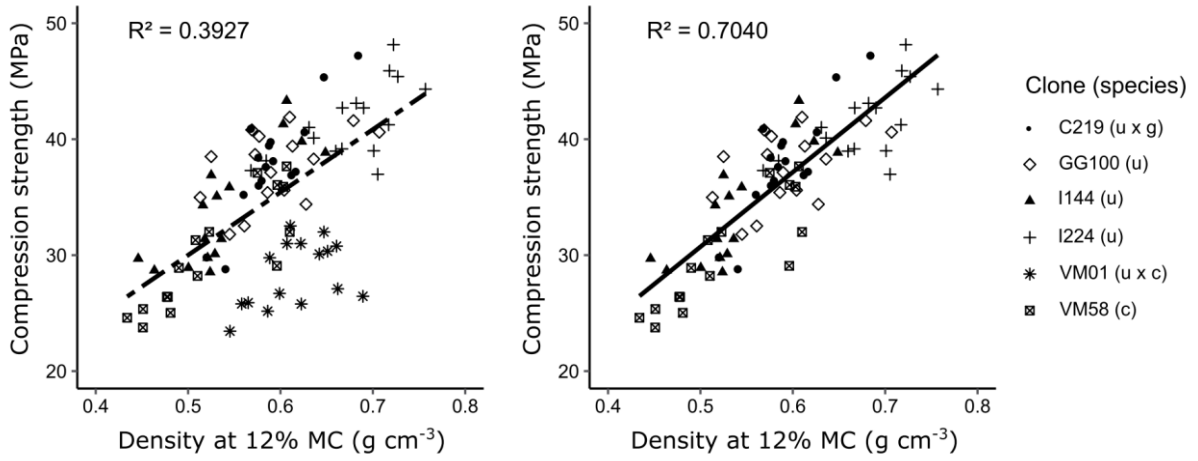

Figure 7. Linear modelling in two situations: model a - with all clones; model b - after removing VM01 from the analysis. $\rho_{12\%}$ = density at 12% moisture content, f_{c0} = strength on compression parallel to grain.
Model a – (all clones): f_{c0}= 54.1914*$\rho_{(12\%)}$+ 2.9079
Model b (excluding VM01): f_{c0}= 64.3564*$\rho_{(12\%)}$ - 1.4579

Table 3. Pearson correlation index between compressive strength and density, and its respective p-value. Bold values represent significant correlations at α= 0.05.

Clone	r	p-value
C219 (u x g)	0.866	0.000014
GG100 (u)	0.470	0.066454
I144 (u)	0.823	0.000090
I224 (u)	0.637	0.007985
VM01 (u x c)	0.454	0.076990
VM58 (c)	0.863	0.000017

VM01 (u × c) and VM58 (c) had the lowest mechanical properties of all six clones (Figures 5 and 6) and also the lowest specific strength and stiffness; VM01 was inferior to VM58 (Figure 8). Curiously, these two clones are pure or hybrids of *E. camaldulensis*. This species usually has denser wood than *E. grandis* and *E. urophylla* but a lower strength-toweight ratio. Specific compression strength was around 63 MNm kg^{-1} in mature planted *E. grandis* (ABNT, 1997) and *E. urophylla* (ABNT, 1997; Lahr et al., 2017), compared with 53.4 MNm kg^{-1} for mature planted *E. camaldulensis* (ABNT, 1997). In native forests, both species have higher specific compression strengths (Bolza and Kloot, 1963), and *E. camaldulensis* (63.2 MNm kg^{-1}) also has lower specific strength than *E. grandis* (83.1 MNm kg^{-1}). As well as its clones, *E. camaldulensis* wood from natural forests has lower specific strength and stiffness on static bending compared with *E. grandis* (Table 4), so lower specific properties might be characteristic of the species.

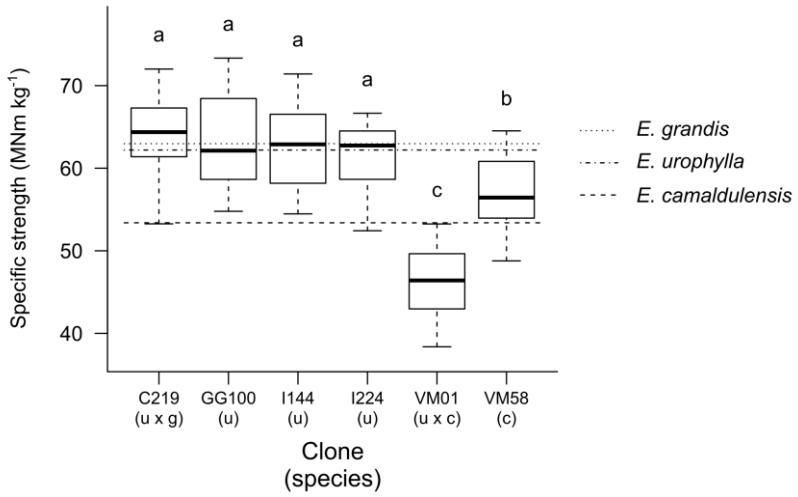

Figure 8. Specific strength in compression parallel to the grain. The same letters mean no difference has been found using the Tukey test (a = 0.05). Source: *Eucalyptus grandis* – ABNT (1997); *Eucalyptus urophylla* – ABNT (1997) and Lahr et al. (2017); *Eucalyptus camaldulensis* – ABNT (1997).

Eucalyptus camaldulensis and its hybrids have many silvicultural advantages, such as drought tolerance (Hakamada et al., 2020), the capacity to thrive in poor soil, slight resistance to frost, and flood tolerance (Martins et al., 2002). Due to its lower specific strength and stiffness compared with *E. grandis* and *E. urophylla*, however, *E. camaldulensis* may be less suitable for timber production, even though it has dense, redcoloured wood, as commonly reported in the literature (Bolza and Kloot, 1963; Hillis, 1984; ABNT, 1997).

Table 4. Wood density at 12% MC ($\rho_{12\%}$), specific bending strength and stiffness of the clones evaluated and two parental species from native forests.

Clone/Species	$\rho_{12\%}$ (g.cm^{-3})	spec. strength (MNm.kg^{-1})	spec. stiffness (GNm.kg^{-1})
C219 (u x g)	0.591	133.55	19.47
GG100 (u)	0.595	137.71	18.80
I144 (u)	0.540	124.66	17.67
I224 (u)	0.677	139.16	18.13
VM01 (u x c)	0.616	114.90	14.38
VM58 (c)	0.524	123.20	15.71
E. camaldulensis(1)	0.894	113.37	12.49
E. grandis(1)	0.804	148.36	19.55

(1) Bolza & Kloot (1963)

The differences we observed in specific properties are a consequence of the complex wood structure (Dinwoodie, 1975) and may not have a single reason. Fibre wall thickness is usually associated with wood strength and stiffness but, because it is the main anatomical feature driving wood density (Zieminska et al., 2013), it probably does not fully explain our results. Although lignin content plays a major role in compression (Gindl and Teischinger, 2002; Horváth et al., 2010), microfibril angle (MFA) has strong influences on bending stiffness (Yang and Evans, 2003; Takahashi et al., 2021) and strength (Yang and Evans, 2003), as well as on compression strength (Gindl and Teischinger, 2002; Vaněrek et al., 2017). Although increased MFA is usually associated with juvenile wood (Zobel and Sprague, 1998), *E. camaldulensis* wood might have a higher MFA than other *Eucalyptus* spp., and this could explain

the lower specific strength and stiffness observed here and in previous studies (Bolza and Kloot, 1963; ABNT, 1997). Another possibility is that *E. camaldulensis* has a lower amount of crystalline cellulose than other eucalypts. Ordered areas give higher mechanical properties to fibrous materials (Drożdżek et al., 2014), and wood bending stiffness has been reported to be correlated with cellulose crystallinity (Fujimoto et al., 2007).

2.3.3. Modelling strength properties

Wood density is one of the main criteria for the selection of clones for charcoal production (Ramos et al., 2019), but it is not as reliable when the goal is selecting genetic material for timber. To build an adequate model to predict compressive strength based on density at 12% MC (Figure 7), it was necessary to remove the VM01 (u × c) clone from the data; this created two models – model a (with all clones) and model b (with VM01 removed).

Applying both built models to the wood data of 17 species of mature planted eucalypts in Brazil (Figure 9), model b generated more approximate values than model a, with the sum of squared errors equalling 913 and 1253, respectively. Model b also had a lower sum of squared errors than a model built for 174 tree species native to Australia (Armstrong et al., 1984). Model a had a worse fit than the model from Armstrong et al. (1984), where the sum of squared errors was 1037. The relationship between compressive strength and density in mature wood from planted forests is much closer to wood from native forests than to juvenile wood (Balboni et al., 2020). It was unexpected, therefore, that a model built with young trees fitted the data from mature trees better than a model for native forests.

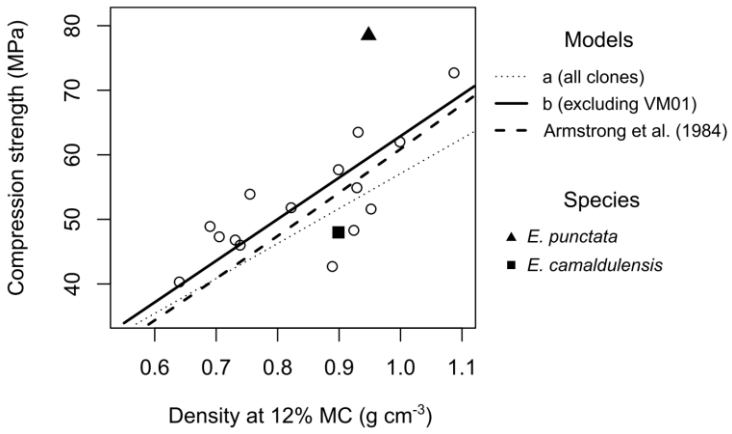

Figure 9. Relationship between compressive strength and density at 12% moisture content of 17 planted *Eucalyptus* species in Brazil. Source: ABNT (1997).

A generic model to predict compression strength parallel to grain would be very useful for the selection of eucalypt genetic material for timber production because density can be measured rapidly and does not require expensive equipment (Nickolas et al., 2020). However, the existence of genetic material with different strength–density ratios makes generic models unreliable for genetic selection. The clone VM01 (u × c) is an example of a variety in which wood density is high but strength is low. Hence, the genetic selection of wood by density alone might result in material with low quality for solid wood products because one of the greatest advantages of wood for many applications is its good strength-to-weight ratio (Ramage et al., 2017).

Some species of eucalypts behave differently from the modelled curve. *Eucalyptus camaldulensis*, along with three other species (*Eucalyptus maidenii* F.Muell., *Eucalyptus propinqua* H.Deane & Maiden and *Eucalyptus umbra* R.T.Baker), fell below the curve, meaning they have lower specific strength. Thus, they might not be good genetic material when the main objective of selection is to produce timber.

Eucalyptus punctata DC., on the other hand, has a higher specific strength (82.8 MNm kg^{-1}) and lies above the modelled curve. Not much information was found in the researched literature on this species regarding its cultivation or wood properties. However, *E. punctata* is considered a highly durable timber (Rudman and Da Costa, 1961), and there are reports of *E. punctata* plantations where its DBH was only inferior to some provenances of fast-growing species such as *E. grandis*, *E. urophylla* and *Eucalyptus saligna* Sm. (Dianese et al., 1984). In Nigeria, it was reported that a plantation of *E. punctata* suffered from dieback at the age of eight years, but the authors associated this condition with a probable boron deficiency (Adegbehin, 1983).

Eucalyptus punctata is from the subgenus *Symphyomyrtus* (Nicolle and Jones 2018), as are *E. grandis*, *E. urophylla* and *E. camaldulensis*. These species are grown in monospecific plantations or are used for compound hybrids. Hence, combining *E. grandis* or *E. urophylla's* fast growth with the high strength and good durability of *E. punctata* might produce genetic material with superior properties for timber. *Eucalyptus longirostrata* (Blakely) L.A.S.Johnson & K.D.Hill, previously a subspecies of *E. punctata* (Henson et al. 2008), easily hybridises with *E. grandis* and *E. urophylla* (Gardner et al., 2007), so breeding the aforementioned hybrid seems plausible. A fast-growing clone with a high strength-to-weight ratio and in-ground durability would have an advantage over available genetic materials, especially if it produces wood with the same strength and stiffness as mature trees but over a shorter rotation.

2.3.4. Suitability of clones for manufacture of timber and wood composites

The clone I224 (u) had the highest density, with equivalent mechanical properties except for shear strength, which was the second-highest. Despite its lower age, the wood properties of this clone were similar to those of a 17-year-old stand of *E. grandis* (Cademartori et al. 2014); commercial Amazon woods *Vochysia* spp., *Couratari* spp. (IPT 2020); and 21-year-old *Hevea brasiliensis* (Willd. ex A.Juss.) Müll.Arg. (planted), considered to have interesting properties for glued-laminated timber (glulam) production (Parra-Serrano et al., 2018). Hence, I224 has potential for use in engineered wood products with structural proposes, such as glulam beams and columns and crosslaminated timber. Although, among the clones analysed, it had the densest wood, I224 is within the acceptable threshold density of 0.7−0.8 g cm^{-3}, beyond which adhesive bonding starts becoming inefficient (Frihart and Hunt 2010).

I144 (u), however, had the lowest wood density, and it may be suitable for glued wood products for which a lighter material is desired. Edge-glued panels made with I144 wood could be a potential substitute for pine wood products and used for furniture, doors, windows and door frames, etc. Its mechanical properties were similar to those of some commercial timbers described in the literature, such as *Pinus elliottii* Engelm. and *Cedrelinga cateniformis* Ducke (Ducke) (IPT 2020).

The light wood-frame building system is under expansion in Brazil (Sotsek and Santos, 2018); although its use is not widespread, this system is starting to be adopted for new construction to replace masonry buildings. The associated future increase in timber demand, together with a lack of expansion of pine (*Pinus* spp.) plantations (IBA 2020), will result in the need for alternative timber sources. If a solution from planted forests is not presented, the industry will start looking towards native forests, which, in the current global situation, is arguably undesirable.

Among the six clones, I144 is the best candidate as a substitute for pine wood, especially due to its low density and good compression specific strength. Because its specific strength and stiffness in static bending were lower than for the other *E. urophylla* and *E. urophylla* × *E. grandis* clones (C219, GG100, and I224), I144 wood would be best suited to columns and wall frames rather than beams.

The properties of C219 (u × g) and GG100 (u) were similar, and the two clones were part of the same statistical group for all properties except shear strength. C219 had the highest shear strength among all clones, which can be useful for some products, such as short beams and some types of roof truss connections. C219 and GG100 had intermediate properties between I224 and I144 and could have similar applications, although their density differences should be considered. When thinking about light buildings, C219 and GG100 are probably the best options for glulam beams because they have the lightest wood among the three clones with higher specific bending strength and stiffness.

Both clones whose parental species is *E. camaldulensis* had lower specific strength in compression and static bending, as well as specific bending stiffness. As a result, they would require a higher amount of mass than other clones to support the same load. Timber from VM01 (u × c) and VM58 (c) would be less suitable for structures and would probably be better destined for other uses, such as bioenergy (the end use for which they were originally selected).

The lower mechanical properties in relation to wood from mature forests observed in the six clones are probably due to their lower density combined with juvenile-wood features. Although specific strength was lower than for native wood, it was similar to mature *Eucalyptus* spp. wood. We evaluated wood properties from tangential boards, which were free of material close to the pith; more significant reductions in wood properties might have occurred in samples located next to the pith.

Even if the mechanical properties of timber from shortrotation forests are lower than those of mature wood, the timber may still be suitable for conversion into composites. With glulam, a greater area can compensate for lower compressive strength and stiffness, and a larger beam height can compensate for lower flexural properties. Through the second moment of area (Equation 1), beam height influences flexural stiffness to the third power. The addition of extra lamellas brings considerable structural gains to glulam beams, possibly supporting the adoption of wood from young forests for structural purposes, even from those clones with lower moduli of elasticity.

$$I = \frac{w\,h^3}{12} \qquad (1)$$

I – second moment of area,

w – beam width;

h – beam height.

The considerable recent development of spindleless and centreless veneer lathes allows the peeling of small-diameter logs (McGavin et al., 2013), so these clones can also be adopted for the production of plywood and laminated veneer lumber. Peeling small logs results in higher recovery than sawmilling (McGavin and Leggate, 2019) and can generate products suitable for structural purposes (Hopewell et al., 2008). There are also reports that *Eucalyptus* spp. wood is suitable for the production of oriented strand-board (OSB) (Iwakiri et al. ,2008; Da Rosa et al., 2017), and our results could help the selection of clones for this objective. The clones with lighter wood and higher specific bending strength and stiffness would be better suited for manufacturing plywood and OSB, especially

if the goal is to substitute pine wood, the main raw material used for plywood in Brazil and the only one used for OSB.

Young, productive, high-quality plantations growing specific clones could increase the use of eucalypts by the timber industry and shorten rotation lengths. With that, timber sources could be located closer to consumer markets, and products from planted forests could replace those from native forests, potentially reducing deforestation. These short-rotation forests for timber products have requirements that are distinct from young bioenergy forests and mature sawnwood forests-high productivity must be accompanied by straight trees, the wood of which meets the demands of the timber industry. Proper forest management must accompany the selection of suitable clones, and the interaction of these two factors in the use of wood by the timber industry must be evaluated.

Many other characteristics need to be assessed to select the best clones for solid wood products. In this paper, we have evaluated the mechanical properties of clear wood, but wood from young trees has strength-reducing characteristics, such as knots and drying defects (Derikvand et al., 2018). Because of their small size (Crafford and Wessles, 2016), knots in young *Eucalyptus* spp. trees are not considered to have major effects on the mechanical properties of timber of structural sizes (Nocetti et al., 2017; Pagel et al., 2020). This characteristic favours the use of young trees for engineered wood products because removing all knots and fingerjointing timber pieces would not be economically viable (Derikvand et al., 2017). However, the effect of knots on the mechanical properties of timber of different dimensions should be investigated. Also, it is important to understand the effect of these knots on gluing and adhesion properties because they may influence grain angles and the properties of adjacent wood. In addition, their high extractives content might reduce glue-bond performance (Davis, 1997).

Growth stress should also be assessed because this affects yield and timber quality during primary processing (Gril et al., 2017). Small-diameter logs usually have lower yields (McGavin and Leggate, 2019), but these smaller dimensions allow the adoption of twin-blade sawing, which minimises the effects of growth stresses and is a fast primary-processing technique (Washusen, 2013). Drying defects are frequent in eucalypts due to their low wood permeability and high shrinkage rate (Vermaas, 1995), so wood behaviour during seasoning is another important feature for selecting suitable clones for timber production.

2.4. Conclusion

Although all six clones evaluated had the same increment rate and were developed for bioenergy purposes, they have wood with considerably different densities and mechanical properties. Each clone has different potential applications, which is beneficial for the timber industry because it provides more options for the selection of raw material according to the final intended use. Our results indicate which clones have the potential to substitute for pine wood, to be used in glulam, and those clones whose wood is better destined for their original purpose (bioenergy). A better understanding of the clones' wood properties and ease of processing (e.g. number and size of knots, growth stress levels, and drying behaviour) may help minimise future shortages of timber in Brazil resulting from a lack of expansion of pine plantations and an increase in the adoption of light wood-frame building systems.

Density should not be the only indicative property for breeding trees when the goal is timber production because some species and clones have lower mechanical properties for the same density value; such was the case for both clones whose parent species was *E. camaldulensis*. The reason why *E. camaldulensis* has lower specific properties should be investigated; it might be related to the high specific compression strength found in *E. punctata* wood. This information could be valuable, not only for the development of varieties and clones for timber production but also

for a better understanding of how some timbers are more mechanically efficient than others. If a higher cellulose crystallinity, as hypothesised, is responsible for differences in specific properties, *E. punctata* might be a good source of cellulosic nanofibre, a product that is attracting attention.

Acknowledgments

We thank 'Fazenda Dourada' and its staff for all the support with the study, Ms. Laís Muniz for the great help with the manufacture of the map, and anonymous reviewers, the comments of whom greatly improved this paper.

References

ABNT 1997. Projetos de estruturas de madeira – NBR 7190. Rio de Janeiro (Brazil): Associação Brasileira De Normas Técnicas; p. 107. Portuguese.

Adegbehin JO. 1983. A preliminary survey of growth of Eucalyptus species in the Sudan and Guinea zones and montane areas of Nigeria. International Tree Crops Journal. 2(3–4):273–289. doi:10.1080/ 01435698.1983.9752761.

Andrade TCGR, Barros NF, Dias LE, Azevedo MIR. 2013. Biomass yield and calorific value of six clonal stands of Eucalyptus urophylla S.T.Blake cultivated in Northeastern Brazil. Cerne. 19(3):467–472. doi:10.1590/ S0104-77602013000300014.

Armstrong JP, Skaar C, Zeeuwde C. 1984. The effect of specific gravity on some mechanical properties of some world woods. Wood Science and Technology. 18:137–146. ASTM. 2014. Standard test methods for small clear specimens of timber – D143. West Conshohocken (PA): ASTM International; p. 31.

Balboni BM, Batista AS, Rodrigues RA, Garcia JN. 2020. Relationship between strength and density in juvenile and mature Eucalyptus sp. wood. Brazilian Journal of Animal and Environmental Research. 3(3):983–991. doi:10.34188/bjaerv3n3-019.

Bolza E, Kloot NH. 1963. The mechanical properties of 174 Australian timbers. Melbourne (Australia): Division of Forest Products, CSIRO. Technological Paper No. 25.

Cademartori PHG, Missio AL, Gatto DA, Beltrame R. 2014. Prediction of the modulus of elasticity of Eucalyptus grandis through two nondestructive techniques. Floresta e Ambiente. 21(3):369–375. doi:10.1590/ 2179-8087.042313.

Crafford PL, Wessels CB. 2016. The potential of young, green fingerjointed Eucalyptus grandis lumber for roof truss manufacturing. Southern Forests. 78(1):61–71.

Da Rosa TS, Trianoski R, Iwakiri S, Bonduelle GM, de Souza HP. 2017. Utilização de Cinco Espécies de Eucalyptus para a Produção de Painéis OSB. Floresta e Ambiente. 24:e20160049. Portuguese. Davis G. 1997. The performance of adhesive systems for structural timbers. International Journal of Adhesion and Adhesives. 17 (3):247–255. doi:10.1016/S0143-7496(97)00010-9.

Derikvand M, Kotlarewski N, Lee M, Jiao H, Chan A, Nolan G. 2018. Visual stress grading of fibre-managed plantation Eucalypt timber for structural building applications. Construction and Building Materials. 167:688–699. doi:10.1016/j.conbuildmat.2018.02.090.

Derikvand M, Kotlarewski N, Lee M, Jiao H, Nolan G. 2020. Flexural and visual characteristics of fibre-managed plantation Eucalyptus globulus timber. Wood Material Science & Engineering. 15(3):172–181. doi:10.1080/17480272.2018.1542618.

Derikvand M, Nolan G, Jiao H, Kotlarewski N. 2017. What to do with structurally low-grade wood from Australia's plantation eucalyptus; Building application? BioResources. 12(1):4–7. Dianese JG, Haridasan MA, Moraes TS. 1984. Tolerance to "Mal do Rio Doce", a major disease of Eucalyptus in Brazil. Tropical Pest Management. 30(3):247–252. doi:10.1080/09670878409370890.

Dinwoodie JM. 1975. Timber – a review of the structure-mechanical property relationship. Journal of Microscopy. 104(1):3–32. doi:10.1111/j.1365-2818.1975.tb04002.x.

Drożdżek M, Zawadzki J, Zielenkiewicz T, Kłosińska T, Gawron J, Golofit T, Borysiak S. 2014. The influence of method of cellulose isolation from wood on the degree and index of crystallinity. Wood Research. 60 (2):255–262.

Dufourny A, Van De Steene L, Humbert G, Guibal D, Martin L, Blin J. 2019. Influence of pyrolysis conditions and the nature of the wood on the quality of charcoal as a reducing agent. Journal of Analytical and Applied Pyrolysis. 137:1–13. doi:10.1016/j.jaap.2018.10.013.

Frihart CR, Hunt CG. 2010. Adhesives with wood materials: bond formation and performance. In: Centennial, editor. General technical report FPL; GTR-190. Wood handbook: wood as an engineering material: chapter 10. Madison (WI): US Department of Agriculture, Forest Service, Forest Products Laboratory; p. 10.1–10.24.

Fujimoto T, Yamamoto H, Tsuchikawa S. 2007. Estimation of wood stiffness and strength properties of hybrid larch by near-infrared spectroscopy. Applied Spectroscopy. 61(8):882–888. doi:10.1366/000370207781540150.

Gardner RAW, Little KM, Arbuthnot A. 2007. Wood and fibre productivity potential of promising new eucalypt species for coastal Zululand, South Africa. Australian Forestry. 70(1):37–47. doi:10.1080/ 00049158.2007.10676261.

Gava JL, Gonçalves JLM. 2008. Soil attributes and wood quality for pulp production in plantations of Eucalyptus grandis clone. Scientia Agricola. 65(3):306–313. doi:10.1590/S0103-90162008000 300011.

Gere JM, Goodno BJ. 2008. Mechanics of materials. 6th ed. New York (NY): McGraw-Hill. Gindl W, Teischinger A. 2002. Axial compression strength of Norway spruce related to structural variability and lignin content. Composites Part A: Applied Science and Manufacturing. 33 (12):1623–1628. doi:10.1016/S1359-835X(02)00182-3.

Gonçalves JLM, Alvares CA, Higa AR, Silva LD, Alfenas AC, Stahl J, Ferraz SFB, Lima WP, Brancalion PHS, Hubner A, et al. 2013. Integrating genetic and silvicultural strategies to minimize abiotic and biotic constraints in Brazilian eucalypt plantations. Forest Ecology and Management. 301:6–27. doi:10.1016/j.foreco.2012.12.030.

Gril J, Jullien D, Bardet S, Yamamoto H. 2017. Tree growth stress and related problems. Journal of Wood Science. 63:411–432. doi:10.1007/s10086-017- 1639-y.

Hakamada RE, Hubbard RM, Moreira GG, Stape JL, Campos O, Ferraz SFB. 2020. Influence of stand density on growth and water use efficiency in Eucalyptus clones. Forest Ecology and Management. 466:1–8. doi:10.1016/j.foreco.2020.118125.

Henson M, Smith H, Boyton S. 2008. Eucalyptus longirostrata: a potential species for Australia's tougher sites? New Zealand Journal of Forestry Science. 38(1):227–238.

Hillis W. 1984. Wood quality and utilization. In: Hillis WE, Brown AC, editors. Eucalypts for wood production. Orlando (FL): Academic Press.

Hopewell GP, Atyeo WJ, McGavin RL. 2008. The veneer and plywood potential of tropical plantation eucalypts in North Queensland: 19- year-old Gympie messmate, Eucalyptus cloeziana, and 15-year-old red mahogany Eucalyptus pellita. Melbourne (Australia): Forestry and Wood Products Australia.

Horváth L, Peszlen I, Peralta P, Kasal B, Li L. 2010. Mechanical properties of genetically engineered young aspen with modified lignin content and/or structure. Wood and Fiber Science. 42(3):310–317.

IBA. 2020. 2020 Relatório Anual. São Paulo (Brazil): Indústria Brasileira de Árvores. Portuguese. Available from: https://iba.org/datafiles/publica coes/relatorios/relatorio-iba-2020.pdf

IBGE. 2021. Portal de Mapas. Rio de Janeiro Instituto (Brazil): Brasileiro de Geografia e Estatística. Portuguese. [accessed 2021 Mar 25]. Available from: https://portaldemapas.ibge.gov.br/portal.php IPT. 2020. Informações Sobre Madeiras. São Paulo (Brazil): Instituto de Pesquisas Tecnológicas. Portuguese. [accessed 2020 Jan 23]. Available from: https://www.ipt.br/consultas_online/informacoes_sobre_ madeira/busca

Iwakiri S, De Albuquerque CEC, Prata JG, Costa ACB. 2008. Utilização de madeiras de Eucalyptus grandis E Eucalyptus dunnii para produção de painéis de partículas orientadas – OSB. Ciênc Florestal. 18(2):265–270. Portuguese. doi:10.5902/19805098463.

Japarudin Y, Lapammu M, Alwi A, Warburton P, Macdonell P, Boden D, Brawner J, Brown M, Meder R. 2020. Growth performance of selected taxa as candidate species for productive tree plantations in Borneo. Australian Forestry. 83(1):29–38. doi:10.1080/00049158.2020.172 7181.

Kissell R, Poserina J. 2017. Chapter 4 – advanced math and statistics. In: Kissel R, Poserina J, editors. Optimal sports math, statistics, and fantasy. Cambridge (MA): Academic Press, Elsevier; p. 103–135.

Kretschmann DE. 2010. Mechanical properties of wood. In: Centennial, editor. General technical report FPL; GTR-190. Wood handbook: wood as an engineering material: chapter 5. Madison (WI): US Department of Agriculture, Forest Service, Forest Products Laboratory; p. 5.1–5.46.

Lahr FAR, Nogueira MCJA, Araujo VA, Vasconcelos JS, Christoforo AL. 2017. Physical-mechanical characterization of Eucalyptus urophylla wood. Engenharia Agrícola. 37(5):900–906.

Liao Y, Tu D, Zhou J, Zhou H, Yun H, Gu J, Hu C. 2017. Feasibility of manufacturing cross-laminated timber using fast-grown small diameter eucalyptus lumbers. Construction and Building Materials, 132:508–515.

Martins IS, Pires IE, Oliveira MC. 2002. Divergência genética em progênies de uma população de Eucalyptus camaldulensis DEHNH. Floresta e Ambiente. 9(1):81–89. Portuguese.

McGavin R, Bailleres H, Lane F, Blackburn D, Vega M, Ozarska B. 2013. Veneer recovery analysis of plantation eucalypt species using spindleless lathe technology. BioResources. 9(1):613–627. doi:10.15376/biores.9.1.613-627.

McGavin RL, Leggate W. 2019. Comparison of processing methods for small-diameter logs: sawing versus rotary peeling. BioResources. 14 (1):1545–1563.

Moutinho VHP, Tomazello M, Brito JO, Ballarin AW, Andrade FWC. 2016. Influence of the wood physical properties on the charcoal physical and mechanical properties. Scientia Forestalis. 44(111):557–561. doi:10.18671/scifor.v44n111.02.

Nickolas H, Williams D, Downes G, Harrison PA, Vaillancourt RE, Potts BM. 2020. Application of resistance drilling to genetic studies of growth, wood basic density and bark thickness in Eucalyptus globulus. Australian Forestry. 83(3):172–179. doi:10.1080/ 00049158.2020.1808276.

Nicolle D, Jones RC. 2018. A revised classification for the predominantly eastern Australian Eucalyptus subgenus Symphyomyrtus sections Maidenaria, Exsertaria, Latoangulatae and related smaller sections (Myrtaceae). Telopea. 21:129–145.

Nocetti M, Pröller M, Brunetti M, Dowse G, Wessels BC. 2017. Investigating the potential of strength grading green Eucalyptus grandis lumber using multi-sensor technology. BioResources. 12 (4):9273–9286.

Pagel CL, Lenner R, Wessels CB. 2020. Investigation into material resistance factors and properties of young, engineered Eucalyptus grandis timber. Construction and Building Materials. 230:1–10. doi:10.1016/j. conbuildmat.2019.117059.

Parra-Serrano LJ, Piva MEM, Cerchiari AMF, Lima IL, Garcia JN. 2018. Use of Hevea brasiliensis rubberwood for glulam beam production. Floresta e Ambiente. 25(2):1–7. doi:10.1590/2179-8087.038616.

Pereira BLC, Carvalho AMML, Oliveira AC, Santos LC, Carneiro ACO, Magalhães MA. 2016. Efeito da carbonização da madeira na estrutura anatômica e densidade do carvão vegetal de Eucalyptus. Ciênc Florestal. 26(2):545–557. Portuguese. doi:10.5902/1980509822755.

Queiroz MM, Arriel DAA, Filho AAT, de Oliveira OE, de Moraes PM, Skowronski L, Da Costa RB. 2019. Early selection in Eucalyptus camaldulensis Dehnh. progenies in Savanna. Brazil. African Journal of Biotechnology. 18(16):347–351. doi:10.5897/AJB2018.16729.

R Development Core Team. 2019. R: a language and environment for statistical computing. Vienna (Austria): R Foundation for Statistical Computing. Available from: http://www.r-project.org

Ramage MH, Burridge H, Wicher MB, Fereday G, Reynolds T, Shah DU, Wu G, Yu L, Fleming P, Tingley DD, et al. 2017. The wood from the trees: the use of timber in construction. Renewable and Sustainable Energy Reviews. 68(1):333–359. doi:10.1016/j.rser.2016.09.107.

Ramos DC, Carneiro ACO, Tangstad M, Saadieh R, Pereira BLC. 2019. Quality of wood and charcoal from Eucalyptus clones for metallurgical use. Floresta e Ambiente. 26(2):1–8. doi:10.1590/2179- 8087.043518.

Resende MDV, Resende MFR, Sansaloni CP, Petroli CD, Missiaggia AA, Aguiar AM, Abad JM, Takahashi EK, Rosado AM, Faria DA, et al. 2012. Genomic selection for growth and wood quality in Eucalyptus: capturing the missing heritability and accelerating breeding for complex traits in forest trees. New Phytologist. 194(1):116–128. doi:10.1111/j.1469- 8137.2011.04038.x.

Ribeiro-Oliveira JP, De Santana DG, Pereira VJ, dos Santos CM. 2018. Data transformation: an underestimated tool by inappropriate use. Acta Scientiarum – Agronomy. 40:e35300. doi:10.4025/actasciagron. v40i1.35300. RNC (National Registry of Cultivars). 2019. Portuguese. [accessed 2019 Nov 15]. Available from: http://sistemas.agricultura.gov.br/snpc/culti varweb/cultivares_registradas.php

Rudman P, Da Costa E. 1961. The cause of natural durability in timber, IV, Variation in the role of toxic extractives in the resistance of durable eucalypts to decay. Holzforschung. 15(1):10–15. doi:10.1515/ hfsg.1961.15.1.10.

Sotsek NC, Santos APL. 2018. Panorama do sistema construtivo light wood frame no Brasil. Ambiente Construído. 18(3):309–326. Portuguese. doi:10.1590/s1678-86212018000300283.

Takahashi Y, Ishiguri F, Aiso H, Takashima Y, Hiraoka Y, Iki T, Ohshima J, Iizuka K, Yokota S. 2021. Inheritance of static bending properties and classification of load-deflection curves in Cryptomeria japonica. Holzforschung. 75(2):105–113. doi:10.1515/hf-2019-0316.

Vaněrek J, Martinek R, Cada P, Kuklík P. 2017. The influence of microfibril angle on the wood stiffness parameters. Procedia Engineering. 195:259–264. doi:10.1016/j.proeng.2017.04.552.

Vermaas HF. 1995. Drying eucalypts for quality: material characteristics, pre-drying treatments, drying methods, schedules and optimization of drying quality. Suid-Afrikaanse Bosboutydskrif. 174:41–49.

Washusen R. 2013. Processing methods for production of solid wood products from plantation-grown Eucalyptus species of importance to Australia. Australian Government Department of Agriculture, Fisheries and Forestry. Melbourne (Australia): Forest and Wood Products Australia. Project No: PNB291-1112A.

Wessels CB, Nocetti M, Brunetti M, Crafford PL, Pröller M, Dugmore MK, Pagel C, Lenner R, Naghizadeh Z. 2020. Green-glued engineered products from fast growing Eucalyptus trees: a review. European Journal of Wood and Wood Products. 78:933–940. doi:10.1007/ s00107-020-01553-6.

Yang JL, Evans R. 2003. Prediction of MOE of eucalypt wood from microfibril angle and density. Holz als Roh und Werkst. 61:449–452. doi:10.1007/s00107-003-0424-3.

Zhang SY. 1997. Wood specific gravity-mechanical relationship at species level. Wood Science and Technology. 31:181–191. doi:10.1007/ BF00705884.

Zieminska K, Butler DW, Gleason SM, Wright IJ, Westoby M. 2013. Fibre wall and lumen fractions drive wood density variation across 24 Australian angiosperms. AoB Plants. 5:plt046. doi:10.1093/aobpla/plt046.

Zobel BJ, Sprague JR. 1998. Juvenile wood in forest trees. Berlin (Germany): Springer; p. 256.

3. A LENGTH-INDEPENDENT INDEX FOR TIMBER BOW AND SPRING VALIDATED ON *Eucalyptus grandis*

Bruno Monteiro Balboni[1,2], C. Brand Wessels[2] & José Nivaldo Garcia[1]

[1]Department of Forest Sciences, University of São Paulo, Piracicaba, Brazil;

[2]Department of Forest and Wood Science, Stellenbosch University, Stellenbosch, South Africa

https://doi.org/10.1080/17480272.2021.2010802

Abstract Warping is a frequently encountered defect in wood products which is evaluated in different ways by various sawn timber product standards. However, there are weaknesses in the current evaluation methods especially when comparing warp in different board lengths. The objective of the work described in this paper was to develop a theoretical model of bow and spring based on pure bending theory and to evaluate the model experimentally. A warp index was developed that allows comparison of bow and spring in timber boards independent of the length. The theoretical model was evaluated in experimental trials with *Eucalyptus grandis* of board warping caused by growth stress release as well as board warping caused by differences in longitudinal shrinkage after drying. The model explained the warping phenomenon well and the errors between theoretical and observed data were, on average, very small. The warp index developed allows assessment of bow and spring in any length, and might be useful with segregating portions of lower distortions for modern production systems of finger-jointed lamellas for engineered wood products, as well as for assessing growth stress levels, sawmilling processes and timber seasoning techniques.

Keywords Crook; distortion; board length; elastic line; pure bending; constant bending moment.

3.1. Introduction

Warping is considered as a big disadvantage of sawn timber compared to other materials (Johansson and Kliger, 2002). Bow and spring, where distortion is on the board face and edge respectively, can be caused by differences in longitudinal wood shrinkage (Shelly et al., 1979) as well as by the release of growth stresses (Chauhan and Entwistle, 2010, Gril et al., 2017). Measuring timber warping is not only useful for assessing timber quality but also for comparing wood drying processes (Tenorio et al., 2012), sawing techniques (Waugh and Northway, 2002) and for selecting genetic material (Schacht et al., 1998). Although warp generally refers to any distortion in timber including bow, spring, twist, and cup, in the work described below, the term warp will only refer to bow and spring.

Different proposals for measuring bow and spring can be found in timber standards throughout the world. In the European Standard EN 1309-3 (CEN, 2018), bow and spring assessment is made by measuring the maximum distortion within a two-meter long segment, regardless of the timber dimensions. The Australian Standard AS 4785.1 (Standards Australia 2002) provides maximum bow and spring values for distinct length and thickness dimensions, suggesting that bow and spring values for dimensions other than the provided ones should be calculated by interpolation and extrapolation. The Brazilian Standard NBR14806 (ABNT 2002), in turn, provides an index for bow and spring, calculated using Equation 2 below. The South African standard SANS 1783-2 (SANS 2012) has bow and spring limits established for each meter of a given length, following the same rationale as the Brazilian standard.

$$E = \frac{x}{L_1} \quad (2)$$

E is the spring or bow index, in mm/m

x is the deflection, in mm

L_1 is the timber length, in m

According to Garcia (1995), static bending and bow or spring from growth stresses show very similar behavior, although, while in the former distortion is caused by the application of stress, in the latter it is caused by stress release. Applying tensile stress is equivalent to the release of compression stress (and vice versa), which explains the generation of bending moment caused by the release of growth stress. Figure 10 presents a board (before sawmilling) kept straight by the tree through balanced growth stress distribution. The growth stress release was split in two displacement components and the effect of each one to the board is presented separately. While the release of one component results in elongation (or shortening) of the board, releasing the other causes bending, in this case, bow or spring.

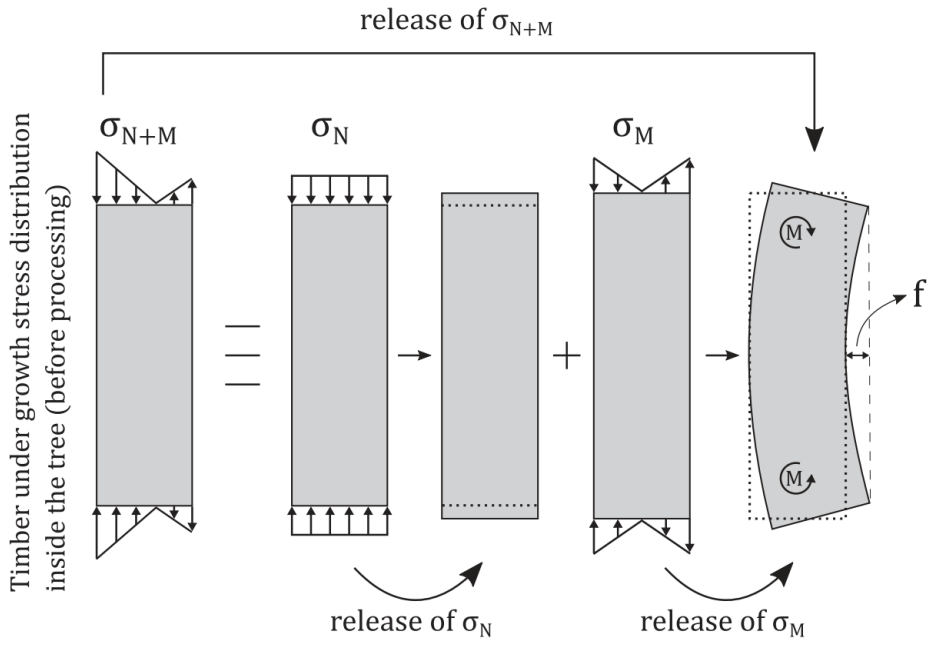

Figure 10. Growth stress release after primary processing. Growth stress distribution (σ_{N+M}) keeps the board straight inside the tree and was split in two components: N (normal) and M (bending). While the release of σ_N causes the elongation of the board, releasing σ_M results in warping (bow or spring) caused by bending moment (M).
Source: Adapted from Garcia (1995).

Bow and spring resulting from timber drying follows the same logic, but in this case, the differences of longitudinal shrinkage cause the bending moment (Gril et al., 2017). The longitudinal axis of a beam forms a circular curve under the action of bending stress (Gere and Goodno, 2008) and it can be represented by the arc of a circle (Figure 11) when assuming a small central angle. An arc of radius = R and length = L is formed by an angle, called 2α (Equation 3). In this case, Equation 4 describes the arc height (f), which can be interpreted as the distortion of a board of length L.

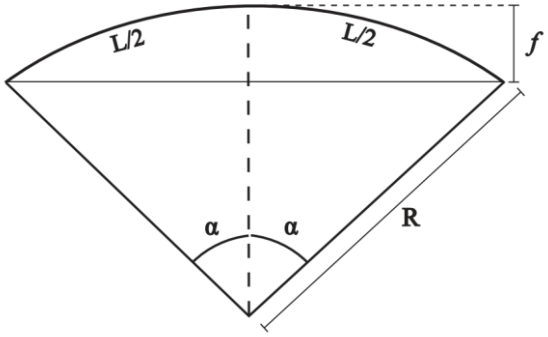

Figure 11. Arc of length *L* and central angle 2α, from a circumference of ray *R*, resulting in an arc of height *f*.

$$L = \frac{2\alpha\pi R}{180} \quad (3)$$

$$f = R - R\cos(\alpha) \quad (4)$$

Where:

L is the arc's length of a circumference segment of central angle 2α and radius *R*

α is the arc semi-angle, in degrees

R is the circumference radius

f is the height of a circumference arc of central angle 2α and radius *R*

When measuring the bow deflection of a warped timber board, we can define the value as f_1. If this same board is cut longitudinally in two halves, the half-board deflection value can be defined as f_2. Two arcs of the same circumference of radius *R*, mathematically differ solely by their length and central angle, which is *L* and 2α for the entire board; and is *L*/2 and α for the half-board.

Applying equations 3 and 4 to the example above, the full board length (L_1) would be $2\alpha\pi R/180$ and its deflection (f_1) will be $R - R\cos(\alpha)$. The half-board would have length (L_2) of $\alpha\pi R/180$ and deflection (f_2) of $R - R\cos(\alpha/2)$. The theoretical lengths L_1 and L_2 of the full and half-boards, respectively, are consistent, as L_1 is twice the value of L_2. For the Brazilian standard index to be appropriate and consistent with the theory as developed above, the deflection has to follow the same proportion: f_1/L_1 has to be equal to f_2/L_2. Replacing the theoretical length and deflection for both the full and the half-board into the Brazilian warp index (Equation 2), we obtain the expressions below:

full board warp index (f_1/L_1)

$$90.\frac{1-\cos(\alpha)}{\alpha\pi}$$

half-board warp index (f_2/L_2)

$$180.\frac{1-\cos(\alpha/2)}{\alpha\pi}$$

The fact that the two equations above do not return the same value, shows that the warp index as described in the Brazilian standard NBR14806 (ABNT 2002) is not appropriate to be used as a universal index for timber bow and spring. We are dealing with the same curvature, so the indexes should be the same for both boards. If an appropriate method is applied to assess the curvature of an entire board, the application of the method to both halves of the same board should result in similar values. If this is not true for the same board, it cannot be used to compare different boards, nor boards of different lengths, because it would underestimate the curvature of short boards, and overestimate it for long boards. Hence, even though the Brazilian Standard (and consequently the South

African standard, SANS 1783-2 2012) allows one to calculate warping for boards of any length, it provides a relationship between bow or spring and length that is mathematically inaccurate.

An index without the board length limitation would allow universal comparison of timber bow and spring as the log length used varies considerably in different markets. Measuring bow and spring within short lengths of a longer board would permit the evaluation of localized strong distortions (LSD), a feature only considered by the measurement of the greatest distortion along a 2m length, according to the European Standard EN 1309-3 (CEN 2018). This method, however, does not help to decide whether the LSD should be removed to generate a timber piece of higher quality (but of shorter length).

A better theoretical understanding of the phenomenon of bow and spring can potentially lead to ways of overcoming the limitations presented previously. The objective of the work described in this paper was to develop a theoretical model of bow and spring based on pure bending theory and to evaluate the model experimentally. We also propose a warp index that allows comparisons of timber boards independent of the length. We hypothesize that bow and spring can be explained by pure bending theory, which applies when an object is subjected to a constant bending moment. According to our hypothesis, in timber bow and spring, growth stress release or differences in longitudinal shrinkage generates a constant bending moment along a sawn timber board's longitudinal axis, resulting in bending with no shear stress involved.

3.2. Materials and Methods

3.2.1. Equation and index development

A parallel between bending a timber piece with imposed and released stresses was established (Garcia, 1995): the release of growth stress is treated as the application of opposite stress, i.e. released tensile stress was analogous to the application of compression stress and vice versa. The differential equation describing the displacement of an elastic line, Equation 5, was used as the starting point and has the small angle assumption. First of all, the differentials on Equation 5 were solved. Since we are considering a case of pure bending, M will be a constant along the board length. If Equation 5 is integrated twice it will result in Equation 6, which represents distortion (y) along the beam's length (z) with the origin of the z-axis located at the center of the beam's length (Figure 12).

$$\frac{d^2y}{dz^2} = -\frac{M}{EI} \tag{5}$$

Where:

y is the position on the vertical axis (or deflection)

z is the position on the horizontal axis

M is the bending moment

E is the modulus of elasticity

I is the second moment of area

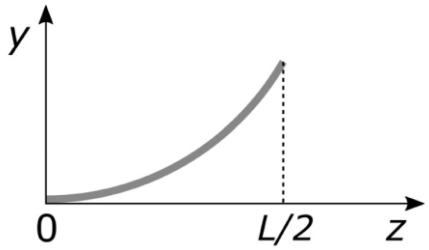

Figure 12. Relationship between y and z as given in Equation 5 with the origin of the z-axis located at the center of the beam's length.

Setting the boundary conditions $z = 0$, so $y = 0$, and then $C_2 = 0$. When $z = 0$, $dy/dz = 0$, so C_1 is also 0. We attributed a null value to both integration constants, and obtained Equation 7. At point z where $= L/2$, displacement perpendicular to the main axis is at a maximum, so y represents the deflection (f). From that, we obtained equation 8.

$$\frac{EI}{M}y = \frac{z^2}{2} + C_1\, z + \, C_2 \tag{6}$$

$$y = \frac{M}{2EI}z^2 \tag{7}$$

$$f = \frac{M}{8EI}L^2 \tag{8}$$

Where:

C_1 is the integration constant 1

C_2 is the integration constant 2

f is the board deflection

L is the length at which f is measured

If we are evaluating deflections of the same board at different lengths, the bending moment (M), the modulus of elasticity (E) and the second moment of area (I) have the same values. From that, $M/8EI$ can be considered a constant k. Two deflections of the same board, f_1 and f_2, measured at different points (at the center of the measured section), L_1 and L_2, follow the same equation: $f_j = kL_j^2$. Isolating k and matching the equations for $j = 1$ and $j = 2$, we got Equation 9, which was first proposed in Garcia (1992).

$$\frac{f_1}{(L_1)^2} = \frac{f_2}{(L_2)^2} \tag{9}$$

Where:

L_1 is the length at which f_1 was measured

f_1 is the distortion measured in L_1

L_2 is the length at which f_2 was measured

f_2 is the distortion measured in L_2

As our objective was the proposal of a universal index of deflection for any length, we have standardized the deflection for $L_1 = 1$ (dimensionless). The formulae used to calculate the index is shown in Equation 10. The

unit for the developed index is, then, mm/m², so the deflection of a specific board can be obtained by multiplying the index by its squared length. However, if one prefers, the unit mm/m can be adopted as the deflection index (f_i), which is equivalent to a deflection of a one-meter-length board.

$$f_i = \frac{f}{L^2} \quad (10)$$

Where:

f_i is the bow or spring index

L is the length used for the deflection measurement

f is the measured deflection

3.2.2. Equation and index validation

We have done two experimental trials to validate the equation and the index using the species *Eucalyptus grandis* W. Hill ex Maiden. *Eucalyptus* is the most planted hardwood genus worldwide (Myburg et al. 2014) and is known for having high growth stresses (Murphy et al., 2005). As *E. grandis* is a model species for the genus (Mostert-O'Neill et al., 2020), we selected this species for our study.

Both warping due to growth stress release as well as caused by different longitudinal shrinkage were considered. As bow and spring have the same cause but in different planes on the board, our experiments were done measuring bow on boards. To evaluate bow due to growth stress release, we used *E. grandis* trees from a 20 years-old stand originally planted in with 3 x 2 m spacing and thinning of 50% of the trees after 6 years. The plantation was located at the municipality of Rio Claro, State of São Paulo, Brazil, and the trees' diameter at breast height (DBH) was 33.7 cm, ranging from 29.2 to 38.7 cm. For the bow caused by wood drying, we used trees from a seven-years-old *E. grandis* plantation managed for fiber production. The stand was located at the municipality of Itirapina, State of São Paulo, Brazil, where trees were spaced 3 x 2.5m and their DBH ranged from 13.5 to 21.8 cm (average = 16.3cm).

In the first trial (growth stress release), eighteen 3.5-meter-long logs from different trees of mature *E. grandis* were sawn to deliberately produce bowed tangential boards. The sawing strategy presented in Figure 13 was followed, producing two boards per log, 36 in total. The initial board length was 3,500 mm, but we discarded both ends, measuring 250 mm each, to avoid undesired influences of stress release resulting from the end splits. This experiment assumed a uniform bending moment along the board length, so we selected trees and logs of a cylindrical shape, and saw the boards parallel to the bark. We then obtained a uniform stress release along the board and virtually no residual growth stress, meeting the theoretical assumptions required for the subsequent analysis.

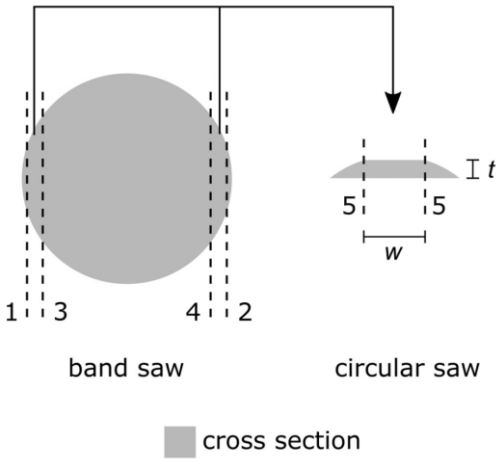

Figure 13. Sawing strategy adopted to avoid residual growth stress. Numbers indicate the sawing sequence; w = 50 mm and t = 25 mm.

We measured the deflection on the 36 boards (25 x 50 x 3,000 mm) at three different points between 1 - 2 m, 0.5 - 2.5 m, and 0 - 3 m, in the center, as shown in Figure 14. We calculated the indexes provided by NBR14806 (ABNT, 2002) and the one proposed in this study, for three different sizes on the 36 mature *E. grandis* boards. To check if the method influenced the calculation of each index, we used the Kruskal-Wallis test (a = 0.05) to compare means. We chose this non-parametric test as data did not present homoscedasticity or normal distribution of errors, even after mathematical transformations.

From the 36 boards mentioned above, twelve were selected from different trees and, using a digital caliper with a precision of 0.01 mm, we measured their deflection every 100 mm longitudinally, from z = 0 to z = 3,000 mm. After that, we assessed their modulus of elasticity in static bending (E_{M0}) according to the secondary method of the ASTM D143 standard (American Society for Testing and Materials, 2014), each board represented by 3 samples (25 x 25 x 410 mm) from both ends and from the center. The samples were bent in the same direction of distortion caused by growth stress release: rays were aligned parallel to the load direction. Both deflections and modulus of elasticity were assessed using wood in the green state (moisture content above the fiber saturation point) to avoid the influence of drying. With the E_{M0} values and Equation 5, we calculated the bending moment necessary to generate the observed deflection at $z = L/2$.

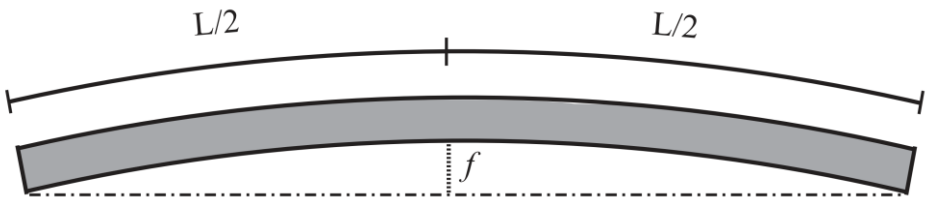

Figure 14. Deflection measurement (f) for a section of length L.

To understand if the bow and spring phenomenons, when isolated, can be explained by pure bending theory, we compared the observed deflection to the theoretical deflection curve caused by the bending moment calculated in each board. For that, the values were mathematically transformed to be equivalent to the observed deflection on the 3,000-mm-long boards: on the horizontal axis, z was substituted by z + 1,500 and, on the vertical axis, f was substituted by $max(f) - f$ (Figure 15). The difference between the elastic curve and the observed value (error) and the error divided by the elastic curve value (a proportional error) were calculated. The theoretical

deflection is symmetric from the center to the board ends, so we evaluated both errors considering the position in relation to the board end, resulting in the analysis of 24 half-boards.

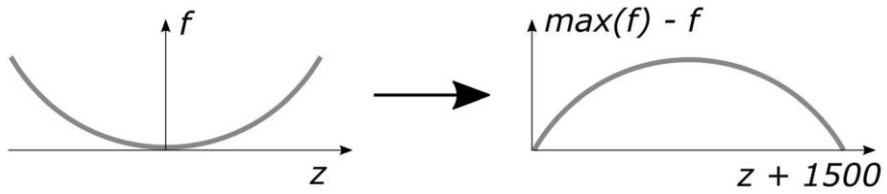

Figure 15. Mathematical conversion of the theoretical deflection.

To check if localized strong distortions (LSD) generated during wood drying followed the pure bending theory and if they could be evaluated using the index developed, we processed the young *E. grandis* logs into boards of 25 mm x 90 mm x 2,000 mm. Only straight logs were processed as it is a requirement of the sawmill, whose processing apparatus consisted of twin blades and multiple saws, both composed by circular blades. Green boards showing no visual localized distortion were stacked to dry until they reached moisture content in equilibrium with the environment. After drying, we selected 20 boards showing LSD, from different trees. We considered that a board had LSD when it showed a severe distortion compared to the other portions of the board, and with the LSD portion shorter than 1 m. However, the LSDs evaluated did not contain knots or other random defects: these types of defects were considered singularities on the mechanism of bow or spring, so the theory developed does not cover their influence.

We measured the distortions within LSDs. Since LSDs do not have the same length, we split every distortion in ten equal parts and measured at every tenth of its total length. As the deflection values were very small, we performed the measurements in digital images using the software ImageJ (Schneider et al., 2012). To avoid image distortions caused by the edge of the lens or perspective, the area of interest and the scale were kept in the very center of the camera during the shots, which were taken with the camera parallel to the timber distortion plane. The observed deflections were compared to the theoretical deflections as described for mature *E. grandis* boards (Figure 15).

To evaluate the effectiveness of the developed method for the assessment of warping in boards showing localized distortions, we compared it to current procedures. We measured the distortion of these 20 boards from young *E. grandis* in four different ways: i) according to the European Standard EN 1309-3 (CEN, 2018), ii) measuring the entire boards using the developed index, iii) measuring the portion within the LSD, and iv) measuring the portions out of the LSD. In methods i and ii, the distortion value for the entire board was a direct measurement. For the methods iii and iv, the value obtained from the measurement of a portion of the board was adjusted through the use of Equation 9 to obtain an equivalent value for the entire board. We converted the distortion values from methods iii and iv, as methods i and ii cannot be converted due to measurements not taken on the distortion center (assumption from Equation 7 to 8). We also used the Kruskal-Wallis test (a = 0.05) to compare the averages of these three distortion values for the same reasons explained previously. All the data analysis and plots were produced using the software R (R Development Core Team, 2020).

To calculate the load necessary to flatten a board, we applied Equation 11. We considered the distributed load that generates a certain deflection to be of the same value as the load necessary to flatten this deflection. The boards simulated were similar to those described earlier for mature *E. grandis*, but with a higher E_{M0} since we considered the boards to be flattened straight after reaching a lower moisture content.

$$f = \frac{5wL^4}{384EI} \quad (11)$$

Where:

w is the distributed load that generated deflection f

3.3. Results and Discussion

3.3.1. Index and equation development

The index provided by the Brazilian standard NBR14806 (ABNT, 2002) does not conform to the theoretical index derived in this study as described by Equation 9: distortion is not proportional to the length, it is proportional to the squared length. A similar relationship between bow or spring and length of measurement is found in the Uruguayan Standard UNIT1262 (UNIT, 2018), in which warping is measured similar to the European Standard EN 1309-3 (CEN, 2018). The former document does not explain how this relationship was obtained though, and its use is different to the one proposed here: an equation is provided to adjust the maximum deflection of shorter boards to a two-meter-long board. The deflection unit on both standards cited above is mm/2m. To avoid this non-standard unit (non-unitary unit in the denominator), we adjusted our index to one meter, i.e., it describes the deflection of bow or spring curves in a one-meter-long segment (Equation 10).

The theoretical assumption of the relationship from Equation 9 is that distortion is measured at the center, as it can be observed from the step that goes from Equation 7 to 8. Thus, caution is needed concerning the transformation of distortions not measured at the center of length assessed. The conversion provided by the standard UNIT1262 (UNIT, 2018) is an approximation and will surely work better when the length of measurement is as close as possible to two meters and the maximum distortion is closest to the center.

Since Equation 8 describes a parabolic curve, using segments that were not centered could also lead to mistakes, as the radius of curvature changes. However, the parabolic curve, when close to its vertex, is similar to a circular curve, which has the same curvature in all sections. This approximation is valid only when dealing with small arc angles, such as the deflections we observed – central angles were smaller than 0.07 radians in all observations. Thus, measuring deflections in sections not from the board center does not configure a problem, different from measuring deflections not in the section center.

3.3.2. Equation and index validations

The deflection of the mature *E. grandis* boards, their modulus of elasticity (E_{M0}), and the bending moment necessary to generate such deflection at the board center are shown in Table 5. In general, we found higher deflections on boards of lower E_{M0}, similar to what Raymond et al. (2004) found in one of the provenances analyzed in their study.

Two curves representative of the collected data are presented: Figure 16A, showing the best fit to the theoretical curve (lower sum of squared errors) among the samples analyzed, and Figure 16B, showing the worst fit. As the theoretical curve was calculated to deliberately match the observed deflection on both board ends and at its center, the greater errors were found far from these positions (Figure 17A). Please note that deflection was zero at

both board ends and that similar length and deflection at board center are assumptions for the theoretical curve. The fit of the curve to the data was evaluated by the sum of squared errors. The average error along the z-axis was virtually null, meaning there was no difference between the observed deflection and the theoretical curve. The proportional error presented a trend: its average was higher where the theoretical deflection value was lower (Figure 17B), a clear association with the precision of the deflection measurement.

Table 5. Deflection, modulus of elasticity (E_{M0}) in the green state, and bending moment of the mature *E. grandis* boards evaluated. Values in parentheses represent standard deviation.

Board	Deflection at z = L/2 (mm)	EM0 (GPa)		Bending moment (N.m)
1	24.34	8.80	(0.606)	10.94
2	15.23	11.32	(0.557)	8.81
3	19.05	10.77	(0.641)	10.47
4	12.46	11.95	(0.244)	7.6
5	19.46	10.64	(0.478)	10.58
6	19.18	10.43	(0.800)	10.22
7	16.98	11.00	(0.537)	9.54
8	23.41	10.81	(0.354)	12.92
9	18.19	12.71	(0.786)	11.8
10	17.95	12.04	(1.205)	11.03
11	30.55	9.36	(0.882)	14.61
12	24.17	10.47	(0.735)	12.92

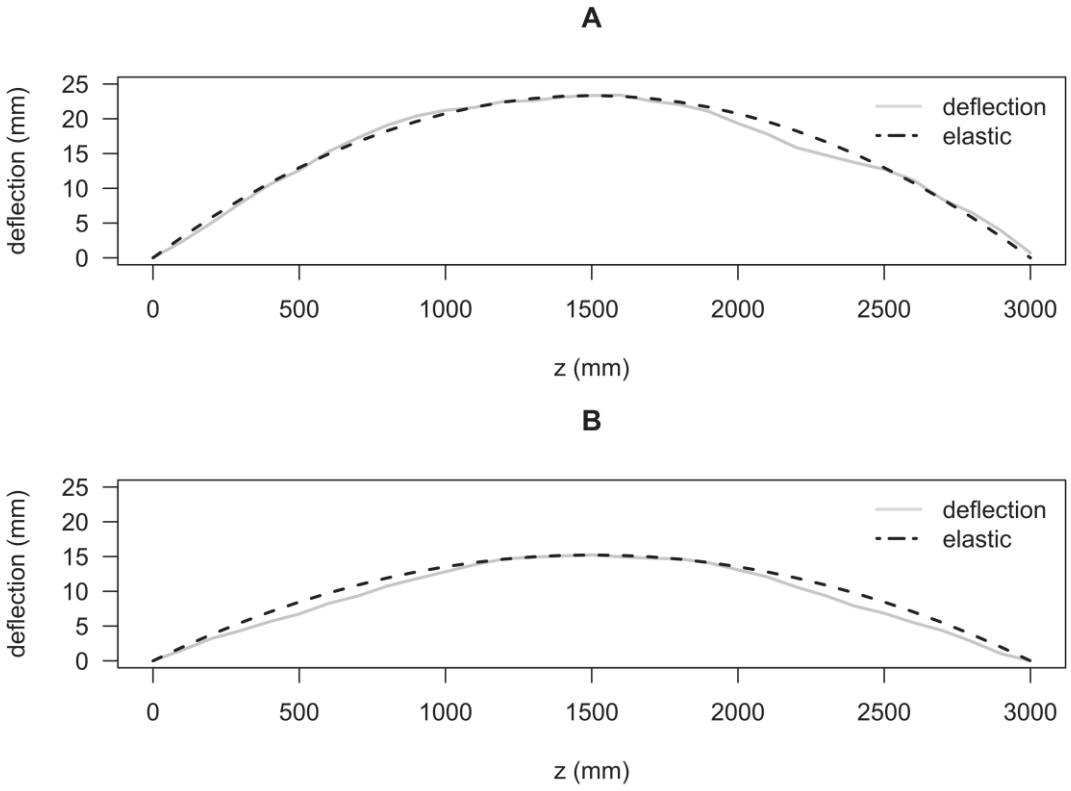

Figure 16. Observed deflection curve and theoretical elastic line curve along the length of green *E. grandis* boards 1 (A) and 2 (B).

Although we have selected cylindrical logs, they were part of living beings subjected to several genetic and environmental influences and, in practice, surely differ from a perfect cylinder. This fact adds variation not considered in the theory, which is based on parallel fiber direction along the entire board. The surface of boards processed in a band saw is not smooth, which probably influenced the measurements. Additionally, wood is known for not being a homogeneous material. Besides grain slope and surface roughness, variations on the modulus of elasticity and growth stress along the board probably added deviations from the theoretical deflection curve. With that in mind, we considered pure bending theory adequate to explain the warping phenomenon and to describe the deflection curve on boards after growth stress release, being the errors observed associated with timber heterogeneity.

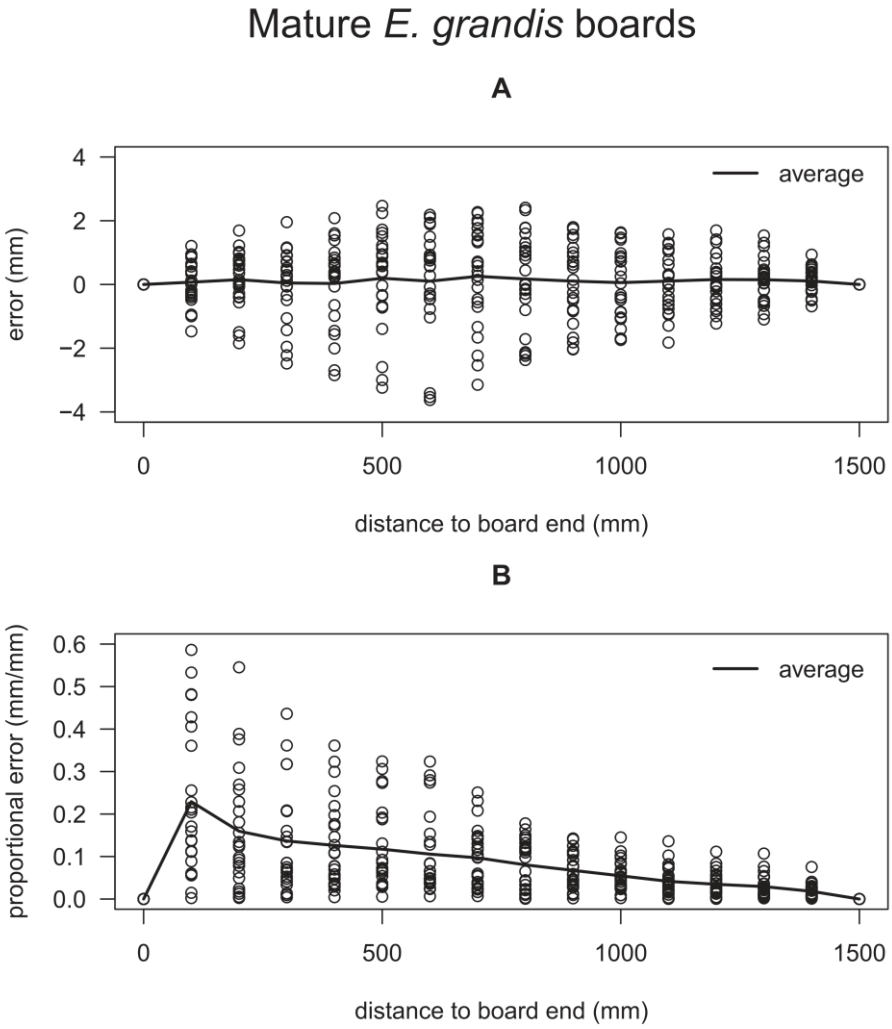

Figure 17. Error (A) and Proportional Error (B) of the observed deflection measured in mature *E. grandis* boards compared to the theoretical elastic curve measured in distinct positions in relation to the board ends.

Stress caused by differences in longitudinal shrinkage showed results similar to those caused by the release of growth stress. The localized distortions generated during wood drying followed the same pattern observed for distortion caused by growth stress release. Errors were greater in positions far from the LSD center and ends, but the average was virtually zero (Figure 18A), while proportional errors were greater where theoretical distortions were very small (Figure 18B). Thereby, LSDs followed the pure bending theory as well and the index proposed can be applied in the evaluation of such distortions.

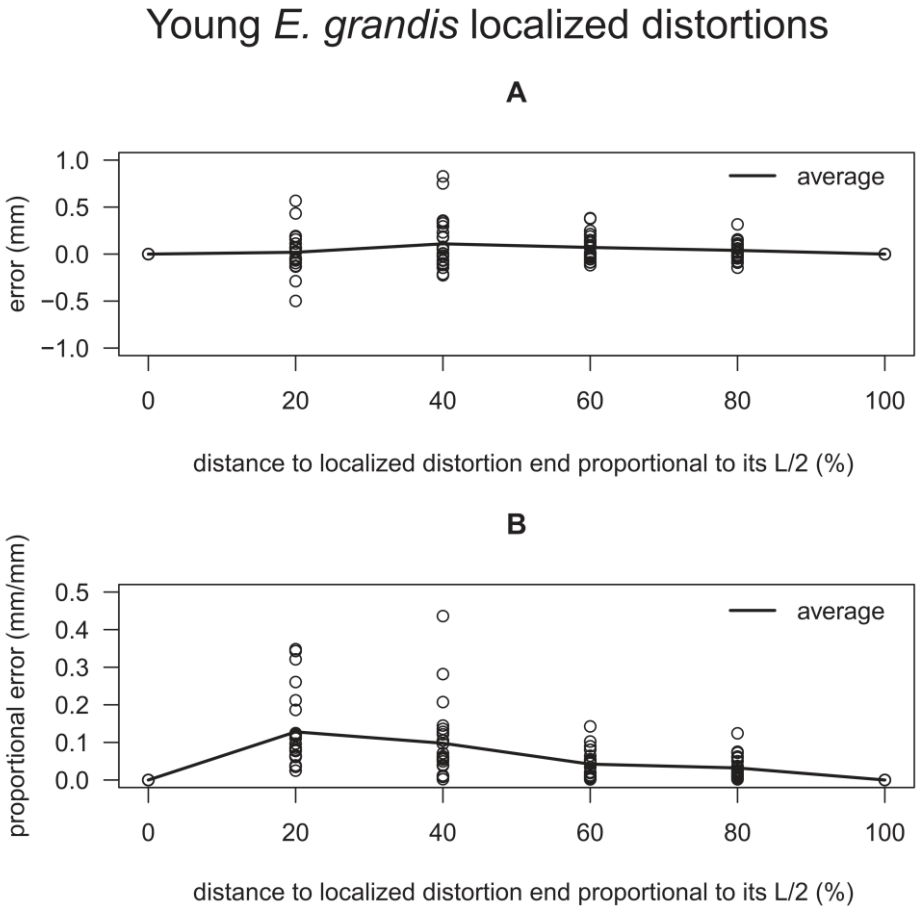

Figure 18. Error (A) and Proportional Error (B) of the observed deflection compared to the theoretical elastic curve in distinct positions (proportional to half of the LSD length) in relation to the board end of young *E. grandis* boards.

3.3.3. Index applications

The calculation of the index NBR14806 (ABNT, 2002) to assess bow resulted in different values when we performed repeated measurement of bow using sections of different sizes (length) of a given board. This problem would also occur if one followed the standard SANS1783-2 (2012), since it uses the same equations. On the other hand, the use of our method resulted in consistent index values regardless of the dimensions of the sections measured (Figure 19). This confirms the suitability of the developed equation and highlights the fact that distortion measurements can be done in portions of any length for timber pieces showing no LSDs.

Because deflections were small in 1 m-long boards (on average 2.39 mm), its measurement was less precise, which probably resulted in a slightly higher standard error (0.0215) when compared to 2 m- (0.0169) and 3 m-long boards (0.0149). We thus suggest the use of the longest possible sections for the measurement of deflection.

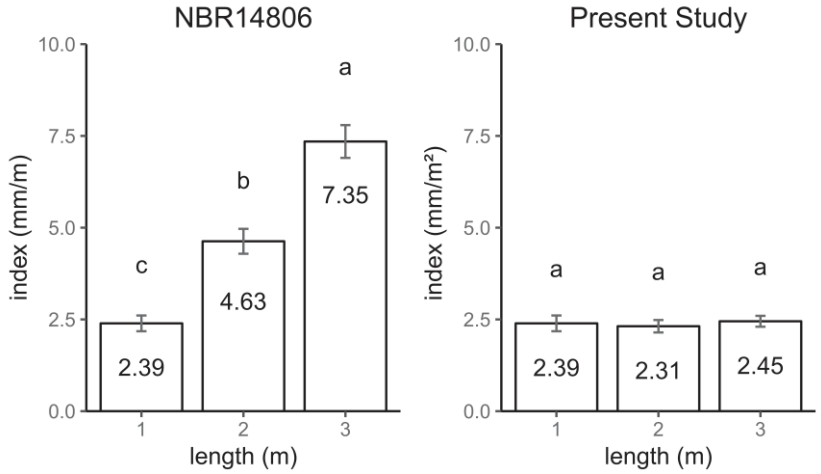

Figure 19. Indexes calculated using two methods, the Brazilian standard NBR14806 (left) and the one proposed by this study (right), measured on 36 timber boards using board sections of three different lengths. Different letters indicate differences in the Kruskal-Wallis test (a = 0.05).

By applying the proposed index to the permissible bow limits provided by the Australian Standard AS 4785.1 (Standards Australia 2002), we obtained the plots shown in Figure 20. The *y*-axis limits were changed for the distinct product classes and thicknesses to highlight the different index profiles. While 25-mm-thick strip flooring boards maintained almost the same warp index, 45 mm joinery boards did not. Joinery 15-mm thick and strip flooring 45-mm thick boards shared the same permissible bow profile, but the index was considerably different on boards of shorter lengths. It means that when a 2.4-meter-long board just below the permissible bow limit is cut in two halves, it produces two boards above the bow limits. On the other hand, the permissible values for 25 and 45-mm-thick joinery boards change differently: shorter boards have higher limits.

In general, thicker boards have lower permissible bow limits, which might be due to the higher difficulty in getting thicker boards flat. However, 1.2-meter-long 25- and 45-mm thick joinery boards have the same bow limit: 0.69444 mm/m. What one would expect is that permissible values are constant for different lengths but the same thickness, so that when boards are cut in halves or thirds, the limits should not change. The high limits for thick short boards might be because a very small deflection (about 1 mm) can be removed using a surface planer, which would not work for longer boards.

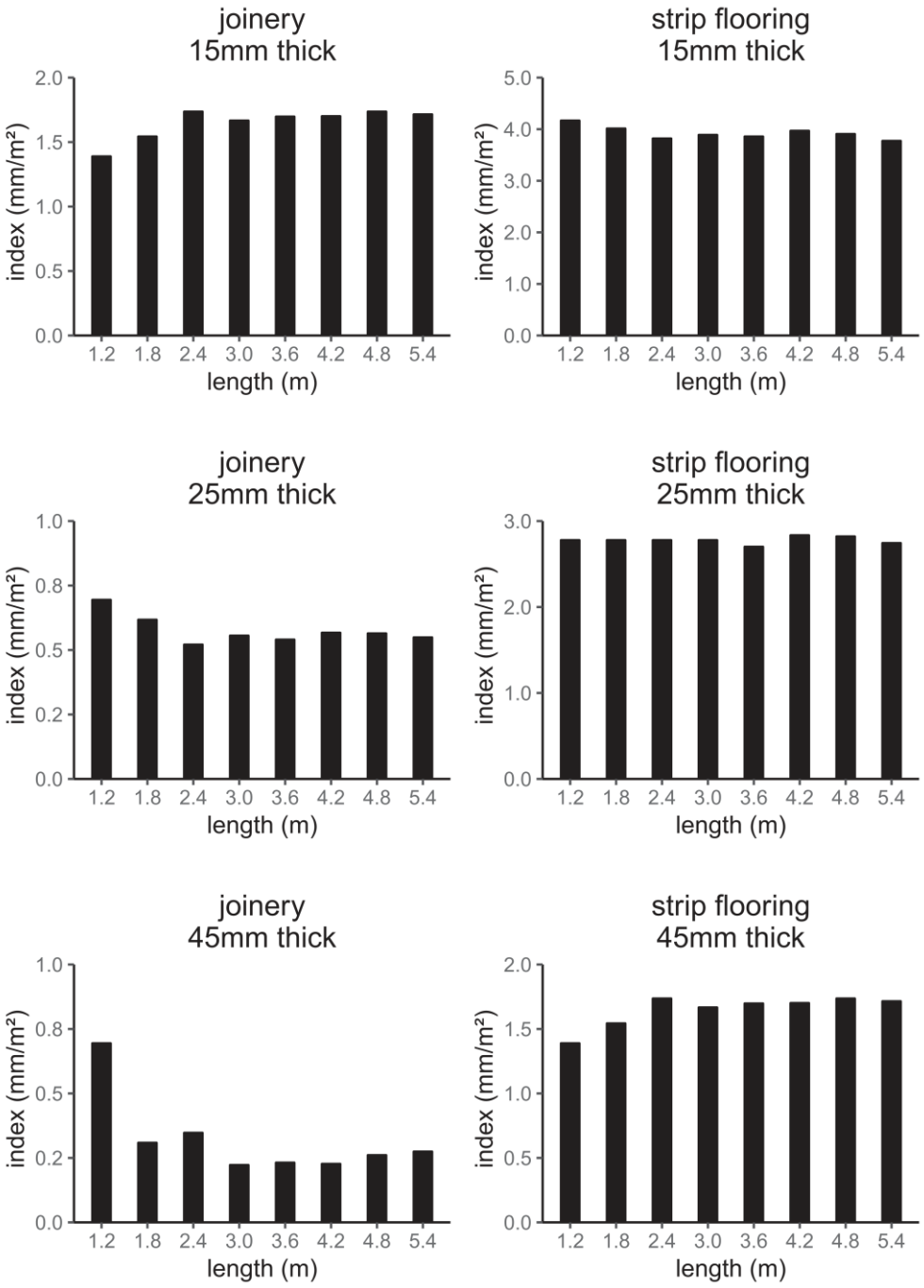

Figure 20. Proposed warping index calculated for the permissible bow deflection values proposed by the Australian Standard AS 4785.1.

Short boards, even with low deflection values, are harder to flatten with a distributed load compared to long boards of the same warp index. An advantage of the developed index is the relationship found between the length of boards of the same index and the distributed load necessary to make them flat. Looking at Table 6, board *a*2 is half of *a*1 in length (both with the same developed bow index) and the distributed load necessary to flat it's distortion is four times the value for *a*1. The board *a*3 has one third of *a*1 length and needs nine times the distributed load. When boards have the same developed bow index, the distributed load is inversely proportional to the squared ratio of their lengths. Board *b*2 also has half of *a*1 length and the same NBR 14806 index, but needs eight times more distributed load; and board *b*3, one third of *a*1 length, needs 27 times the load. In the case of the NBR 14806 index,

the distributed load seems to be inversely proportional to the cubic ratio of their lengths, but it only happens for specific developed index ratios – boards *c*2 and *c*3 do not follow the pattern nor the ratio for distributed loads. Equation 12 shows the relationship of distributed loads necessary to flatten two boards when they have the same second moment of area and modulus of elasticity. The relationship described can be used by industries and companies for establishing their own bow and spring limits according to each distinct need.

Table 6. Distributed loads (according to Equation 11) necessary to flatten straight mature *E. grandis* boards. Boards *a*1, *a*2 and *a*3 have the same developed bow index, while boards *b*2 and *b*3 have the same NBR 14806 bow index as *a*1; boards *c*2 and *c*3 have shorter lengths than *a*1 and indexes with ratios different than 1/2 or 1/3. The E_{M0} adopted was 15 GPa, thickness = 25 mm, width = 50 mm.

board	length (m)	bow deflection (mm)	index (mm/m²)	NBR index (mm/m)	distributed load (N/m)
a1	3.0	22.500	2.50	7.50	20.833
a2	1.5	5.625	2.50	3.75	83.333
a3	1.0	2.500	2.50	2.50	187.500
b2	1.5	11.250	5.00	7.50	166.667
b3	1.0	7.500	7.50	7.50	562.538
c2	1.5	9.750	4.33	6.50	144.444
c3	1.2	5.700	3.96	4.75	206.177

$$\frac{w_2}{w_1} = \left(\frac{L_2}{L_1}\right)^{-2} \left(\frac{f_{i_2}}{f_{i_1}}\right) \quad (12)$$

Where:

w_i is the distributed load to flatten a board with deflection f_i straight when boards 1 and 2 have the same second moment of area and modulus of elasticity

A board showing a localized distortion, when sectioned transversally, generates pieces of distinct warp indexes. Although the measurement of the maximum distortion in a two-meter-long section (CEN, 2018, UNIT, 2018) aims to consider the influence of LSDs on the timber distortion, its effectiveness is limited. When an LSD is outside the portion measured, it is not considered in the distortion value. In cases when the LSD is within the portion measured (Figure 21), the European Standard (CEN 2018) method does compute the LSD, returning distortion values 27% higher than those found when applying our method to the entire board. Nevertheless, distortions of the LSD zones are almost three times those obtained by the standard method, and the timber portions outside LSDs have distortions of about 50% the latter. Not only is the standard method closer to the distortion outside the LSD, but it also returns similar variances viz. 7.90 and 7.27, respectively, when compared to the LSD, 67.19; while for the developed method, the variance is slightly higher than the first two (13.16). The calculated index for the LSDs was, in average 5.75 mm/m², from 2.95 to 10.38 mm/m², considerably higher than the mature *E. grandis* boards, 2.38 mm/m² in average.

Amongst the 20 young *E. grandis* boards evaluated, three of them (15%) presented concavity of the LSD on one face, while for the portion outside the LSD it was on the opposite face. This is another limitation of the method described in the European Standard EN 1309-3 (CEN, 2018) to assess distortion on boards showing LSDs. Using the method proposed, both zones could be evaluated separately, with no concerns regarding distortion conversion, as LSDs do follow the theory presented.

Understanding whether LSDs should be removed is especially useful for the new generation of engineered wood products from young *Eucalyptus* plantations proposed by Derikvand et al. (2017). As these authors stated, grading standards are rigid and do not consider that timber boards can be used as components of engineered products. After the removal of the LSD portion of a board showing warping values above the limits, one might be able to produce timber of adequate quality to compose a finger-jointed lamella. For that, more than grading a whole board, it is essential to have a method such as the proposed index, which can evaluate distortion in portions of timber boards. Identifying low-warping portions in a high-warping board will certainly increase the yield of the conversion of rough sawn timber to lamellas. With the reduction in the volume of rejected timber, engineered wood products from young eucalyptus forests are one step closer to economic viability.

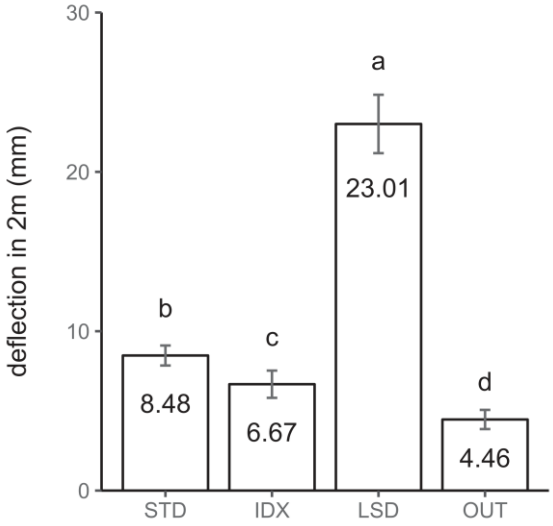

Figure 21. Deflections (means and standard error bars) measured according to the standard (STD) EN 1309-3 (CEN 2018), according to the developed index in the entire board (IDX), in the localized strong distortion (LSD) and outside the LSD (OUT). Both LSD and OUT distortion values were adjusted to values of a theoretical 2 m long board using equation 9.

A fourth example for which the application of the proposed method is useful can be found in Chauhan and Entwistle (2010). They presented a strong model ($R^2 = 0.92$) for predicting timber warping when a log showing growth stress is sawn longitudinally in two halves. When comparing the distortion on the bottom and upper logs, they found a considerable difference and attributed it to the position of the log in the trunk. The distortion measurement, called log opening, was performed slightly differently from what we did in this study. The two halves of the log were realigned together and the distance between them, at the ends, was measured, representing the sum of distortion of both half-logs. Applying our index to Chauhan and Entwistle's (2010) data after dividing it by 2, we obtained the results shown in Table 7. While the cited authors found a difference in distortion for both treatments, they would have probably concluded that both log positions had the same distortion values if they had used the proposed index, because it neutralizes the influence of log length – note the large difference in "distortion" between butt and upper logs compared to similar "warp index" values for the two logs in Table 7.

Table 7. Log opening values from Chauhan and Entwistle (2010) and distortion values used for calculating the proposed warp index.

	length (m)	log opening (mm)	distortion (mm)	warp index (mm/m^2)
butt log	1.3	19.05	9.53	5.64
upper log	2.0	47.29	23.65	5.91

Another example is found in Hornburg et al. (2012), where the authors compare bow and spring directly to other studies using distinct board lengths. Because they were following the equation from NBR 14806 (ABNT, 2002), they may have made imprecise analogies. This problem was avoided in another study from the same year, Souza et al. (2012). Indeed, they limited their comparison to the differences between treatments found by other authors and not the values themselves.

As we could observe, a better understanding of the warping phenomenon, generated by growth stress release or difference in longitudinal shrinkage, helped to reduce some limitations of grading timber showing bow or spring. The developed method allows the correct measurement of bow and spring in boards of any length, including the evaluation of distortion within timber boards. There is a limitation, though: the deflection has to be accessed in the warping center, as the development of the theory uses this assumption.

Knots and other features that may cause a stronger and more localized distortion then the LSDs presented in this study. As stated on the methodology section, our theory does not cover these elements, as they are points of heterogeneity. This limitation is not exclusive to our method since the current methodologies also lack a warping classification for such distortions. The index we developed provides, at least, a way to classify the portions before and after the knot distortion. Variations of width or thickness along the board may also bring a limitation to our method since it is a change on the second moment of area, which we considered to be constant along the board. But, this is another restriction also found in the current methodologies. It is important to highlight that the evaluation of a board's warping is commonly realized visually on the production line and needs to be fast and may configure a disadvantage of the proposed method for segregating board sections or short boards. The application of technology (laser scanners returning the ratio deflection by squared length) or training the staff (measurement always in a specific length) may be a solution for turning the application of the proposed index to a feasible option.

It is advisable for timber standards which indicate the measurement of maximum distortion using two-meters-long boards to have an additional method to evaluate shorter boards or localized distortions. The recent return of the global trend of using wood for construction is based on Mass timber systems (Mayencourt and Mueller, 2020), and classifying portions of timber boards gains even more relevance, so they can be used to compose these engineered products. The possibility of using finger jointed low-warping portions depends on our capacity to identify them within timber boards, and can increase the volume of sawn wood to be used in structures and buildings.

Regarding further developments, we consider it relevant to evaluate how wood properties influence the measured errors in each position, i.e., if measured deflection values are greater than theoretical ones because of a lower modulus of elasticity. After understanding the causes of deviations from the theory, it will be possible to calculate growth stress in trees. It is an alternative to the several available methods, generally based on the measurement of very small deformations on standing trees after stress release (Gril et al., 2017).

3.4. Conclusion

Pure bending theory (assuming a constant bending moment along the board) is adequate to describe the deflection curve of warping caused by growth stress release and by differences of longitudinal shrinkage during wood drying. Distortion is proportional to the squared length of its measurement, and this relationship has the theoretical assumption that distortion is assessed at the center. We suggest the addition of the proposed method on standards dealing with timber visual grade, especially to assess distortions within board sections. The developed method allows the classification of portions of timber boards according to their warping levels, which can be useful for selecting raw material for mass timber products. The proposed index also helps to calculate the increase of distributed load required, after cut to a different length, to flatten the board. Evaluations of growth stress for areas such as tree breeding, genetics, and sawmilling strategies can benefit as well since the index is independent of the length of boards.

Acknowledgements

We thank Dr. Gustavo Burin Ferreira for reviewing this manuscript and suggesting relevant modifications for its improvement.

Funding

This study was financed in part by the Coordenação de Aperfeiçoamento de Pessoal de Nível Superior – Brasil (CAPES).

References

ABNT. (2002). NBR 14806: Madeira serrada de eucalipto - Requisitos. Associação Brasileira de Normas Técnicas, Brasília, 11 pp.

American Society for Testing and Materials. (2014). ASTM D143 — standard test methods for small clear specimens of timber. ASTM International, West Conshohocken, PA

CEN (2018) EN 1309-3. Round and sawn timber - Methods of measurements - Part 3: Features and biological degradations; European Committee of Standardization (CEN): Brussels, Belgium, 2018.

Chauhan, S., Entwistle, K. (2010). Measurement of surface growth stress in Eucalyptus nitens Maiden by splitting a log along its axis. Holzforschung, 64: 267–272.

Derikvand, M., Nolan, G., Jiao, H., Kotlarewski, N. (2017). What to Do with Structurally Low-Grade Wood from Australia's Plantation Eucalyptus; Building Application ? BioResources, 12(1): 4–7.

Garcia, J. N. (1992). Estados de tensão em árvores e de deformação em peças de madeira serrada. Ph.D. Thesis. Universidade de São Paulo.

Garcia, J. N. (1995). Técnicas de desdobro de eucalipto. Seminário Internacional de Utilização da Madeira de Eucalipto para Serraria. Anals of the Seminário Internacional de Utilização da Madeira de Eucalipto para Serraria.

Gere, J. M., Goodno, B. J. (2008). Mechanics of Materials 7th Edition. Cengage Learning, 1022 pp.

Gril, J., Jullien, D., Bardet, S., Yamamoto, H. (2017). Tree growth stress and related problems. Journal of Wood Science, 63:411–432.

Hornburg, K. F., Eleotério, J. R., Bagattoli, T. R., Nicoletti, A. L. (2012). Qualidade das toras e da madeira serrada de seis espécies de eucalipto cultivadas no litoral de Santa Catarina. Scientia Forestalis, 40(96): 463-471.

Johansson, M., Kliger, R. (2002). Influence of material characteristics on warp in Norway spruce studs. Wood and Fiber Science, 34 (2): 325-336.

Mayencourt, P., Mueller, C. (2020). Hybrid analytical and computational optimization methodology for structural shaping: Material-efficient mass timber beams. Engineering Structures, 215, 110532.

Mostert-O'Neill, M. M., Reynolds, S. M., Acosta, J. J., Lee, D. J., Borevitz, J. O., Myburg, A. A. (2020). Genomic evidence of introgression and adaptation in a model subtropical tree species, Eucalyptus grandis. Molecular Ecology. doi:10.1111/mec.15615

Murphy, T. N., Henson, M., Vanclay, J. K. (2005). Growth stress in Eucalyptus dunnii. Australian Forestry, 68(2), 144–149. doi:10.1080/00049158.2005.10674958

Myburg, A., Grattapaglia, D., Tuskan, G. et al. The genome of Eucalyptus grandis. Nature 510, 356–362 (2014). https://doi.org/10.1038/nature13308

R Development Core Team. (2020) R: A Language and Environment for Statistical Computing Vienna, Austria R Foundation for Statistical Computing.

Raymond, C. A., Kube, P. D., Pinkard, L., Savage, L., Bradley, A. D. (2004). Evaluation of non-destructive methods of measuring growth stress in Eucalyptus globulus: relationships between strain, wood properties and stress, Forest Ecology and Management, 190(2–3): 187-200.

SANS - South African National Standard. (2012). Sawn softwood timber Part 2: Stress-graded structural timber andtimber for frame wall construction. Standards South Africa, Pretoria, 19 pp.

Schacht, L., Garcia, J. N., Vencovsky, R. (1998). Variação genética de indicadores de tensão de crescimento em clones de Eucalyptus urophylla. Genetic variation of growth stress indicators in clones of Eucalyptus urophylla. Scientia Forestalis, 54: 55–68.

Shelly, J. R., Arganbright, D. G., Birnbuch, M. (1979). Severe warp development in young-growth ponderosa pine studs. Wood and Fiber, 11(1): 50-56.

Schneider, C. A., Rasband, W. S., Eliceiri, K. W. (2012). NIH Image to ImageJ: 25 years of image analysis. Nature methods, 9 (7): 671-675.

Souza, J. T., Trevisan, R., Denardi, L., Stangerlin, D. M., Vivian, M. A., Haselein, C.R., Santini, E. J. (2012). Qualidade da madeira serrada proveniente de árvores dominantes e médias de Eucalyptus grandis submetidas à secagem. CERNE, 18(1): 167-174.

Standards Australia, 4785.1 (2002) Timber – Softwood – Sawn and Milled Products. Part 1: Product Specification. Standards Australia International, Sydney. 42 pp

Tenorio, C., Moya, R., Quesada-Pineda, H. J. (2012). Kiln drying of Acacia mangium wood: colour, shrinkage, warp, split and check in dried lumber. Journal of Tropical Forest Science 24(1): 125–139.

UNIT Instituto Uruguayo de Normas Técnicas. (2018). UNIT 1262:2018 Madera Aserrada de Uso Estructural – Casificación Visual – Madera de Eucalipto (Eucalyptus grandis) Montevideo, Uruguay.

Waugh, G., Northway, R. (2002). Best practice for sawing and drying plantation eucalypts for appearance grade products, Proceedings of the Forest Industry Engineering Association Wood Technology Clinic, Rotorua, New Zealand

4. INFLUENCE OF KNOTS ON THE ADHESION OF WOOD FROM YOUNG *Eucalyptus grandis*

Bruno Monteiro Balboni[1,2], C. Brand Wessels[2] & José Nivaldo Garcia[1]

[1]Department of Forest Sciences, University of São Paulo, Piracicaba, Brazil;

[2]Department of Forest and Wood Science, Stellenbosch University, Stellenbosch, South Africa

Abstract The structural use of wood from young *Eucalyptus grandis* trees requires the gluing of smaller pieces to form larger elements. Although knots do not reduce the wood mechanical properties in *Eucalyptus* timber of structural dimensions significantly, the influence of knots on wood adhesion has not been studied extensively. The objective of this study was to assess the relationship of knot features with the bond quality of face-glued wood from young *E. grandis* trees. Wood from a seven-year-old *E. grandis* stand was glued with a single component polyurethane adhesive for testing shear strength and wood failure percentage using paired specimens of knot-containing and clear wood samples. The size and position of the knots did not correlate with shear strength or wood failure percentage. Knot-containing samples had 5.8% lower percent of wood failure, but the same shear strength as that of clear wood samples. Below a wood density of 0.65 g cm^{-3}, clear and knot-containing wood behaved similarly, but above this value the adhesion of wood with knots was worse than that of clear samples. By simulating glued laminated timber beams composed of high-density specimens on the outer lamellas, we showed that shear stress on those glue lines is lower than the minimum shear strength observed on dense knot samples. Lower adhesion caused by knots on denser wood, probably do not represent a significant problem in the manufacture of glued laminated products from young *Eucalyptus grandis* trees.

Keywords Shear; wood density; wood failure; juvenile wood.

4.1. Introduction

Short forest rotations have the advantage of a faster investment return when compared to classic long rotation management regimes (Pleguezuelo et al., 2015). The practice of short rotation forestry is not new (Betters et al., 1991) and its increase has been driven by the pulp and paper and the reconstituted panel industries (FAO, 2009). In some cases, such as in Brazil, the bioenergy industry provided further impetus in the movement towards shorter rotations (Betters et al., 1991). A great variety of species have been tested and are used in different regions depending on the site conditions, with a clear preference for fast-growing trees, such as species from the genera *Eucalyptus*, *Acacia*, and *Populus* (Moya et al., 2019).

Besides providing fiber and biomass, recent studies have shown that wood from young *Eucalyptus* spp. plantations have potential to be used for cross laminated timber (Liao et al., 2017), glued laminated timber beams (Pagel et al., 2020) as well as for roof structures (Crafford & Wessels, 2016), a product already established on the South African market. There is, to the best of our knowledge, no genetic material developed for sawn timber production from short rotation *Eucalyptus*, so varieties developed for other end uses are being planted to provide wood for timber. We have recently identified some Brazilian bioenergy clones that are suitable for producing timber, based on their clear-wood properties (Balboni et al., 2021). Short rotation trees have different properties to mature trees including knot features (Derikvand et al., 2018), besides being composed mainly of juvenile wood, a material

with lower density and mechanical properties (Zobel & Sprague, 1998). The knot properties of softwoods, as commonly reported in the literature (Abbott & Whale, 1987; As et al., 2006; Wright et al., 2019), are different to those from young *Eucalyptus* spp. which are typically small (Crafford & Wessels, 2016) and were reported to not represent a major problem for timber of structural sizes (Nocetti et al., 2017; Pagel et al., 2020). Knots, however, can reduce wood adhesion strength due to different grain angles and higher extractive contents (Davis, 1997). As young trees have lower diameters and generate timber with small cross sections, gluing is a fundamental processing step to manufacture products with structural dimensions and the presence of knots might have implications on the use of wood from young forests.

Understanding how knots from young *Eucalyptus* spp. influence wood adhesion is essential for the manufacturing of engineered wood products such as glued laminated timber when using this wood source (Gaspar et al., 2015). Removing knots and finger jointing clear wood sections is an expensive process (Derikvand et al., 2017) which need to be minimised or avoided. The objective of this study was, therefore, to assess the relationship of the knot features with the bond quality of face-glued wood from young *E. grandis* trees. Additionally, we wanted to understand which knots reduce the bond strength of laminates and should be removed.

4.2. Materials and Methods

4.2.1. Material

A total of 45 bottom logs from different trees were randomly selected from a seven-year-old *Eucalyptus grandis* plantation (spacing 3 x 2 m) located in the municipality of Itirapina, State of São Paulo, Brazil. While the smaller diameter of the logs ranged from 13 to 22.5 cm (average = 15.73 cm), the larger diameter ranged from 13.6 to 25.7 cm (average = 17.26 cm). The logs, 2.2 meters in length, were then processed in a twin circular saw followed by a multiple circular saw, generating 25 x 90 x 2200 mm boards. All boards were labelled with their respective log number, and stacked for air drying. After reaching the moisture content (MC) in equilibrium with the environment, one board per log was selected. Boards with extreme drying defects, such as warping and splits, were avoided. The selected boards were processed in a circular saw to reduce their width to 55 mm and, subsequently, in a thicknesser planer to reach 20 mm thickness and prepare the surface for adhesion. About 48h after planing, each board was cut in half and glued with 200 g m^{-2} one-component polyurethane adhesive under a pressure of 0.7 MPa. From each of these glued samples two shear test specimens were produced, one containing a knot on only one face and another one free of knots (Figure 22). The two test specimens from the same board composed a pair of samples, and were analysed together. Knots were sampled with the aim to represent all size ranges and to establish the relationship between knot features and shear test results.

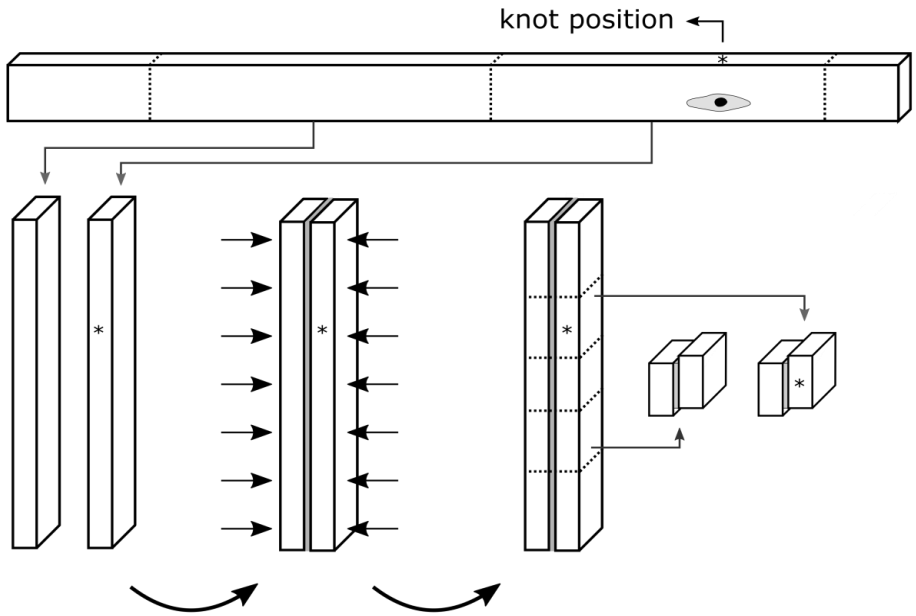

Figure 22. Sampling methodology to produce shear sample pairs of one knot containing sample and one clear sampling per laminate. Black arrows represent the load applied for the wood adhesion.

4.2.2. Knot features, wood density and shear test

Before timber was glued, each knot had a picture with scale taken, and the knot features were measured with the ImageJ software (Schneider et al., 2012). The features measured were: knot and wound wood area, as well as the distance between the knot's edge and the glued area edge in both directions, along with and across the wood grain (Figure 23).

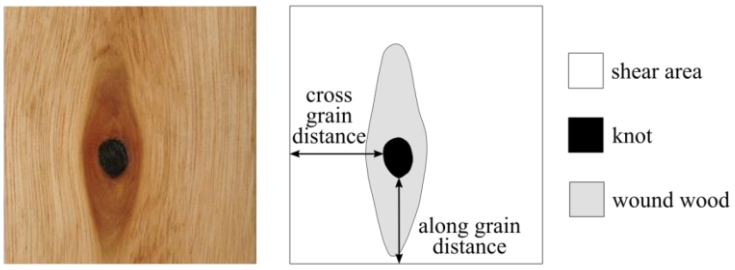

Figure 23. Knot features measurements.

The shear test was conducted following the ASTM D905 standard (ASTM, 2008), with a small adjustment on the glued shear area to turn it in a 50 x 50 mm square. All specimens were kept in an acclimatisation room at a temperature of 23°C and 65% air relative humidity until they stabilize their mass, meaning they reached the equilibrium MC around 12%. After the shear test, the percentage of wood failure was measured with the ImageJ software (Schneider et al., 2012). The wood density at 12% MC ($\rho_{12\%}$) was assessed on one clear solid wood specimen per sample pair by the gravimetric method: dimensions measured with a digital calliper (precision of 0.01 mm) and mass assessed in a semi-analytical digital scale (precision of 0.01 g). Two specimens were discarded, and consequently their pairs, as the rupture took place in a position which does not reflect the shear strength on the glue line.

4.2.3. Shear data analysis

The variations of shear strength (f_{v0g}) and percentage of wood failure (πf) within the paired specimens were calculated using Equation 13. In order to return negative variations when knot samples have lower values than clear wood samples, we multiplied the right side of the equation by -1.

$$var(x) = -100\frac{(x_{clear} - x_{knot})}{x_{clear}} \quad (13)$$

var(x) is the pair-wise variation of *x* in percentage;
x is the shear strength on the glue line or percentage of wood failure.

To test the hypothesis that knots decrease the shear strength, the one-sided paired T-test was applied, as the difference between the specimens pairs followed a normal distribution. For the pair wise difference of wood failure to achieve a normal distribution the data had to be transformed taking the squared root of these values. Normal distribution of the data was evaluated graphically, comparing the observed with the theoretical quantiles. We used linear models to test the relationship of the knot features with the shear strength and wood failure of the knot samples. The level of confidence of 95% was adopted for all statistical tests conducted.

In order to visualize how the high wood density is affecting the shear strength on the glue line, linear models were built removing the densest samples progressively. These models were built with knot-containing and clear samples separated and together. For the latter, four types of models (following Equation 14) were evaluated, where clear and knot samples have: i) the same a and b coefficients; ii) the same a and different b; iii) different a and the same b; iv) different a and b coefficients.

$$f_{v0g} = a + b(\rho_{12\%}) \quad (14)$$

f_{v0g} is the shear strength on the glue line;
$\rho_{12\%}$ is the wood density at 12% MC;
a is the linear coefficient;
b is the angular coefficient.

4.2.4. Static bending mechanical tests and theoretical beam simulations

From the same batch of timber, we produced 48 clear wood specimens and tested them in static bending, following the ASTM D143 standard (ASTM, 2014). We obtained the modulus of rupture (f_M), modulus of elasticity (E_{M0}) and density at 12% MC ($\rho_{12\%}$); the latter assessed by the gravimetric method. An adaptation on the dimension of the bending samples was necessary as timber boards were originally 25 mm thick and after planing were reduced to 22 mm. With that, we reduced the samples' cross sections dimensions to 20 x 20 mm, keeping the span to height ratio, thereby resulting in a distance between supports of 280 mm (Mack, 1979). The relationship between f_M and E_{M0} with wood density was assessed through linear regressions.

In order to estimate how our results affected glued laminated timber (glulam) beams with timber from young *Eucalyptus grandis*, we have done simulations (Figure 24) considering an extreme situation regarding shear stress: i) rupture occurs by shear and normal stresses simultaneously, ii) the maximum f_M value found on small clear specimens represents the beam flexural strength, as it would be the material composing the top and bottom lamellas,

and iii) the average f_{t0g} from clear samples represents the shear strength of the material from central lamellas, those with the lowest density. The glulam beams were simulated using the equations derived from the classical beam theory. We followed the Equation 15, provided by the ASTM D198 standard (ASTM, 1999) to simulate beams under four points bending tests that theoretically break by normal and tangential stresses simultaneously, adopting, for that, the span-to-height ratio described by the same standard cited above ($3f_M/4f_{t0}$). All theoretical beams were composed by 20-mm-thick lamellas, starting from 2 up to 15 lamellas. With the Equation 16 (Gere & Goodno, 2008), we calculated the shear stress which occurs on the glue line of the bottom lamella, and compared with the lowest f_{t0g} values found for knot and clear samples. Additional 60 boards were selected from the same batch of timber, from which we assessed their density (by the gravimetric method) and counted the number of knots. The influence of the number of knots on their density was analysed through linear regression.

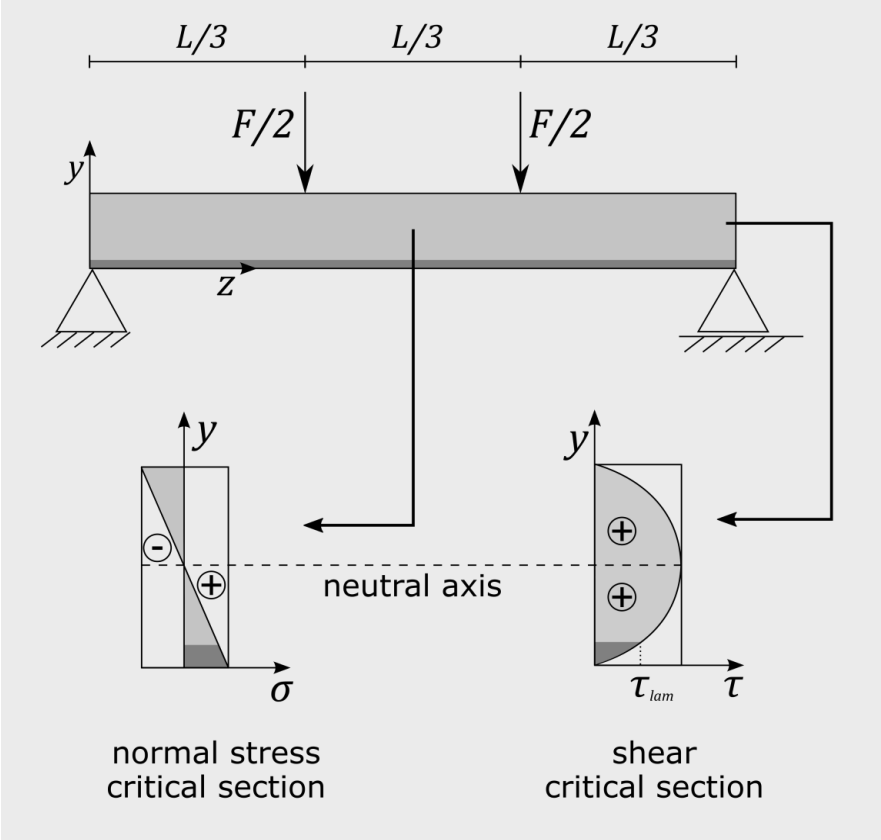

Figure 24. A beam with rectangular cross section under four points static bending (ASTM, 1999) and considering the linear normal stress (σ) distribution and parabolic tangential stress distribution (τ). F is the load applied to the beam, L is the span length, dark grey represents a lamella on the maximum tension zone and τ_{lam} is the shear stress on the glue line from the bottom lamella.

$$f_M = \frac{3Pa}{bh^2} \quad (15)$$

$$\tau = \frac{V}{2I}\left(\frac{h^2}{4} - y_1^2\right) \quad (16)$$

f_M is the modulus of rupture on static bending;

P is the load;

a is the distance from support to the nearest load-point ($L/3$);

b is the width of the cross section;

h is the depth of the beam;

τ is the shear stress

V is the shear force;

I is the second moment of area;

y_1 is the distance from the region of interest and the neutral axis.

4.3. Results and Discussion

Large variation was found for the knot features and can be related to the sampling strategy, which was designed to obtain the full range of knot sizes (Table 8). The coefficient of variation obtained for wood density was as expected from literature (Gomez & Gomez, 1984). Zziwa et al. (2017) found an average knot area in *E. grandis* equal to 436 mm², more than four times the knot area we observed. Although the cited authors did not provide the age of the sampled trees, we believe the higher knot area was probably due to a greater stand age which is the norm for *Eucalyptus* grown for sawn timber. Most of the knots we sampled did not have a round shape (not all boards were back-sawn), thereby it was not possible to measure their diameter properly. Calculating the theoretical knot diameter considering the circle area equation, it resulted in an average of 11.41 mm. This value was considerably lower than the knot diameters described by Moberg (2000) for *Pinus sylvestris*, from 7 to 68 mm (23 in average). Šušnjar et al. (2006) also found greater knot diameter values, from 20 to 80 mm, on another conifer species, *Abies alba*. These results reinforced what was reported by Crafford and Wessels (2016): knots on young *Eucalyptus grandis* trees are generally fairly small.

Table 8. Descriptive statistics of the evaluated knot features as well as wood density. The surface where the knot features were assessed had 2500 mm² (50 x 50 mm, see Figure 23).

Variable	Unit	Mean	Stand dev.	Min	Max	CV (%)
Knot area	mm²	102.28	108.71	9.38	594.09	106.28
Wound wood area	mm²	359.96	224.39	54.51	1008.99	62.34
Distance grain	mm	16.12	4.97	0.00	22.14	30.83
Distance cross grain	mm	16.47	8.25	5.31	55.88	50.12
Density*	g cm^{-3}	0.56	0.09	0.45	0.78	15.48

*density was measured on clear wood samples

CV = coefficient of variation

The samples with knots did not show a significant difference in shear strength compared to their clear wood sample pairs (Table 9). The percentage of wood failure in knot samples was only 5.80% lower than that of clear wood samples and the difference was significant.

Besides the average value, the presence of knots also influenced the variation of the data, with the knot samples presenting a higher CV% than clear wood samples, in both f_{v0g} and *wf*. Although lower variation is beneficial to wooden structures, the differences observed on the coefficients of variation were small, between 3% and 7%. It is important to highlight that these tests were conducted on small wood specimens, where knots represent higher area proportions if we compare it to glued laminated products. Nevertheless, none of the knot features had significant relationships with f_{v0g}, wf or even to the pair-wise variation of these two variables (P-values ranging from 0.228 to 0.955).

Table 9. Shear strength on the glue line (f_{v0g}) and percentage of wood failure (*wf*) for clear and knotty wood. Average ± standard deviation (coefficient of variation).

Property	Unit	Clear	Knot	T-test
f_{v0g}	MPa	11.17 ± 1.95 (17.45)	10.70 ± 2.15 (20.12)	n.s. p = 0.07115
w_f	%	81.67 ± 24.31 (29.77)	76.93 ± 28.32 (36.81)	* p = 0.01753

*significant difference on paired one-sided T-test

According to literature, knots are zones of lower adhesion strength due to their higher fiber angle, roughness and extractive contents (Davis, 1997), therefore, some influence of their size on the f_{v0g} was expected. Grunwald et al. (2014) found a significant relationship between defect area and wood adhesion strength, however, they were studying wood with artificial defects with virtually no adhesion (Teflon patches). Knots probably have better adhesion than Teflon, so we expected it to have a lower decrease than that reported by the cited authors, which was that a loss of 50% of the adhesion area cause a decrease of 30% of the shear strength.

In contrast with the knot features, wood density did show a significant relationship with shear strength. While there was no relationship between f_{v0g} and $\varrho_{12\%}$ on knot samples, on clear wood samples we found a weak but significant relationship (Figure 25). Wood failure, on the other hand, not only is influenced by wood density on both treatments, but their coefficients of determination were considerably higher (Figure 26). Another difference is that samples with denser wood were stronger in shear and the percentage of wood failure was lower when wood had higher density. With the increase of density, wood shear strength also increases (Kretschmann, 2010), but the adhesion strength might be reduced (HUNT et al., 2018), so it is natural to observe a higher failure on the adhesive on wood of higher density values.

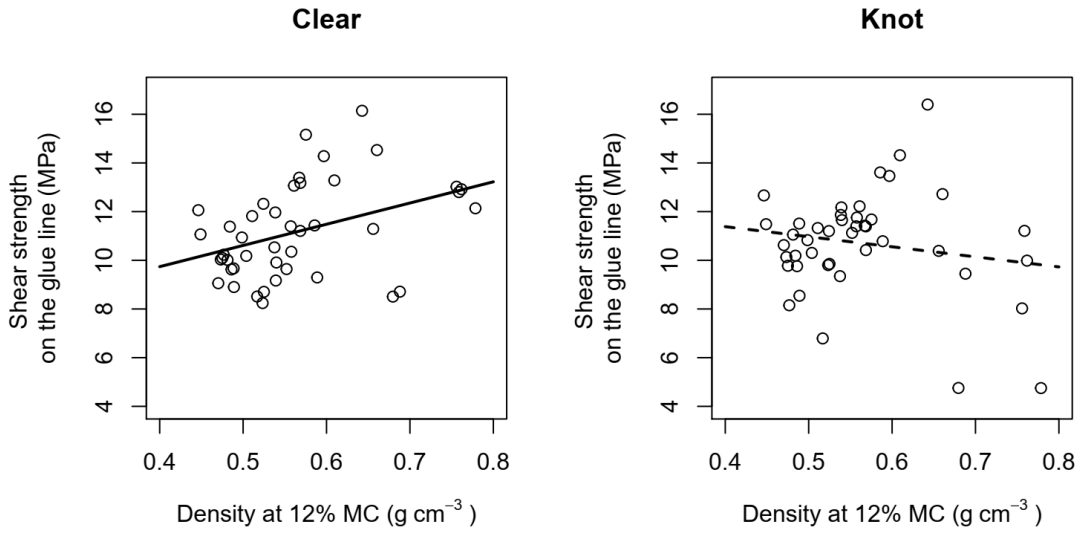

Figure 25. Relationship between shear strength on the glue line (f_{t0g}) and wood density ($\varrho_{12\%}$) for both treatments, clear wood (left) and knotty wood (right).
Clear: f_{t0g} = 6.242 + 8.690 [$\varrho_{12\%}$]; R^2 = 0.1356, P = 0.008731
Knot: f_{t0g} = 13.037 – 4.137 [$\varrho_{12\%}$]; R^2 = 0.005084, P = 0.2768

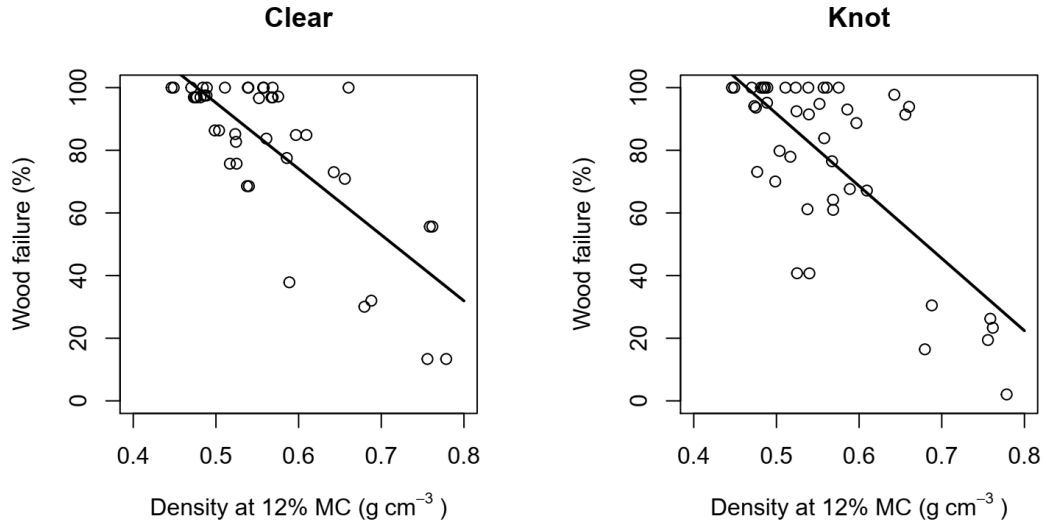

Figure 26. Relationship between percentage of wood failure (*wf*) and density ($\varrho_{12\%}$) for both treatments, clear wood (left) and knotty wood (right).
Clear: *wf* = 199.86 - 212.62[$\varrho_{12\%}$] ; R^2 = 0.5758, p = 2.257 10^{-09}
Knot: *wf* = 206.60 + 232.82 [$\varrho_{12\%}$] ; R^2 = 0.5075, p = 5.09 10^{-08}

The shear strength on clear wood samples had no significant relationship with percentage of wood failure (p-value = 0.8397), a feature some authors believe should not be used as a criteria for assessing bonding quality of one component polyurethane adhesives (Lehringer & Gabriel, 2014; Pröller, 2017). On knot samples, however, we observed a weak but significant relationship. Knot samples with higher percentage of wood failure had also higher shear strength on the glue line (Figure 27). This relationship was particularly strong when wf was close to zero and returned very low f_{t0g} values, reinforced by the power model, which had a better fit than the linear model.

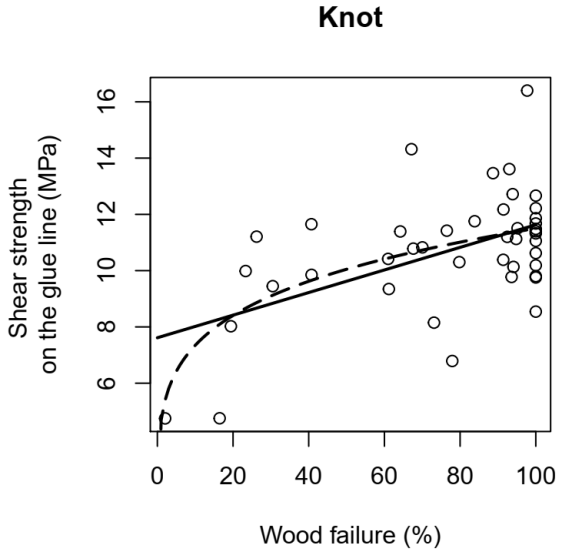

Figure 27. Relationship between shear strength on the glue line (f_{t0g}) and percentage of wood failure (*wf*) on knot samples.
Solid line: f_{t0g} = 7.61537 + 0.04015[*wf*] ; R^2 = 0.261, P = 0.0002752, sum of squared errors = 140.5705
Dashed line: f_{t0g} = 4.69219 [*wf*] 0.19467 ; sum of squared errors = 125.7725

Although no difference in f_{t0g} was observed between the treatments, knots seem to affect the adhesion of denser wood (Figure 27). The decrease of shear strength on knot samples in comparison to their clear wood pair was higher with the increase of wood density, having up to 60% of decrease in relation to its clear wood pair. Wood density did not present relationship with the pair-wise difference of wf, however, the variance of wf from knot samples in relation to their clear wood pair increased with the increase of wood density (Figure 28).

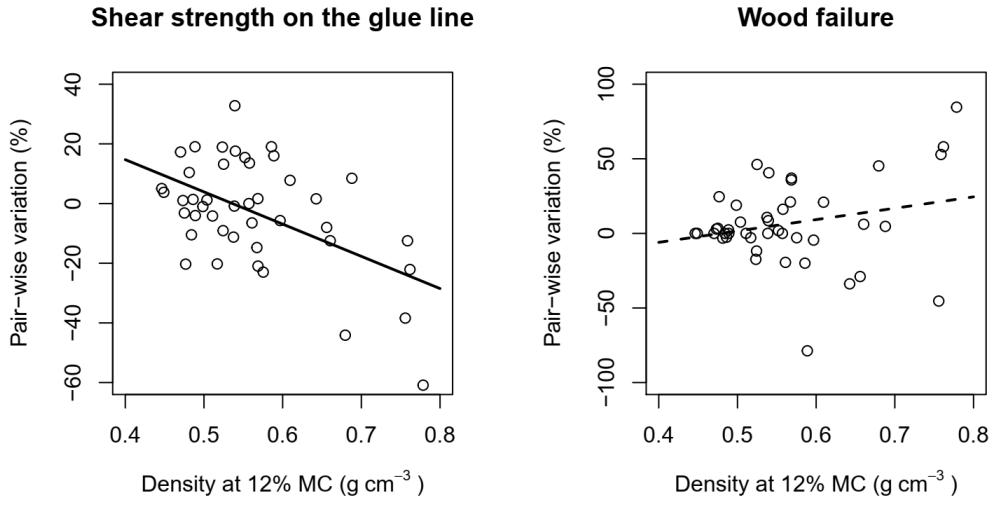

Figure 28. Pair-wise variation of shear strength on the glue line (f_{t0g}) and percentage of wood failure (*wf*) in relation to wood density.
Pair-wise variation = - 100 $(x_{clear} - x_{knot})/x_{clear}$ for each pair of samples, where x is the variable.
var f_{t0g} = 57.91 - 108.01[$\varrho_{12\%}$]; R^2 = 0.2561, P = 0.000317
var *wf* = -36.50 + 76.22[$\varrho_{12\%}$]; R^2 = 0.03305, P = 0.1263

Considering the reported influence of density on the adhesion strength of knot samples, a sensitivity analysis was conducted on knot samples to better understand the relationship between f_{v0g} and $\varrho_{12\%}$ (Table 10). When removing samples with density above 0.65 and 0.675 g cm^{-3}, significant relationships were achieved between shear strength and density (Figure 29); similar to that observed on clear wood samples. These results reinforce the fact that the negative impact of knots is higher on denser wood, and showed that the wood density on young *Eucalyptus* are more important than the size or position of the knots. This negative influence of knots on the adhesion of denser wood has a probable explanation related to the fact that wood of higher densities has already lower adhesion (HUNT et al., 2018), and the presence of a knot makes it even lower.

Table 10. Linear models relating shear strength to wood density on knot samples only. Bold values represent the highest coefficient of determination and lowest p-value found.

Density ($\varrho_{12\%}$)	Equation	R^2	P-value
All density values	$f_{v0g} = 13.037 - 4.137\ [\rho_{12\%}]$	0.005084	0.2768
Density < 0.700 g cm^{-3}	$f_{v0g} = 8.551 + 4.379\ [\rho_{12\%}]$	-0.007094	0.3976
Density < 0.675 g cm^{-3}	$f_{v0g} = 2.461 + 16.194\ [\rho_{12\%}]$	0.2466	0.001046
Density < 0.650 g cm^{-3}	$f_{v0g} = -0.165 + 21.329\ [\rho_{12\%}]$	**0.3198**	**0.0002384**
Density < 0.625 g cm^{-3}	$f_{v0g} = 2.472 + 16.151\ [\rho_{12\%}]$	0.1986	0.004817
Density < 0.600 g cm^{-3}	$f_{v0g} = 3.989 + 13.134\ [\rho_{12\%}]$	0.1273	0.02361

*density was measured on clear wood samples

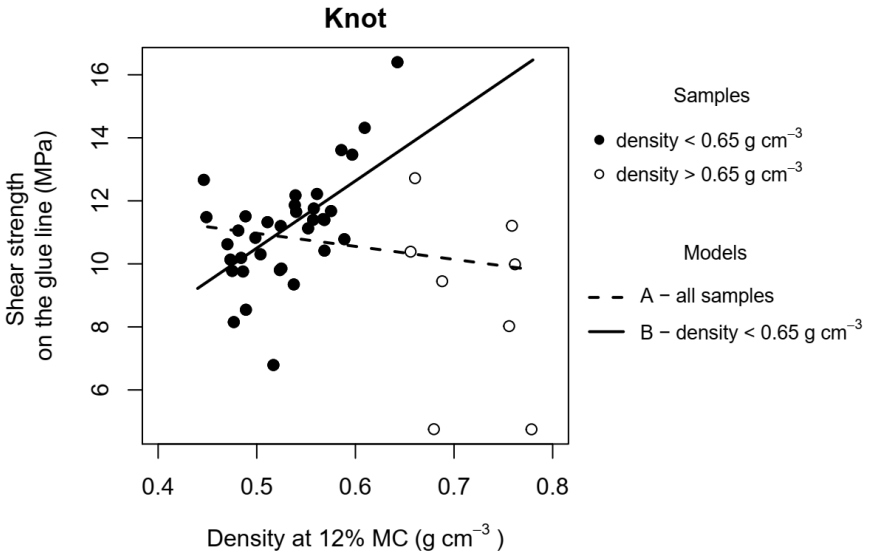

Figure 29. Relationship between shear strength (f_{v0g}) and wood density at 12% MC ($\varrho_{12\%}$) for knot samples only.
Model A: f_{v0g} = 13.037 – 4.137[$\varrho_{12\%}$]; R^2 = 0. 005084, P = 0.2768
Model B: f_{v0g} = -0.1651 + 21.3294[$\varrho_{12\%}$]; R^2 = 0.3198, P = 0.0002384

When we also removed clear wood samples with density above 0.650 and 0.675 g cm^{-3} from the data, f_{v0g} by $\varrho_{12\%}$ models were improved (Table 11), similar to what was found for knot samples. It suggests that denser wood also affected the adhesion of specimens without knots. Observing the coefficients of determination from Table 12, the stronger models are those with the same linear and angular coefficients for clear and knot samples, i.e. one single curve, and it happens when samples with density above 0.650 and 0.675 g cm^{-3} were removed. It means that bellow these density values, the adhesion of the wood evaluated behaved in the same way, with or without knots. Frihart

and Hunt (2010) indicate the adhesion of woods above values between 0.7 and 0.8 g cm^{-3} became inefficient. The results from the tables 11and 12 suggest the limit of density for an efficient adhesion for wood from young *E. grandis* plantations is slightly below 0.7 g cm^{-3}.

Table 11. Coefficient of determination (R^2) from the significant (α = 0.05) linear models of shear strength considering various clear and knot sample model coefficients. The bold value represents the highest R^2 among the models tested.

Density*	Clear wood only		Clear and knot wood				
(g cm^{-3})	n	linear model	n	model i	model ii	model iii	model iv
all	43	0.136	86	n.s.	n.s.	n.s.	0.065
< 0.700	39	0.076	78	0.039	n.s.	n.s.	n.s.
< 0.675	37	0.307	74	0.287	0.277	0.277	0.27
< 0.650	35	0.292	70	**0.315**	0.305	0.305	0.295
< 0.625	34	0.183	68	0.202	0.19	0.19	0.178
< 0.600	33	0.14	66	0.147	0.133	0.133	0.121

*density was measured on clear wood samples

Model i – the same a and b coefficients

Model ii – the same a, different b

Model iii – different b, the same a

Model iv – different a and b coefficients

a is the linear coefficient

b is the angular coefficient

Suleimana et al. (2020), on the other hand, found no significant adhesion strength reduction on wood denser than 0.675 g cm^{-3}. The shear strength on the glue line was higher than the one on solid wood, even when the former had lower density (0.739 g cm^{-3}) than the latter (0.857 g cm^{-3}). We have two possible explanations for our results to be distinct from Suleimana et al. (2020). First, the type of adhesive used by the cited authors (melamine urea formaldehyde) may have a stronger interaction with *Eucalyptus* wood than the single component polyurethane we used. Second, in the present study, the wood surface was exposed for about 48h and, over time, this exposed surface becomes less hydrophilic, decreasing the wood-adhesive interaction (Hunt et al., 2018). A higher bonding strength on denser wood samples will probably be obtained if the timber pieces are glued with freshly exposed surfaces.

4.3.1. Critical glue shear stress in glulam beams

Knots in timber from young *Eucalyptus* spp. trees, are not considered a major structural problem (Pagel et al., 2020) and other studies did not find a significant relationship between knot properties and the flexural wood properties (Nocetti et al., 2017) of timber pieces above 100mm width. However, we have reported a negative influence of knots on adhesion of wood of higher densities as described in the section above. Results from bending tests on clear wood specimens can be seen in Table 12. These results showed that density had a significant positive relationship with modulus of rupture (R^2 = 0.5609) and modulus of elasticity (R^2 = 0.4859). The clear-wood bending samples were representative of the samples from glued shear tests as they did not show a significant difference (P = 0.7795) in mean wood density with the shear test group (Table 12).

Table 12. Descriptive statistics of the variables from clear wood specimens under bending (n = 50). Sd = standard deviation; CV = coefficient of variation; f_M is the bending strength and E_{M0} is the bending stiffness. Density was measured at 12% moisture content.

Variable	Unit	Mean	Sd	Min	Max	CV (%)
Density	g cm^{-3}	0.5597	0.0582	0.4297	0.7241	10.39
f_M	MPa	90.68	15.05	50.45	128.12	16.59
E_{M0}	GPa	11.90	2.41	8.37	17.21	20.27

For glued laminated timber beams, lamellas composed of stiffer wood should be positioned in the regions of higher mechanical stress demand viz. the top and bottom lamellas (Abbott & Whale, 1987; Castro & Paganini, 2003). The bending stiffness of a glulam beam, the product of the modulus of elasticity (E_{beam}) by the second moment of area (I_{beam}), can be calculated by the summation of the bending stiffness of each lamella (E_{lam} x I_{lam}) that composes the beam (Espíndola & Silva Neto, 2001). According to the Steiner Theorem (Morales, 2009), Ilam is influenced by the squared transport of area (Equation 17), so arranging the lamellas with highest E_{lam} far from the geometric center of the beam increases E_{lam} x I_{lam} and, consequently, E_{beam} x I_{beam}.

$$I_{lam} = \frac{bh^3}{12} + bhT^2 \qquad (17)$$

I_{lam} is the second moment of area of a lamella composing a glulam beam;

b is the width of the lamella;

h is the height of the lamella;

T is the transport of area, the distance between the geometric center of the lamella and the geometric center of the beam in the y axis.

The positions where we find the higher normal stresses (tension and compression) are also where the tangential stresses (shear) are lower (Figure 24). It means that when we arrange glulam beams to have the stiffest (and densest) lamellas on the top and bottom positions, we have a double gain: higher beam bending stiffness and lower shear stresses where the adhesion performance is low.

In Table 13 we can observe the results from the theoretical beam simulations considering situations with high shear demand: where the beams break by normal and shear stresses simultaneously, the beams' bending strength is the maximum f_M value from the clear wood specimens (128.12 MPa) and shear strength is the average f_{v0g} from clear wood (11.17 MPa). The shear stress on the glue line from the bottom (or top) lamella exceeds the lowest f_{v0g} from knot samples when beams have 8 laminations or less. However, these lamellas are not composed only by knotty surfaces; they present an average of 4.3 knots (from 0 to 9) in a length of 2.1 m, with no relationship between the number of knots and wood density (P = 0.153). If we consider each knot has an influence area of 2500 mm² (the area from glue shear samples), the lamellas (25 x 90 x 2100 mm) have between 88.1% and 100% of clear wood surface (mean of 94.3%). Establishing the lowest f_{v0g} value from the clear samples as the limit, only beams with 4 lamellas or less would fail on the bottom or top glue line. In the simulated beam with 4 lamellas (80 mm height), the rupture would occur under a load of 5.98 tons in a span of 0.688 m, a situation unlikely to happen in practice.

Even when beams are submitted to high shear stress, the low adhesion values observed on dense knotty wood did not seem to be a problem on glulam beams. However, it is important to evaluate these situations experimentally, in order to verify what we have observed in theory. In any case, if knots are considered a problem on the adhesion of denser lamellas, it is always an option to remove these knots and finger-joint the clear wood sections.

Although this is an expensive process (Derikvand et al., 2017), only the densest lamellas would have knots removed, a minor timber volume in a whole beam, and may not affect its economic viability. However, before replacing knots for these joints, it is essential to find out what knot features would result in strength lower than finger joints, to remove knots only when it is really necessary.

Table 13. Data from the simulated glued laminated timber beams (20 mm lamellas) with equation 15 (4-point bending test), considering bending strength (f_M) = 128.12 MPa, shear strength (f_{v0}) = 11.17 MPa and a span-to-height ratio = $3f_M/4f_{v0}$

h (mm)	n lam	L (mm)	Fmax (kN)	τ_{lam} (MPa)	% min $f_{v0g,k}$	% min $f_{v0g,c}$
40	2	344.1	29.8	11.17	**235.2**	**135.5**
60	3	516.2	44.7	9.93	**209.0**	**120.5**
80	4	688.2	59.6	8.38	**176.4**	**101.6**
100	5	860.3	74.5	7.15	**150.5**	86.7
120	6	1032.3	89.4	6.21	**130.6**	75.3
140	7	1204.4	104.3	5.47	**115.2**	66.4
160	8	1376.4	119.1	4.89	**102.9**	59.3
180	9	1548.5	134.0	4.41	92.9	53.5
200	10	1720.5	148.9	4.02	84.7	48.8
220	11	1892.6	163.8	3.69	77.7	44.8
240	12	2064.6	178.7	3.41	71.9	41.4
260	13	2236.7	193.6	3.17	66.8	38.5
280	14	2408.7	208.5	2.96	62.4	36.0
300	15	2580.8	223.4	2.78	58.5	33.7

h = depth of the beam; n lam = number of lamellas; L = span in which the beam breaks by normal and shear stresses simultaneously, F = load in which the beam breaks by normal and shear stresses simultaneously; τ_{lam} = shear stress on the glue line of the bottom lamella (equation 16); % min $f_{v0g,k}$ = the percentage of τ_{lam} in relation to the minimum f_{v0g} value from knot samples; % min $f_{v0g,c}$ = the percentage of τlam in relation to the minimum f_{v0g} value from clear samples.

4.4. Conclusion

On average, knot-containing samples had a lower wood failure area, but the same shear strength on the glue line in relation to clear wood samples. None of the knot features evaluated had significant correlations with wood failure area, shear strength on the glue line or the variation of these properties in relation to the clear wood sample pair.

The negative influence of knots on wood adhesion only occurs when wood density was above 0.65 – 0.675 g cm^{-3}. With lower density values, clear and knotty wood behave similarly in adhesion. When wood density is high, knots cause an increase in the variation of wood failure area and a decrease in shear strength on the glue line.

Optimized glulam have their stiffer (and denser) lamellas on the top and bottom positions, where the shear stress is low. Even in extreme shear situations, the glue line of denser lamellas are subjected to a shear stress lower than the minimum values of shear strength observed, so delamination should not be a problem on glulam containing knots from young *Eucalyptus grandis* trees.

References

Abbott, A. R., & Whale, L. R. J. (1987). An overview of the use of glued laminated timber (glulam) in the UK. Construction & Building Materials, 1(2), 104–110.

As, N., Goker, Y., & Dundar, T. (2006). Effect of knots on the physical and mechanical properties of scots pine (Pinus sylvestris L.). Wood Research, 51(3), 51–58.

ASTM. (1999). ASTM D198 - Standard Test Methods of Static Tests of Lumber in Structural Sizes. ASTM International, 20.

ASTM. (2008). Standard Test Method for Strength Properties of Adhesive Bonds in Shear by Compression Loading - D905. ASTM International, 1–5.

ASTM. (2014). Standard Test Methods for Small Clear Specimens of Timber - D143. ASTM International, 31. https://doi.org/10.1520/D0143-09.2

Betters, D. R., Wright, L. L., & Couto, L. (1991). Short rotation woody crop plantations in Brazil and the United States. Biomass and Bioenergy, 1(6), 305–316. https://doi.org/10.1016/0961-9534(91)90011-Z

Castro, G., & Paganini, F. (2003). Mixed glued laminated timber of poplar and Eucalyptus grandis clones. 61, 291–298. https://doi.org/10.1007/s00107-003-0393-6

Crafford, P. L., & Wessels, C. B. (2016). The potential of young, green finger-jointed Eucalyptus grandis lumber for roof truss manufacturing. Southern Forests, 78(1), 61–71. https://doi.org/10.2989/20702620.2015.1108618

Davis, G. (1997). The performance of adhesive systems for structural timbers. International Journal of Adhesion and Ahesives, 17(3), 247–255.

Derikvand, M., Kotlarewski, N., Lee, M., Jiao, H., Chan, A., & Nolan, G. (2018). Visual stress grading of fibre-managed plantation Eucalypt timber for structural building applications. Construction and Building Materials, 167, 688–699. https://doi.org/10.1016/J.CONBUILDMAT.2018.02.090

Derikvand, M., Nolan, G., Jiao, H., & Kotlarewski, N. (2017). What to Do with Structurally Low-Grade Wood from Australia ' s Plantation Eucalyptus ; Building Application ? BioResources, 12(1), 4–7.

Espíndola, J. J., & Silva Neto, J. M. da. (2001). Identification of Flexural Stiffness Parameters of Beams. Journal of the Brazilian Society of Mechanical Sciences, 23, 217–225.

FAO. (2009). State of the World's Forests. FAO.

Frihart, C. R., & Hunt, C. G. (2010). Adhesives with wood materials : bond formation and performance. In R. J. Ross (Ed.), Wood Handbook (Centennial, p. 509). USDA Forest Service, Forest Products Laboratory.

Gaspar, F., Cruz, H., & Gomes, A. (2015). Modeling the influence of delamination on the mechanical performance of straight glued laminated timber beams. Construction and Building Materials, 98, 447–455. https://doi.org/10.1016/j.conbuildmat.2015.08.011

Gere, J. M., & Goodno, B. J. (2008). Mechanics of Materials (6th ed.). Thomson Learning.

Gomez, K. A., & Gomez, A. A. (1984). Statistical Procedures for Agricultural Research (2nd Editio). John Wiley & Sons Inc (Verlag).

Grunwald, C., Fecht, S., Vallée, T., & Tannert, T. (2014). Adhesively bonded timber joints - Do defects matter? International Journal of Adhesion and Adhesives, 55, 12–17. https://doi.org/10.1016/j.ijadhadh.2014.07.003

Hunt, C. G., Frihart, C. R., Dunky, M., & Rohumaa, A. (2018). Understanding wood bonds-going beyond what meets the eye: A critical review. Reviews of Adhesion and Adhesives, 6(4), 369–463. https://doi.org/10.7569/RAA.2018.097312

Kretschmann, D. E. (2010). Mechanical Properties of Wood. In Wood Handbook, Wood as an Engineering Material (Centennial, p. 508). U.S. Department of Agriculture, Forest Service, Forest Products Laboratory.

Lehringer, C., & Gabriel, J. (2014). Review of Recent Research Activities on One-Component PUR-Adhesives for Engineered Wood Products. In S. Aicher, H.-W. Reinhardt, & H. Garrecht (Eds.), Materials and Joints in Timber Structures: Recent Developments of Technology (1st ed., Vol. 9, pp. 405–406). Springer Netherlands. https://doi.org/10.1007/978-94-007-7811-5

Liao, Y., Tu, D., Zhou, J., Zhou, H., Yun, H., Gu, J., & Hu, C. (2017). Feasibility of manufacturing cross-laminated timber using fast-grown small diameter eucalyptus lumbers. Construction and Building Materials, 132, 508–515. https://doi.org/10.1016/j.conbuildmat.2016.12.027

Mack, J. J. (1979). Australian methods for mechanically testing small clear specimens of timber.

Moberg, L. (2000). Models of Internal Knot Diameter for Pinus sylvestris. Scandinavian Journal of Forest Research, 15(2), 177–187. https://doi.org/10.1080/028275800750014984

Morales, C. A. C. (2009). Prototipo para la Enseñanza de la Dinámica Rotacional (Momento de Inercia y Teorema de Ejes Paralelos). Latin American Journal of Physics Education, 6–11.

Moya, R., Tenorio, C., & Oporto, G. (2019). Short rotation wood crops in Latin American: A review on status and potential uses as biofuel. Energies, 12(4). https://doi.org/10.3390/en12040705

Nocetti, M., Pröller, M., Brunetti, M., Dowse, G. P., & Wessels, C. B. (2017). Investigating the potential of strength grading green Eucalyptus grandis lumber using multi-sensor technology. BioResources, 12(4), 9273–9286. https://doi.org/10.15376/biores.12.4.9273-9286

Pagel, C. L., Lenner, R., & Wessels, C. B. (2020). Investigation into material resistance factors and properties of young, engineered Eucalyptus grandis timber. Construction and Building Materials, 230, 117059. https://doi.org/10.1016/j.conbuildmat.2019.117059

Pleguezuelo, C. R. R., Zuazo, V. H. D., Bielders, C., Bocanegra, J. A. J., PereaTorres, F., & Martínez, J. R. F. (2015). Bioenergy farming using woody crops. A review. Agronomy for Sustainable Development, 35(1), 95–119. https://doi.org/10.1007/s13593-014-0262-1

Pröller, M. (2017). An investigation into the edge gluing of green Eucalyptus grandis lumber using an one-component polyurethane adhesive. Stellenbosch University.

Schneider, C. A., Rasband, W. S., & Eliceiri, K. W. (2012). "NIH Image to ImageJ: 25 years of image analysis." Nature Methods, 9(7), 671–675. http://imagej.nih.gov/ij

Suleimana, A., Sena, C. S., Branco, J. M., & Camões, A. (2020). Ability to glue portuguese eucalyptus elements. Buildings, 10(7), 1–10. https://doi.org/10.3390/buildings10070133

Šušnjar, M., Krpan, A. P. B., Pentek, T., Horvat, D., & Poršinsky, T. (2006). Influence of knots on classification of timber assortments of silver fir into quality classes. Wood Research, 51(1), 51–58.

Wright, S., Dahlen, J., Montes, C., & Eberhardt, T. L. (2019). Quantifying knots by image analysis and modeling their effects on the mechanical properties of loblolly pine lumber. European Journal of Wood and Wood Products, 77(5), 903–917. https://doi.org/10.1007/s00107-019-01441-8

Zobel, B. J., & Sprague, J. R. (1998). Juvenile Wood in Forest Trees. Springer.

Zziwa, A., Robert, K., Kizito, S., & Syofuna, A. (2017). The Effect of Knot Size on Flexural Strength of Eucalyptus Grandis Structural Size Timber. Modern Agricultural Science and Technology, 3(1), 43–47. https://doi.org/10.15341/mast(2375-9402)/01.03.2017/00

5. INVESTIGATING THE USE OF BOW FOR PRESTRESSING LAMELLAS OF GLULAM BEAMS MADE WITH YOUNG *Eucalyptus grandis* TIMBER

Bruno Monteiro Balboni[1,2], C. Brand Wessels[2] & José Nivaldo Garcia[1]

[1]Department of Forest Sciences, University of São Paulo, Piracicaba, Brazil;

[2]Department of Forest and Wood Science, Stellenbosch University, Stellenbosch, South Africa

Highlights

- Glulam beams were manufactured from seven-year-old *Eucalyptus grandis* timber containing knots and with different levels of bow
- Beams were prestressed by straightening the inherent bow present in the lamellas
- No influence of prestress was found, but lamellas with higher bow levels returned improved flexural properties
- Use of lamellas with bow above the allowable distortion limits can result in high value products

Abstract Young plantation forests can be used as a resource for structural sawn timber products to help reduce the embodied carbon emissions of buildings. *Eucalyptus* spp. are amongst the most promising species due to their adaptability and high growth rates. However, young *Eucalyptus* forests often produce timber containing defects such as excessive warp (due to growth stresses) and knots. We hypothesize that the straightening of bowed lamellas can result in prestressed glulam beams and, in this way, improve their load capacity and lower the impact of knots. Eighteen (18) glulam beams were manufactured with lamellas of varying bow distortion levels. Nine of the beams had the pre-tensioned side coincident with the tension side of the beam, and the other nine with the compression side. Results indicate that the prestress added to the beams through the straightening of lamellas did not influence the beams' stiffness or strength. However, it was found that lamellas with increased bow did have better inherent flexural properties than straight lamellas, and hence resulted in beams with improved bending strength and stiffness. In total, 80% of the lamellas had bow above the limits established by the Australian Standard which would normally result in a rejected product. Utilising bowed timber for laminated beams result in a high value product and reinforces the potential of young fast-growing plantation forests to provide raw material to the timber and construction industries.

Keywords warp, bow, glulam, knots, short-rotation forest.

5.1. Introduction

The construction industry was responsible for more than 40% of global energy-related carbon emission in 2015 (Abergel et al., 2017). With efforts to improve the energy efficiency of buildings bearing fruit, the focus is turning to the reduction of embodied emissions of buildings (Huang et al., 2018). Embodied emissions can be defined as the carbon emitted by the manufacturing of the materials used in the building and during the construction

process itself (Cabeza et al., 2014). Utilising timber as a structural and building material, instead of high emission materials such as steel and concrete, is one of the main strategies for reducing CO_2 emissions (Oliver et al., 2014).

Although plantation forests usually need long rotations for the production of timber, some species are able to provide raw material for the timber industry at very early ages, such as *Populus* sp. (Casado et al., 2012; Castro & Paganini, 2003), and *Schizolobium parahyba* (Rosa et al., 2019). Species from the genus *Eucalyptus* stand out in this matter, though. Besides being the most planted hardwood in the world (Myburg et al., 2014) and one of the fastest growing trees (Japarudin et al., 2020), *Eucalyptus* trees can adapt to a wide variety of environments (Gonçalves et al., 2013). However, together with *Eucalyptus'* fast growth come some undesired features, such as an increased portion of juvenile wood, knots, warping and splitting.

Juvenile wood from hardwoods, although weaker than mature wood, is less of a problem than for softwoods (Zobel & Sprague, 1998). For *Eucalyptus* research results showed that juvenile wood has returned adequate mechanical properties for structural timber use (Balboni et al., 2021; Crafford & Wessels, 2016; Liao et al., 2017). It was also shown that knots in timber from young *Eucalyptus* trees were not related to strength and stiffness variation in structural timber (Nocetti et al., 2017; Pagel et al., 2020). *Eucalyptus* are known for having high levels of growth stress (Murphy et al., 2005) which during primary processing usually result in boards with end splits, thickness variation, bow or crook (Yang & Waugh, 2001). National manufacturing standards have rigid limits for acceptable bow distortion and timber that exceed these limits are rejected for structural use, resulting in lower value products (Derikvand et al., 2017).

One option for timber with excessive bow is that it can be used as lamellas for glued laminated timber to produce straight beams and result in a high value addition products. In the process of straightening lamellas, there is a generation of stresses: compression on the convex face and tension on the concave face. These stresses can potentially be used to benefit the structural element for prestressing the beams. Adding an opposite stress to the side of the beam that will be tensioned can increase its bending strength since, under tension, wood has a more brittle behavior than under compression (Negrão, 2012; Van der Put, 2010). Prestressing is a technique commonly used in concrete structures for increasing its low tension strength in comparison to compression strength. Prestressing have been investigated in timber and to have higher gains, usually prestressing timber is accompanied by reinforcements (Estévez-Cimadevila et al., 2018) with fibers (Halicka & Ślósarz, 2021; H. Yang et al., 2016), steel (Bohannan, 1964; de Lima et al., 2018; de Luca & Marano, 2012) or densified wood (Anshari et al., 2012), which, in turn, increases the cost. Even without adding other materials, prestressing timber needs additional infrastructure and adds complexity to the manufacturing process. Using bowed lamellas, on the other hand, is simple and takes advantage of an inherent feature of the timber which usually cause a value reduction of the raw material.

Young *Eucalyptus* forests are usually planted to produce paper, reconstituted panels or bioenergy, so they are mostly unpruned. As brittle ruptures caused by defects on the tension side are the main reason for failures in timber beams (Negrão, 2012), precompressing the tension zone can potentially lower the effect knots and other defects (Bohannan, 1964). Our hypothesis is that the prestress caused by straightening bowed lamellas can influence the beam's load capacit. So, adding compression stress to the face to be tensioned will increase the maximum tension stress in service and, in turn, adding tension stress to the face to be tensioned will decrease the maximum stress.

5.2. Materials and Methods

5.2.1. Material

Trees from a seven years-old *Eucalyptus grandis* plantation spaced 3 x 2 m (1667 stems per hectare) were harvested and transported to a sawmill. The logs, 2.5 m long, were processed first in a twin blade circular saw, and after a turn of 90°, the centre cant was sawn with a multirip circular saw. The boards, with nominal thickness and width of 25 and 90 mm, respectively, were stacked to air dry for six months under cover. After reaching equilibrium moisture content with the environment, 150 boards were selected having bow of different levels. Boards with twist or spring were discarded but all knots were considered acceptable. Boards were cross cut on both ends for achieving a final length of 2.2 m. In a thicknesser planer, both board faces were planed, producing parallel and smooth surfaces, yet maintaining the bow deformation. After reducing the boards' width, we obtained 20 x 70 x 2200 mm lamellas.

5.2.2. Lamellas selection and classification

The 150 lamellas were kept in a temperature and humidity-controlled room until reaching 12% moisture content (MC). Then, with a digital caliper (precision = 0.01 mm) the thickness, width and bow distortion was measured (following AS 2796.1, Standards Australia, 1999), while the length was measured with a measuring tape and mass with a semi analytic scale (precision = 0.01 g). Finally, the density of each lamella was calculated at 12% MC.

A non-destructive three-point bending test with a 1.4 m span was used to assess the lamellas' bending stiffness in a universal testing machine (model Pavitest with 300kN capacity). An initial load was applied (30 N) and the test was conducted until reaching 100 N, with a cross head speed of 10 MPa min^{-1}. Applying this data to Equation 18, the modulus of elasticity (E_{M0}) was calculated. This methodology was used to test 12 of the 150 lamellas, with a representative range of densities, and this load range always returned a linear load-deflection curve. Bending stiffness was assessed twice on each of the 138 lamellas left, with convex face of the bow facing up and down, treatments named $\cup$ and $\cap$, respectively. To avoid any influence of the first test on the second, half of the lamellas were tested first on the $\cup$ position and the other half, on $\cap$ first.

Lamellas returned bending stiffness too high for their density, compared to values obtained on clear wood specimens from the same timber batch. The difference found is probably related to the span to depth ratio used in this test (70) which is higher than the values commonly adopted by national standards. We built linear models of bending stiffness by wood density and found that the curves of lamellas and clear wood data have the same slope. Then, we adjusted lamellas' E_{M0} by subtracting 3.665 GPa.

$$E_{M0} = \frac{tg_{\alpha} L^3}{48I} \qquad (18)$$

E_{M0} is the bending stiffness

α is the angle of the load-deflection curve

L is the span length

I is the second moment of area

5.2.3. Glued laminated beams

In order to test the hypothesis and evaluate the effect of prestressing timber through straightening bowed lamellas, beams were produced whose bottom surfaces were increasingly more compressed (where it was expected to have benefits from the added stresses) and beams whose bottom surfaces were increasingly more tensioned (expected to be detrimental). There were two groups of beams: i - the bottom surface of the beam was pre tensioned, group $\cap$. ii - the bottom surface of the beam was pre compressed, group U. Although all beams were straight after gluing, the same terminology of the lamellas was adopted to the beams to indicate the lamellas' orientation during the beams assembling.

Each beam, of seven lamellas each, was designed to have stiffer lamellas in positions where normal stresses are higher. All lamellas were ordered by their stiffness (average of U and $\cap$) and then segregated into four groups with stiffness progressively lower: groups A, B and C with 36 lamellas each, and group D with 18 lamellas. Inside each stiffness group, the lamellas were ordered according to their bow distortion and segregated into nine sub-groups. All 18 beams were planned to have equivalent bending stiffness of lamellas in each position, but with increasing bow distortion, which, in turn, was equivalent between U and $\cap$ beams (Figure 30).

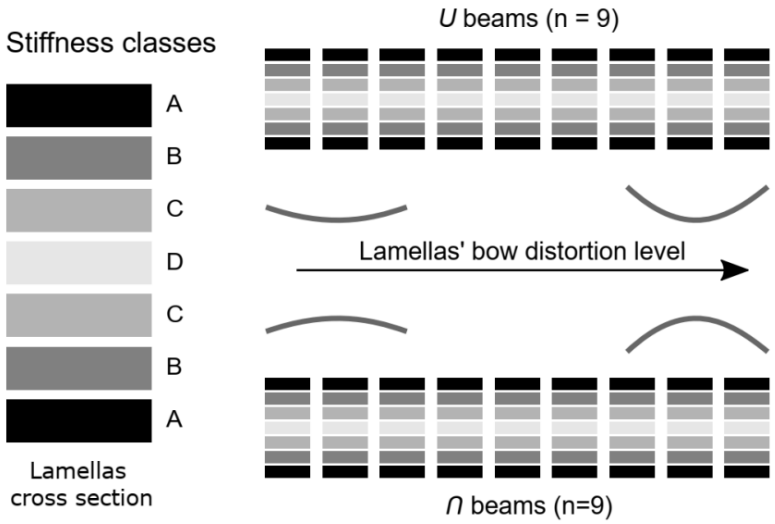

Figure 30. Representation of the lamella's cross sections, their classes according to bending stiffness, their planned vertical distribution in the glulam beams, where class A have the stiffest lamellas and class D, the least stiff, and sub-groups based on bow distortion values.

Just before gluing the lamellas into beams, a thicknesser planer was used to plane both surfaces of each lamella to have freshly exposed wood for better adhesion (Hunt et al., 2018), resulting in 16 mm nominal thickness lamellas. A two-component polyurethane adhesive (donated by Imperveg Ltd) was used with a spread rate of 250 g m^{-2}. All lamellas had the convex surface facing the same side during the assembling, so they fit in the shape of the adjacent lamellas. Each pair of beams (U and $\cap$) from the same sub-group of bow distortion was pressed together under 0.7 MPa for 5 hours. The lamellas from both beams pressed together had the convex side facing down, with the distributed load making them straight. The beams were left for 12 months under cover, for a complete adhesive cure, as well as to pass through a full year cycle, especially the humid, hot summer and the dry, mild winter. Then,

the residual warping was measured and the beams were planed to remove imperfections, resulting in straight beams of approximately 60 x 112 x 2000 mm.

The beams were tested using a four-point bending setup, following the standard ASTM D198 (ASTM, 1999) with 1800 mm span, 600 mm shear span and cross head speed = 50 N min^{-1}. The universal machine used was the same as described earlier for the lamellas' tests.

5.2.4. Calculations and data analysis

With the bending stiffness, deflection and length of the lamellas, the pre-stress of the bottom and top surfaces of each lamella was calculated. Instead of using the average between ∩ and ∪ orientations, the stiffness value of the lamellas in the same orientation they were assembled in the beam, was used. The stress in the center of each lamellas' length were calculated, considering the distributed loads necessary to straighten the lamellas are equivalent to those that generate such bow distortions from a straight timber piece (Equation 19). We calculated the sum of stress imposed to all lamellas (when straightened) forming a glulam beam, when integrating the absolute value of normal stress distribution (considering a linear distribution) at the middle of span.

$$f = \frac{5wL^4}{384EI} \tag{19}$$

f is the deflection;

w is the distributed load that generated deflection f

In each beam, the thickness of lamellas and the distance from the geometric center of each lamella to the beam's center, were measured in the y axis. Then, the second moment of area of the lamellas was calculated applying the Steiner Theorem (Morales, 2009) - Equation 20. The theoretical beam stiffness (E_{theor}) was calculated isolating it according to Equation 21. To simulate a non-optimized glulam beam, a theoretical bending stiffness with the average E_{M0} of all the lamellas composing the beam (E_{avg}) was calculated. In both theoretical beam stiffness values above, the lamellas' stiffness according to their orientation (∩ or ∪) in the beams was considered.

$$I_{lam,i} = \frac{bh^3}{12} + bhT^2 \tag{20}$$

$$E_{beam}I_{beam} = \sum_{i=1}^{i} E_{lam,i}\, I_{lam,i} \tag{21}$$

$I_{lam,i}$ is second moment of area of the lamella i;

b is the lamella's width;

h is the lamella's thickness;

T is the distance of the lamella's geometric center to the beam's geometric center in y axis;

E_{beam} is the beam's stiffness;

I_{beam} is the beam's second moment of area;

$E_{lam,i}$ is stiffness of lamella i.

T-tests were adopted to compare the lamellas' stiffness in both orientations and the first orientation tested (pair wise), and to compare beams' flexural properties of treatments ∩ and ∪. To understand the association of lamellas' features with beams' properties, linear and power models were developed. All statistical analyses were done considering the confidence level of 0.05, and using the software R (R Core Team, 2021).

5.3. Results and Discussion

5.3.1. Lamellas

Segregating lamellas in stiffness classes resulted in four distinct groups A, B, C and D (Table 14). Bow distortion (

Table **15**), in turn, showed differences between classes A and C, despite the aimof having all classes with the same distortion. Density at 12% MC (Table 16) followed the pattern observed in stiffness and was divided in four groups. The coefficients of variation indicate a wide range of bow distortions in each class but low COV's for bending stiffness and density in each lamella class, a consequence of the stratification methodology. The MOE of lamellas when tested in ∪ orientation did not differ from the test done in ∩ orientation (p-value = 0.74). The position in which lamellas were tested first did not influence the second test result either (p-value = 0.75).

Table 14. Bending stiffness (GPa) of lamellas segregated in stiffness classes. Groups according to ANOVA followed by Tukey test; same letter indicates no statistical difference at $\alpha = 0.05$.

Bending stiffness (GPa)						
Lamella class	mean	sd	min	max	cv	group
A	16.03	1.86	13.37	21.50	11.57	a
B	13.00	0.68	11.39	14.35	5.21	b
C	10.75	0.75	9.09	12.24	6.98	c
D	9.08	1.88	7.99	10.05	5.22	d
All	12.72	2.74	7.99	21.50	21.52	-

Table 15. Bow distortion (mm) of lamellas segregated in stiffness classes. Groups according to ANOVA followed by Tukey test; same letter indicates no statistical difference at $a = 0.05$.

Bow distortion (mm)						
Lamella class	mean	sd	min	max	cv	group
A	15.02	7.06	1.41	35.43	46.98	a
B	12.23	6.67	1.07	32.45	54.52	ab
C	8.98	5.40	0.00	19.17	60.10	b
D	11.04	5.25	4.10	19.37	47.59	ab
All	11.93	6.61	0.00	35.43	55.41	-

Table 16. Density at 12% MC (g cm^{-3}) of lamellas segregated in stiffness classes. Groups according to ANOVA followed by Tukey test; same letter indicates no statistical difference at a = 0.05.

Density at 12% MC (g cm^{-3})						
Lamella class	mean	sd	min	max	cv	group
A	0.629	0.064	0.485	0.785	10.24	a
B	0.582	0.067	0.480	0.753	11.53	b
C	0.538	0.050	0.476	0.697	9.21	c
D	0.527	0.048	0.450	0.648	9.18	d
All	0.575	0.071	0.450	0.785	12.32	-

Lamellas' E_{M0} had a significant (p-value = 2.2 x 10-16) association with density (R^2 = 0.42), which explains the similar results mentioned above. When assessing the relationship of bending stiffness (average of $\cup$ and $\cap$) with bow distortion, there was a weak relationship when all lamellas was considered together and when only class A lamellas was considered (Figure 31). Boards from regions close to the bark tend to warp more than those close to the pith (Ikami et al., 2009). In turn, boards close to the pith show more juvenile wood features, which implies lower bending stiffness (Zobel & Sprague, 1998). Lamellas from class A, mostly came from regions closer to the bark, so the relationship between E_{M0} and bow distortion gets slightly lower when compared to all lamellas together, evidenced by the slope of both models.

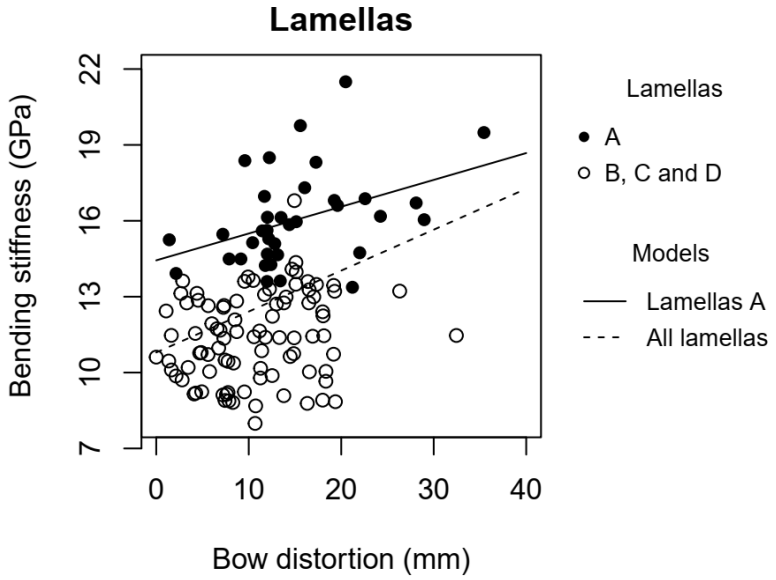

Figure 31. Bending stiffness (average of $\cup$ and $\cap$ tests) and bow distortion of lamellas.
All lamellas: E_{M0} = 10.79471 + 0.16179 [distortion]; R^2 = 0.1526; p-value: 6.13 x 10^{-06}
Lamellas A: E_{M0} = 14.43679 + 0.10601 [distortion]; R^2 = 0.1626; p-value: 0.01475

5.3.2. Beams

Glulam beams (Table 17) returned a higher mean bending stiffness when compared to lamellas, a result that was expected since beams were designed with stiffer lamellas in positions of higher stress. There was low variation in beams' density and stiffness, due to the selection of the lamellas to compose the beams. Bending

strength, in turn, showed higher variation than the former two variables, although the coefficient of variation below 15% suggests the sample size was appropriate to assess f_M (Ferreira, 2018). The higher CV% was most probably due to the presence of knots as they influence the brittle behaviour of wood under tension (Negrão, 2012).

Table 17. Density ($\varrho_{12\%}$), bending stiffness (E_{beam}) and bending strength (f_M) of all beams.

	mean	sd	min	max	CV (%)
$\varrho_{12\%}$ (g cm^{-3})	0.612	0.025	0.574	0.674	4.16
E_{beam} (GPa)	14.08	0.81	12.76	15.60	5.75
f_M (MPa)	74.68	9.58	54.20	89.02	12.83

From all 18 beams, 12 had a knot on the zone of maximum bending moment at the tension side and nine of them at the compression side (six beams had knots on both sides). Knots had a distinct influence when under compression and tension even though they had similar sizes (from 10 to 16 mm). While 11 knots on the tension side were the points of initial rupture, none of knots on the compression side resulted in beam failure. Nevertheless, there was one beam considered to have been negatively influenced by a knot rupture on the tension side. The knot was very close to the edge and the wood around it (wound wood) was apparently very stiff, which caused an early rupture, in the thin knot edge in one side and in the transition of wound wood to regular wood in the other (Figure 32). Due to this divergent behavior from the other beams (early rupture), when evaluating relationships between bending strength and lamellas' features, beam 18 was excluded. Bending stiffness, on the other hand, was not influenced by knots, either in the tension or compression side.

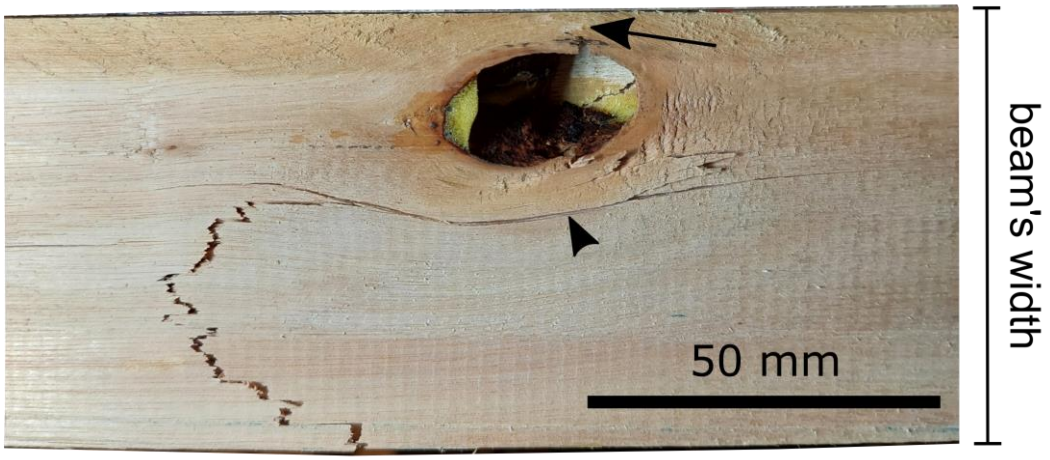

Figure 32. Knot on the tensioned side of beam 18 which caused an early rupture. The arrow points the rupture on the thin knot edge and the arrow head points the rupture in the transition between wound wood and regular wood.

The bending stiffness observed (E_{beam}) on the beams was lower than the theoretical (E_{theor}) bending stiffness (p-value = 8.95 x 10^{-5}), but there was a moderate correlation between observed and predicted results (Figure 33). When comparing to the mean bending stiffness (E_{avg}), Ebeam was 10.7% higher while E_{theor} was 16.5% higher. With a beam design using stratified lamellas, such a result was already expected.

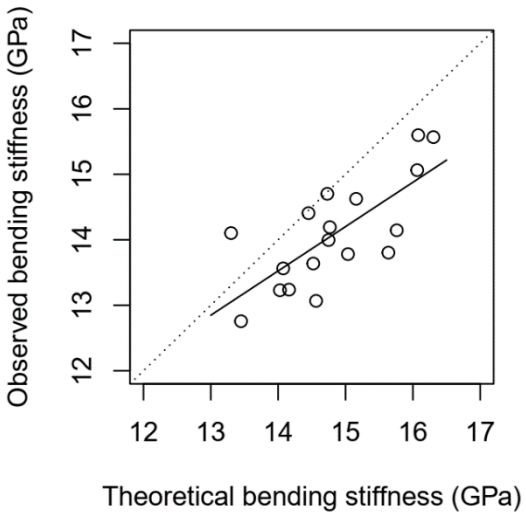

Figure 33. Beams' observed and theoretical bending stiffness.
E_{beam}= 4.0512 + 0.6767 [E_{theor}]; R^2 = 0.5413; p-value: 0.0005013

Although there was a soft trend of ∪ beams being stiffer and ∩ being stronger (Figure 34), we did not find significant differences between beams ∪ and ∩ in any flexural properties assessed (p-value > 0.29). The presence of beams with low lamella distortion in both treatments could be hiding some effects, but even when we keep only six beams with the highest distortion from each treatment, differences are still not significant (p-value > 0.23).

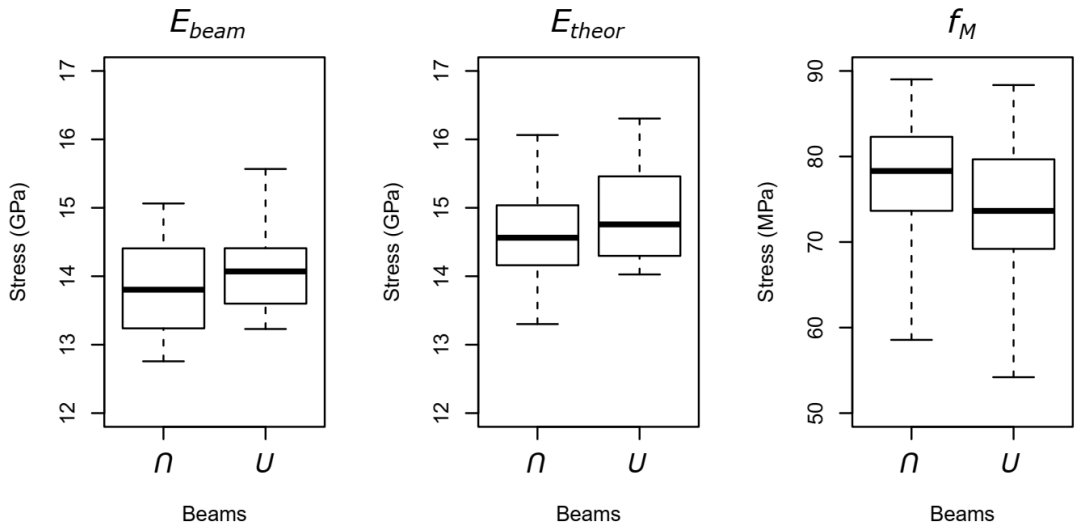

Figure 34. Bending stiffness (E_{beam}), theoretical bending stiffness (E_{theor}) and bending strength (f_M) of the ∩ and ∪ beams. None of these properties returned a significant p-value on t-test when comparing ∩ to ∪ beams for differences.

Beams made from lamellas with higher bow distortion, independent of their orientation, showed higher bending stiffness (R^2 = 0.4472). This association was also observed with theoretical bending stiffness, with a lower coefficient of determination (R^2 = 0.2504). These results indicate that most of the increase of E_{beam} were caused by the higher E_{M0} of lamellas with greater distortion. Bow distortion, through pre-stressing, did seem to have a minor

influence on bending stiffness, evidenced by the higher R^2 and angular coefficient on the model with E_{beam} than that with E_{theor}. As the difference between E_{beam} and E_{theor} did not return a significant relationship with any variable tested (bow distortion, stress added to the tension side, sum of added stress, etc) we considered this influence to be neglectable.

The relationship between bending stiffness and average bow distortion of each beam was moderate and significant ($R^2 = 0.4472$, p-value = 0.00241). Prestress values, on the other hand, only showed significant relationship with E_{beam} when considering the absolute value of stress ($R^2 = 0.448$, p-value = 0.001424).

Compression stress added to the tension side of the beam of $\cup$ beams through straightening lamellas was calculated to be on average -4.40 MPa, ranging from -0.5 to -11.6 MPa. Tensile stress added on compression side of $\cap$ beams, in turn, was 3.78 MPa, from 1.87 to 7.89 MPa. These values represent between 0.92 and 17.46% (5.4% in average) of the maximum bending stress observed.

Summing the absolute value of prestress from all lamellas ($\cup$ and $\cap$ beams), we found a strong association with f_M, and the power model had a higher fit to the data than the linear model, considering the sum of squared errors (Figure 35).

We expected that beams with pre compression on their tension side would show higher bending strength than those whose tension side was pre tensioned, which did not happen. Beams with higher prestress independently of the direction (compression or tension) were the ones that showed higher bending strength and stiffness. However, this effect may be due to the fact that stiffer lamellas also had higher bow distortion. Although the correlation was low, the slightly higher E_{M0} of lamellas might have been amplified by their second moment of area (Equation 20). Because bending strength and stiffness of wood are usually correlated (Kovryga et al., 2020; Lara-Bocanegra et al., 2020), this effect was also observed on the beams' f_M.

With these results, we reject our hypothesis that prestressing beams with the stress generated by straightening lamellas can increase a beams' maximum bending stress. Prestressing timber beams has the aim of increasing the plastic behaviour on compression and reducing the brittle behavior on tension by unbalancing the normal stress distribution: adding compressive stress to the tension side of the beam, a plastic-type rupture on the compression side is induced (instead of a brittle rupture), increasing the beam's bending strength (Bohannan, 1964). In the present study, at the same time that the tension zone was compressed, the compressed zone was tensioned, which might have reduced the stress unbalance and the effectiveness of prestressing. Beams' assembling with bowed lamellas was done also looking to the ease of fitting warped lamellas in the same direction, but further studies can evaluate the addition of compression prestress only on the bottom or on both surfaces.

Besides beam 18, whose rupture was influenced by a knot on the tension side, the highest compression prestress represented 7.2% of maximum bending stress. Bohannan (1964) found positive effects of prestressing when values were around 20% of bending strength. It does not seem feasible to achieve this percentage only using lamellas' bow distortion, unless camber opposite to the bow direction is also used in the beams' manufacturing. However, it will not cause unbalance to the normal stress distribution either.

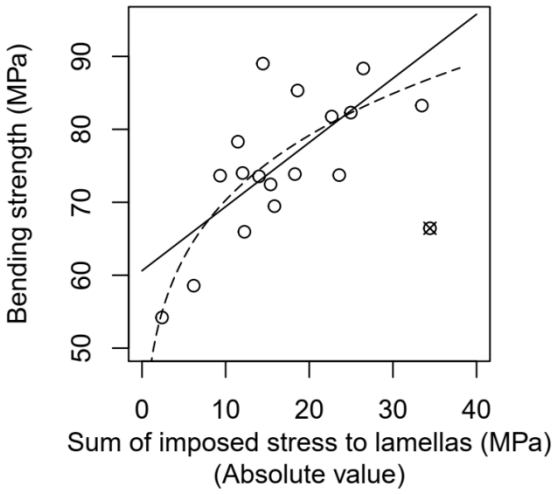

Figure 35. Relationship between bending strenght and sum of stress imposed to lamellas when they were strainghened (absolute value). The crossed circle represents beam 18, which was not used in the models.
Models:
f_M = 60.6109 + 0.8791[*sum.sts*]; R^2 = 0.5123; p-value: 0.001233; sum of squared errors: 725.8573
f_M = 47.28281[*sum.sts*]0.1721 ; sum of squared errors: 565.9263

During the mechanical tests, it was observed that any delamination and all ruptures occurred by brittle behavior on the tension side of the beams. Table 18 illustrate the structural efficiency (ratio of flexural properties with density) of the tested beams. The values are in line with other studies involving *Eucalyptus* in which the material was considered of high quality for the production of glued laminated timber beams (Castro & Paganini, 2003; Martins et al., 2020). None of the studies cited above reports the age of the *Eucalyptus* trees, but we assumed they are older than the one described here (seven-years-old) since both investigations were realized in Europe, where growth rate is expected to be lower than those found in Brazil.

Table 18. Structural efficiency of glulam beams made with young *Eucalyptus grandis* under static bending. Specific stiffness, $E_{beam}/\varrho_{12\%}$, and specific strength, $f_M/\varrho_{12\%}$.

	mean	sd	min	max	cv
$E_{beam}/\varrho_{12\%}$ (GNm kg^{-1})	23.03	1.20	20.93	25.42	5.22
$f_M/\varrho_{12\%}$ (MNm kg^{-1})	121.97	13.98	94.05	138.62	11.46

A common approach for designing beams is to establish a maximum deflection in relation to their span (*L*), called serviceability limit state (Leijten et al., 2010). This method aims to avoid that excess deformations affect the appearance and functioning of the structure in service or inflict damage to non-structural members (Honfi et al., 2012). The most extreme deflection suggested by the EN1995.1 Standard (European Committee for Standardization, 2004) is *L*/250. When applying this value to the studied beams and comparing the bending stress generated by such deflection to the maximum bending stress observed (f_M) we have an average of 22.04%, ranging from 18.16 to 28.06% (Figure 36). The Brazilian standard for timber structures NBR7190 (ABNT, 1997) has a slightly higher limit, *L*/200, which results in 27.54% of the maximum stress (from 22.70 to 35.08%). In none of the situations described the beams reached stress values close to half of their failure stress. Beam 18, whose rupture was affected by a knot on the tension zone, was not the beam with the highest proportion, showing 26.03% for *L*/250 and 32.54% for *L*/200. Despite the negative influence of the knot, the strength of beam 18 was still above the minimum value found among all beams. Other studies with young *Eucalyptus* did not find any influence of knots in timber of structural sizes

(Nocetti et al., 2017; Pagel et al., 2020). However, the results found for beam 18 suggests that the effect of knots under tension should be better understood for the best use of young *Eucalyptus* for timber structures.

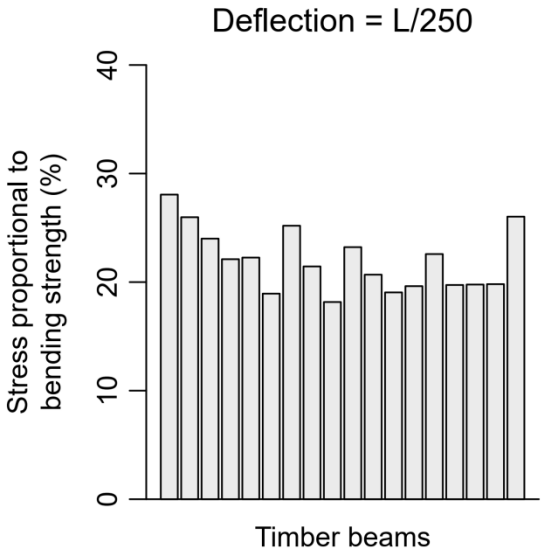

Figure 36. Bending stress of each beam (n=18) tested in relation to their bending strength when deflection is *L*/250.

Having quality products from short rotation forests confirms results from previous studies (Crafford & Wessels, 2016; Liao et al., 2017; Pagel et al., 2020) and can stimulate its adoption where timber is scarce. Young forests can provide material for structural purposes, but we have to learn how to use this material and take advantage of its characteristics, usually considered inadequate (Zobel & Sprague, 1998). In the present study, the majority of lamellas used did not meet the bow limit indicated by the Australian Standard AS 2796.1 (Standards Australia, 1999) and in a regular situation they would be discarded and not be considered suitable for structural products (Figure 37). As stated by Derikvand et al., (2017), the standard procedures do not take into consideration that timber can be applied for engineered wood products and might be too severe.

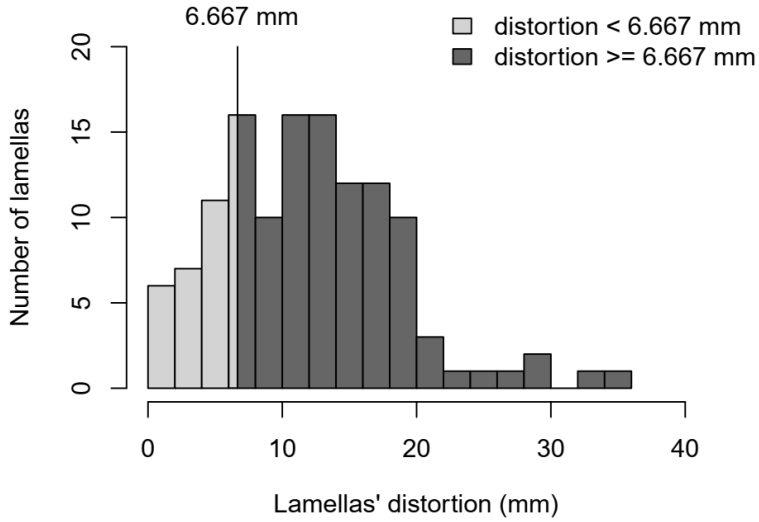

Figure 37. Bow distortion of each lamella used in the present study, assessed according to the Australian Standard AS 2796.1 (Standards Australia, 1999). From the 126 lamelas, 26 (20.6%) are below the limit stablished by the AS 4785.1 standard and 100 (79.4%) are above the limit.

Even with the rejection of our hypothesis, the results obtained are positive, especially when taking into account that the raw material used to manufacture these beams and the final results. The timber comes from a forest plantation not older than seven years-old with no pruning or thinning and did not pass through any genetic improvement toward timber production. The plantation followed a standard practice for the production of wood for the pulp and paper industry or for bioenergy purposes. Besides selecting boards having bow in different levels - to attend to the main objectives of this study - the material did not have any special selection, such as segregation of boards considering knots, sapwood and juvenile wood, or any treatment like kiln drying. Only by stratifying lamellas, we have produced glulam timber beams with adequate mechanical properties for a high value timber product.

5.4. Conclusion

The hypothesis that prestressing of beams through straightening of bowed lamellas was rejected since it did not influence the beams' stiffness or strength when considering the compression or tension sides individually. However, it was found that lamellas with increased bow did have better inherent flexural properties than straight lamellas, and hence resulted in beams with improved bending strength and stiffness.

Although no benefits or disadvantages from prestressing lamellas were observed, the beams made with young *Eucalyptus* returned adequate bending properties values. It indicates this sort of timber source, with almost no selection, can generate, as we observed, products of high quality for structural purposes. Not only the averages were in conformity with data from other studies, but the variation of the properties was low.

With 80% of lamellas not meeting the bow distortion limit from the Australian standard and keeping lamellas with knots, we built glulam beams that we consider of high quality based on their properties and qualitative results. Considering the serviceability limit state allowed by the European standard (deflection = $L/250$), the bending stress in this situation has not reached 30% of the bending strenght in any of the beams tested. It is a strong indication of safety for the product aimed, even though they had ruptures starting at knots on the tensioned side.

The increasing need for timber in our society demands other sources of timber rather than natural forests or classic timber-managed plantations, and our results reinforce the potential of young planted forests to provide raw material to timber and construction industries. The next step for a better understanding of this timber source for structural purposes is to evaluate different species, varieties and clones, considering the knot size and frequency. Addittionally, the effect of knots on timber under tension must be assessed, since it has a distinct behaviour of knots in softwoods, a material with more information available than young *Eucalyptus* wood.

References

Abergel, T., Dean, B., & Dulac, J. (2017). Towards a zero-emission, efficient, and resilient buildings and construction sector. www.globalabc.org

ABNT. (1997). NBR 7190: Projeto de estruturas de madeira. Associação Brasileira de Normas Técnicas, 107.

Anshari, B., Guan, Z. W., Kitamori, A., Jung, K., & Komatsu, K. (2012). Structural behaviour of glued laminated timber beams pre-stressed by compressed wood. Construction and Building Materials, 29, 24–32. https://doi.org/10.1016/J.CONBUILDMAT.2011.10.002

ASTM. (1999). ASTM D198 - Standard Test Methods of Static Tests of Lumber in Structural Sizes. ASTM International, 20.

Balboni, B. M., Batista, A. S., & Garcia, J. N. (2021). Evaluating the potential for timber production of young forests of Eucalyptus spp. clones used for bioenergy: wood density and mechanical properties. Australian Forestry, 84(3), 122–132. https://doi.org/10.1080/00049158.2021.1945238

Bohannan, B. (1964). Prestressed laminated wood beams. Forest Products Laboratory, 8, 1–31.

Cabeza, L. F., Rincón, L., Vilariño, V., Pérez, G., & Castell, A. (2014). Life cycle assessment (LCA) and life cycle energy analysis (LCEA) of buildings and the building sector: A review. Renewable and Sustainable Energy Reviews, 29, 394–416. https://doi.org/https://doi.org/10.1016/j.rser.2013.08.037

Casado, M., Acuña, L., Basterra, L.-A., Ramón-Cueto, G., & Vecilla, D. (2012). Grading of structural timber of Populus × euramericana clone I-214. Holzforschung, 66(5), 633–638. https://doi.org/doi:10.1515/hf-2011-0153

Castro, G., & Paganini, F. (2003). Mixed glued laminated timber of poplar and Eucalyptus grandis clones. Holz Als Roh- Und Werkstoff, 61(4), 291–298. https://doi.org/10.1007/s00107-003-0393-6

Crafford, P. L., & Wessels, C. B. (2016). The potential of young, green finger-jointed Eucalyptus grandis lumber for roof truss manufacturing. Southern Forests, 78(1), 61–71. https://doi.org/10.2989/20702620.2015.1108618

de Lima, L. C. C., Costa, A. A., & Rodrigues, C. F. (2018). On the use of prestress for structural strengthening of timber beams: assessment with numerical support and experimental validation. International Journal of Architectural Heritage, 12(4), 710–725. https://doi.org/10.1080/15583058.2018.1442526

de Luca, V., & Marano, C. (2012). Prestressed glulam timbers reinforced with steel bars. Construction and Building Materials, 30, 206–217. https://doi.org/10.1016/J.CONBUILDMAT.2011.11.016

Derikvand, M., Nolan, G., Jiao, H., & Kotlarewski, N. (2017). What to Do with Structurally Low-Grade Wood from Australia ' s Plantation Eucalyptus ; Building Application ? BioResources, 12(1), 4–7.

Estévez-Cimadevila, J., Suárez-Riestra, F., Otero-Chans, D., & Martín-Gutiérrez, E. (2018). Experimental analysis of pretensioned CLT-glulam t-section beams. Advances in Materials Science and Engineering, 2018. https://doi.org/10.1155/2018/1528792

European Committee for Standardization. (2004). EN 1995-1-1 (2004) (English): Eurocode 5: Design of timber structures - Part 1-1: General - Common rules and rules for buildings.

Ferreira, P. v. (2018). Estatística experimental aplicada às ciências agrárias. UFV.

Gonçalves, J. L. D. M., Gonçalves, D. M., Alcarde, C., Rioyei, A., Duque, L., Couto, A., Stahl, J., Frosini, S., Ferraz, D. B., Paula, W. de, Henrique, P., Brancalion, S., Hubner, A., Bouillet, J. D., Laclau, J., Nouvellon, Y., & Epron, D. (2013). Integrating genetic and silvicultural strategies to minimize abiotic and biotic constraints in Brazilian eucalypt plantations. Forest Ecology and Management, 301, 6–27. https://doi.org/10.1016/j.foreco.2012.12.030

Halicka, A., & Ślósarz, S. (2021). Strengthening of timber beams with pretensioned CFRP strips. Structures, 34, 2912–2921. https://doi.org/10.1016/J.ISTRUC.2021.09.055

Honfi, D., Mårtensson, A., & Thelandersson, S. (2012). Reliability of beams according to Eurocodes in serviceability limit state. Engineering Structures, 35, 48–54. https://doi.org/10.1016/J.ENGSTRUCT.2011.11.003

Huang, L., Krigsvoll, G., Johansen, F., Liu, Y., & Zhang, X. (2018). Carbon emission of global construction sector. Renewable and Sustainable Energy Reviews, 81, 1906–1916. https://doi.org/https://doi.org/10.1016/j.rser.2017.06.001

Hunt, C. G., Frihart, C. R., Dunky, M., & Rohumaa, A. (2018). Understanding wood bonds-going beyond what meets the eye: A critical review. Reviews of Adhesion and Adhesives, 6(4), 369–463. https://doi.org/10.7569/RAA.2018.097312

Ikami, Y., Murata, K., Matsumura, Y., & Tsuchikawa, S. (2009). Einfluss der Lage der Markröhre beim Einschnitt auf Verformungen von Schnittholz aus Sugirundholz (Cryptomeria japonica D. Don) mittlerer Qualität. European Journal of Wood and Wood Products, 67(3), 271–276. https://doi.org/10.1007/s00107-009-0318-0

Japarudin, Y., Lapammu, M., Alwi, A., Warburton, P., Macdonell, P., Boden, D., Brawner, J., Brown, M., & Meder, R. (2020). Growth performance of selected taxa as candidate species for productive tree plantations in Borneo. Australian Forestry, 83(1), 29–38. https://doi.org/10.1080/00049158.2020.1727181

Kovryga, A., Stapel, P., & van de Kuilen, J. W. G. (2020). Mechanical properties and their interrelationships for medium-density European hardwoods, focusing on ash and beech. Wood Material Science & Engineering, 15(5), 289–302. https://doi.org/10.1080/17480272.2019.1596158

Lara-Bocanegra, A. J., Majano-Majano, A., Arriaga, F., & Guaita, M. (2020). Eucalyptus globulus finger jointed solid timber and glued laminated timber with superior mechanical properties: Characterisation and application in strained gridshells. Construction and Building Materials, 265, 120355. https://doi.org/10.1016/J.CONBUILDMAT.2020.120355

Leijten, A. J. M., Larsen, H. J., & van der Put, T. A. C. M. (2010). Structural design for compression strength perpendicular to the grain of timber beams. Construction and Building Materials, 24(3), 252–257. https://doi.org/10.1016/J.CONBUILDMAT.2009.08.042

Liao, Y., Tu, D., Zhou, J., Zhou, H., Yun, H., Gu, J., & Hu, C. (2017). Feasibility of manufacturing cross-laminated timber using fast-grown small diameter eucalyptus lumbers. Construction and Building Materials, 132, 508–515. https://doi.org/10.1016/j.conbuildmat.2016.12.027

Martins, C., Dias, A. M. P. G., & Cruz, H. (2020). Blue gum: assessment of its potential for glued laminated timber beams. European Journal of Wood and Wood Products, 78(5), 905–913. https://doi.org/10.1007/s00107-020-01567-0

Morales, C. A. C. (2009). Prototipo para la Enseñanza de la Dinámica Rotacional (Momento de Inercia y Teorema de Ejes Paralelos). Latin American Journal of Physics Education, 6–11.

Murphy, T. N., Henson, M., & Vanclay, J. K. (2005). Growth stress in Eucalyptus dunnii. Australian Forestry, 68(2), 144–149. https://doi.org/10.1080/00049158.2005.10674958

Myburg, A. A., Grattapaglia, D., Tuskan, G. A., Hellsten, U., Hayes, R. D., Grimwood, J., Jenkins, J., Lindquist, E., Tice, H., Bauer, D., Goodstein, D. M., Dubchak, I., Poliakov, A., Mizrachi, E., Kullan, A. R. K., Hussey, S. G., Pinard, D., van der Merwe, K., Singh, P., … Schmutz, J. (2014). The genome of Eucalyptus grandis. Nature, 510(7505), 356–362. https://doi.org/10.1038/nature13308

Negrão, J. H. (2012). Prestressing systems for timber beams. WCTE - World Conference on Timber Engineering.

Nocetti, M., Pröller, M., Brunetti, M., Dowse, G. P., & Wessels, C. B. (2017). Investigating the potential of strength grading green Eucalyptus grandis lumber using multi-sensor technology. BioResources, 12(4), 9273–9286. https://doi.org/10.15376/biores.12.4.9273-9286

Oliver, C. D., Nassar, N. T., Lippke, B. R., & McCarter, J. B. (2014). Carbon, Fossil Fuel, and Biodiversity Mitigation With Wood and Forests. Journal of Sustainable Forestry, 33(3), 248–275. https://doi.org/10.1080/10549811.2013.839386

Pagel, C. L., Lenner, R., & Wessels, C. B. (2020). Investigation into material resistance factors and properties of young, engineered Eucalyptus grandis timber. Construction and Building Materials, 230, 117059. https://doi.org/10.1016/j.conbuildmat.2019.117059

R Core Team. (2021). R: A Language and Environment for Statistical Computing. R Foundation for Statistical Computing.

Rosa, T. O., Terezo, R. F., Rios, P. D., Sampietro, J. A., & Rosa, G. O. (2019). Schizolobium Parahyba var. Amazonicum Glulam Classified by Non-destructive Tests. In Floresta e Ambiente: Vol. v. vol.26 num.2. Instituto de Florestas da Universidade Federal Rural do Rio de Janeiro.

Standards Australia. (1999). AS 2796.1 — Timber — Hardwood — Sawn and milled products Part 1: Product Specification.

van der Put, T. A. C. M. (2010). Failure criterion for timber beams loaded in bending, compression and shear. Wood Material Science and Engineering, 5(1), 41–49. https://doi.org/10.1080/17480270903582163

Yang, H., Ju, D., Liu, W., & Lu, W. (2016). Prestressed glulam beams reinforced with CFRP bars. Construction and Building Materials, 109, 73–83. https://doi.org/10.1016/J.CONBUILDMAT.2016.02.008

Yang, J.-L., & Waugh, G. (2001). Growth stress, its measurement and effects. Australian Forestry, 64(2), 127–135. https://doi.org/10.1080/00049158.2001.10676176

Zobel, B. J., & Sprague, J. R. (1998). Juvenile Wood in Forest Trees. Springer.

6. CONCLUSIONS

The topics assessed in the present study, usually considered impeditive for the use of wood from young trees, are an obstacle possible to overcome through the use of technology. We believe as happens in other areas of science, that the knowledge acquired by the developed countries has an influence on studies conducted in other regions, sometimes creating a general rule that may not be true for all situations. In our opinion, such is the case of the impacts of juvenile wood and knots on mechanical properties. Both features reduce the wood quality in softwoods more than in hardwoods. Although some authors have pointed that out previously, studies about softwood created an idea that it is not possible to use wood containing such features for solid products or structures. In Brazilian Pine, for example, the juvenile core of logs is large and has low quality, resulting in the timber from that zone to be often discarded. The brittle behavior usually seen in Pine timber from the log cores was not observed in the *Eucalyptus* we used. The fragile rupture in young *Eucalyptus* may be restricted to timber from the first two rings around the pith, so lamellas returned the same mechanical behavior usually observed in mature wood.

The knots showed a similar result. In young *Eucalyptus*, knots are smaller than those in Pine and are not distributed in clusters. These characteristics have a relevant influence on the mechanical behavior of wood with knots from these two types of wood. We did find decreases in adhesion and tensile strength (on beams) caused by knots, while on compression (on beams), knots did not show any qualitative or quantitative impact. We consider these reductions still allow the use of timber from young *Eucalyptus* for structural purposes, especially when considering the good adhesion results we observed.

Timber bow, even above the limits established, was not harmful to the manufacture of glued laminated beams, on the contrary, it seems to be beneficial. The other types of warping, on the other hand, are harder to handle and should be avoided. The developed index for timber bow and spring can be useful to improve yield on the conversion of timber to lamellas, especially finger jointed ones.

Our studies were conducted on a laboratory scale, so the positive results observed in our beams are strongly related to the careful selection and stratification of lamellas. On a commercial scale, the classification of lamellas by stiffness and bow levels must be faster and, consequently, may be less precise. However, we believe it is feasible to obtain results close to what we reported here if a production line is designed specifically for manufacturing glued laminated beams using timber from young *Eucalyptus*.

We also had the opportunity to manufacture a piece of furniture using wood from young *Eucalyptus grandis* (Appendix). We applied different techniques such as edge gluing, biscuit and dowel connections, resin filling and the material behaved normally. This is a positive result and indicate young *Eucalyptus* may also supply the furniture industry with timber, besides the already stablished reconstituted panel based furniture.

There are several benefits of using young forests as a timber source, from the fast raw material production and optimized processing, earlier payout, to the possibility of establishing plantations close to the consumer market. However, there is still relevant information about young *Eucalyptus* timber for structural application. From the material science perspective, the assessment of the behavior of knots under tension and the effect of a thin layer of clear wood on top of the knots under tension. From the industrial side, it might be interesting to develop a production line specifically for young *Eucalyptus* products, assess the losses of timber due to splitting and warping together with the economic viability.

APPENDIX

Item manufactured at the wood workshop course during the doctoral internship at Stellenbosh University: a bedside table made with young *Eucalyptus grandis* timber.

Figure 38. Raw material: finger-jointed boards of young *Eucalyptus grandis* timber.

Figure 39. Pieces of the bedside table before assembling.

Figure 40. Detail of the connections used: biscuit joints at the top and dowel connections at the bottom on both sides.

Figure 41. Final product presented as requirement for the wood workshop course.